SYSTEMIC CHARACTERIZATION OF THE OXYGEN RESPONSE OF THE WINE YEAST *SACCHAROMYCES CEREVISIAE* EC1118 IN OENOLOGICAL CONDITIONS

Tesis entregada a la Pontificia Universidad Católica de Chile en cumplimiento parcial de los requisitos para optar al grado de Doctor en Ciencias Biológicas con mención en Genética Molecular y Microbiología

Por

Felipe Eduardo Aceituno Aceituno

Director de Tesis
Dr. Eduardo Agosín Trumper
Profesor Titular
Departamento de Ingeniería Química y Bioprocesos
Escuela de Ingeniería
Pontificia Universidad Católica de Chile

Patrocinador de Tesis
Dr. Francisco Melo
Departamento de Genética Molecular y Microbiología
Facultad de Ciencias Biológicas
Pontificia Universidad Católica de Chile

Agosto 2013

So, carry on,
There's a meaning to life
Which some day we will find
Never giving up, it's time to forget
The remains from the past to carry on

(Adapted from Andre Matos)

ACKNOWLEDGEMENTS

Personally, I would like to thank my wife, Juanita Larraín-Linton, for her essential support. I would have fallen from this road at an early stage without her. I also thank her for having carried into this world our daughter, Regina Amalia, who was born during the course of this thesis. Thanks to her and to the newcoming baby, Aurelio Román, for the inspiration and encouragement their sole existence invokes.

I also thank the family from my wife's side; Becky, Fanor, Maga and Camilo for the countless times they helped with life tasks or simply by having a good moment to sweeten the sometimes sour road that a PhD thesis is. Also I would like to thank my cousins: Irina and Cesar, for with them we could rebuild the family, and we can foresee a no-more lonely future for us all. This thesis is also a present to them, so they can see goals and dreams can be achieved despite life's hardness.

This is also in memory of my mother and my uncle, who would like to see this achievement, if they were able to.

I also would like to thank the people I met during these years, especially to Marcelo Orellana, my partner, who made possible much of the work in this thesis. His granitic work ethics were both an example and a pillar of our research. I would also like to remember the people that welcomed me to the Biotechnology Lab: Isabel Moenne, Felipe Perez, Felipe Vargas and Sebastián Mendoza, among others, whose help at different specific points of this thesis was fundamental.

I also would like to thank the people from the Plant Systems Biology Lab, especially to Elena Vidal, who was my partner at the beginning of my PhD and Dr. Rodrigo A. Gutierrez. Both helped me with training on bioinformatics and use of microarray facilities, what proved to be fundamental in this thesis. I also thank Alex Slater and Dr. Francisco Melo for bioinformatic support and for providing office space in times of need.

Last but not least, I would like to thank my advisor, Dr. Eduardo Agosín, for having trusted me many times; allowing me to develop this thesis even when it seemed there was no hope. Without him my goal to be a PhD would have never been accomplished.

This thesis was supported by FONDECYT grant #1090520 and the "Doctoral thesis support" grant AT-24100170 from CONICYT, Chile. The laboratory is grateful to Lallemand, Inc. (Canada) for financial support and INDURA S.A. (Chile) for providing gas mixtures. The student was funded by CONICYT and VRI-UC doctoral fellowships.

SUBJECT INDEX

FIGURE INDEX

TABLE INDEX

ABBREVIATION LIST

OUR: Oxygen uptake rate

MFA: Metabolic Flux Analysis

FBA: Flux Balance Analysis

GSMR: genome-scale metabolic reconstruction

ABSTRACT

Discrete oxygen additions play a critical role in alcoholic fermentation. However, few studies have quantified the fate of the dissolved oxygen and its impact on wine yeast cell physiology, under oenological conditions. We simulated the range of dissolved oxygen concentrations that occur after a pump-over during the wine making process, by sparging nitrogen-limited continuous cultures with oxygen-nitrogen gaseous mixtures. Metabolic Flux Analysis was performed with a custom-built model. This indicated that when the dissolved oxygen concentration increases from 1.2 to 2.7µM, yeast cells change from a fully fermentative to a mixed respiro-fermentative metabolism. This transition was characterized by a switch in the operation of the tricarboxylic acid cycle (TCA), and an activation of NADH shuttling from the cytosol to mitochondria. Nevertheless, fermentative ethanol production remained the major cytosolic NADH sink for all oxygen conditions, suggesting the limitation of mitochondrial NADH reoxidation as the major cause of the Crabtree effect. This is reinforced by the induction of several key respiratory genes by oxygen, despite high sugar concentrations, indicating that oxygen overrides glucose repression, which was thought to be the cause of the Crabtree effect. Genes associated with other processes such as proline uptake, mannoproteins and oxidative stress are also significantly affected by oxygen. Our data suggests that oxygen can be beneficial at low levels, improving proline uptake and reducing acetic acid. On the contrary, high oxygen levels can reduce mannoproteins, important for haze removal and wine mouthfeel, and even stress yeast to the point of reducing its metabolic capacity when in excess, highlighting the dual role of oxygen in “making or breaking wines”.

Even though oxygen was promptly consumed under oenological fermentation conditions, we wondered which pathways accounted for biological oxygen consumption. By means of a

genome-scale, unbiased metabolic model, we determined that most oxygen is consumed by respiration. This is concordant with our experimental analyses that showed a minor contribution of non-respiratory pathways (such as ergosterol and lipid biosynthesis) to the overall oxygen consumption, and a major contribution of the respiratory-coupled proline assimilation pathway. Altogether, these results strongly indicate that oxygen consumption, when limiting, is more critical for nitrogen assimilation and respiration than for lipid synthesis.

To the best of our knowledge, this work is the first to globally assess the effects of oxygen on yeast physiology under a high-sugar, nitrogen-limited culture setting simulating oenological conditions. From this data, we determined optimal and deleterious oxygen conditions that can be chosen or avoided in wine making. Regarding yeast physiology, while several data can be extrapolated from carbon-limited physiology (such as TCA splitting in anaerobiosis), it is striking that respiration is responsible for a substantial part of the oxygen response in yeast cells during alcoholic fermentation, contrary to the widespread belief that respiration is under glucose repression in these conditions. Nevertheless, respiration does not surpass fermentation as the main energy-providing pathway, in a way analogous to what is seen in cancer cells that show the “Warburg effect”, this is, aerobic ethanol production. Therefore, the study of the oxygen response in nitrogen-limited yeast cells can provide relevant information on how to manage oxygen to impact positively wine quality, but is also as a model for other relevant biological systems.

1. INTRODUCTION

Alcoholic fermentation is a bioprocess of significant present and future perspectives, both for the production of highly consumed beverages (wine and beer, for example) as well as in the growing biofuel industry (Vargas et al. 2010). However, most of the research related to this field has focused on the overall process and not on the characterization of the yeast physiology at the molecular level. On the other hand, most molecular research in yeast has been conducted in laboratory strains and conditions that do not resemble industrial fermentation environment. A good example of this dichotomy is the research on oxygen additions to the wine fermentations. Oxygen additions are common practice in winemaking, improving yeast fermentative rate, viability and biomass (Sablayrolles et al. 2000); however, the metabolic and regulatory effects on yeast cells under wine fermentation conditions have not been evaluated, with the consequent lack of scientific background to establish optimal oxygen addition regimes in winemaking. The goal of this thesis is to fill this gap.

1.1. A general view of wine fermentation

Wine fermentation is an alcoholic fermentation process of high economical importance to our country. Chilean wine exports accounted for US$ 1.680 million during 2011 (www.vinosdechile.cl 2012). Therefore, research on the critical variables affecting wine quality is imperative to sustain the competitiveness of the Chilean wine industry.

Wine fermentation is a complex process where the quality of the must, the yeast strain, operation temperature and aeration are important variables that affect the final product (Pizarro et al. 2008). On this thesis, we focus on the yeast perspective. To understand to what extent yeast participates of the changes in these processes, we have to consider alcoholic fermentation from a microbiological perspective. Wine fermentation is

a batch culture system, with clearly defined lag, exponential and stationary phases. Exponential phase ends when the nitrogen of the must runs out; the end of the fermentation is when it reaches dryness, *i.e.,* sugar concentration is lower than 2 g/l, what happens at the end of stationary phase. The reason for this is that musts are extremely unbalanced in nutrients, having approx. 200-250 g/l of sugars and only approx. 300 mg/l of nitrogen. This means that winemaking conditions are nitrogen-limited, opposite to most laboratory media, which are carbon-limited. The fermentation time required to consume all the sugars depends on the abovementioned variables; some fermentations do not even reach dryness due to nitrogen scarcity, low or high temperature stress or lack of yeast biomass, among other factors (Sablayrolles et al. 2000; Varela et al. 2004; Pizarro et al. 2008); and one of the most crucial factor is oxygen addition (Sablayrolles et al. 2000).

1.2. The role of oxygen in wine fermentation

Oenologists incorporate oxygen to wine fermentations to ensure they reach dryness. This is most of the times performed through "pump-over", an operation that involves taking out the content of a tank and returning it from the top to the bottom. This may or not involve the exposure of the tank content to the environment by depositing it in an open tub. The turbulence occurring in this process allows that the fermenting must incorporates oxygen at different levels. Work from our laboratory has shown that this operation produces sharp oxygen impulses that range from 0 to 100 μM dissolved oxygen (Moenne and Agosin Personal communication). Other methods, such as "microoxygenation", involve a constant addition of small amounts of air. All these have recognized beneficial effects in winemaking, contributing to the aromatic diversity and intensity, color stabilization, and astringency and roundness (Parpinello et al. 2011). However, they are usually neither well controlled nor reproducible and therefore, oxygen

can also have deleterious effects when in excess, as oxidation can degrade aromatic compounds and, in case of white wines, it can also result in browning of the final product (Waterhouse and Laurie 2006; Cejudo-Bastante et al. 2011).

The effect of aeration operation on the yeast present in the fermenting must is less understood. It is known that CO_2 evolution and biomass content increases after oxygen addition (Rosenfeld et al. 2003). This effect has been attributed to the stimulation of unsaturated lipids and ergosterol syntheses. Supporting this idea, yeast cannot grow in defined media under absolute anaerobiosis, unless there is an exogenous supplement of ergosterol and unsaturated fatty acids, so-called "anaerobic factors". Another effect of oxygen in yeast metabolism is the stimulation of proline consumption (Ingledew et al. 1987). Proline is one of the most abundant amino acids in the must, although it cannot be metabolized in the absence of oxygen. Therefore, oxygen also allows yeast cells to utilize an alternative nitrogen source in a nitrogen-scarce environment such as grape must, minimizing one of the main causes of stuck fermentations (Varela et al. 2004). Despite this knowledge, there are few advances in the understanding of the oxygen effect on yeast physiology. For example, studies differ in how much oxygen is destined to sterol and lipid synthesis or proline assimilation (Valero et al. 2001; Fornairon-Bonnefond et al. 2002; Rosenfeld et al. 2002; Rosenfeld et al. 2003), and no one so far has determined all the pathways that account for oxygen consumption in wine fermentation conditions. To do so, it is necessary to understand yeast metabolism in fermentation conditions. We will summarize this knowledge below.

1.3. Yeast metabolism during alcoholic fermentation

1.3.1. The glycolytic pathway, ethanol and glycerol production.

All alcoholic fermentations required the glycolytic pathway. Glucose is the main substrate of the pathway, although fructose and other sugars present in the must can also link up to the pathway at the level of fructose-6-phosphate (Fig 1).

In the first part of glycolysis, energy expenditure is required in order to "activate" the sugars. Two molecules of ATP are spent at this stage. Later, the activated sugars are split into two molecules of trioses phosphate. These molecules are oxidized and then, energy is recovered by "substrate level phosphorylation" that occurs at the latter stages of the pathway, that ends producing pyruvate. Overall, four molecules of ATP are produced per sugar molecule that entered the pathway.

The oxidation of the trioses phosphate needs the expenditure of 2 NAD^+ molecules. In aerobic conditions, the NAD^+ stock is ultimately replenished by respiration, since the NADH produced transfers electrons to oxygen in the mitochondria. However, in anaerobic conditions, this is not possible. Therefore, the NADH in excess has to be compensated by additional reactions. Those are reactions that use NADH and ultimately lead to ethanol production (from pyruvate) and, to a lesser amount, to glycerol (from glyceraldehyde-3-phosphate, Fig 1). Glycerol is only produced in exponential phase, when biomass (which is more reduced than glucose) is produced and so contributes to redox imbalance. Ethanol and glycerol are the main components of wine (Boulton et al. 1998).

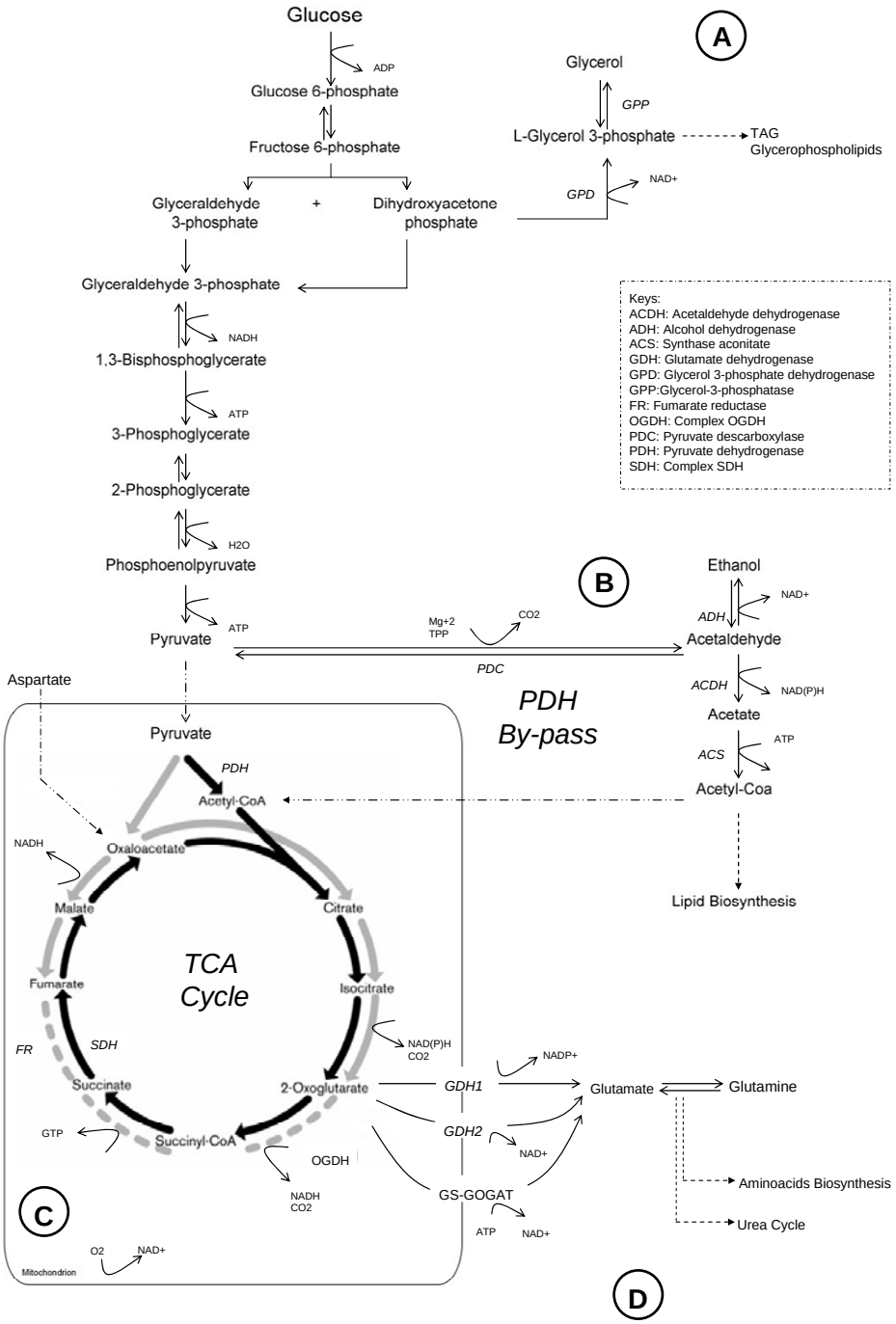

Figure 1. Schematic summary of fermentative and respiratory metabolism of yeast. A) Glycerol synthesis pathway as a branch of fermentation. B) The complete pathway from glucose to ethanol including the PDH by-pass. C) Reductive and oxidative branches of the TCA cycle under anaerobic conditions. The oxidative branch works counter-clockwise from pyruvate and is marked in black. The reductive branch is marked in grey, and ends in 2-oxoglutarate and succinate. For this last branch, needs the involvement of the fumarate reductase (FR) instead of the succinate dehydrogenase (SDH) working in the oxidative branch. The point of cycle interruption is marked as dotted lines. Adapted from Camarasa et al. (2003). D) Synthesis of glutamate fromTCA cycle. Overall figure adapted from (Vargas et al. 2010)

A secondary role of glycerol production is protection against the osmotic stress caused by high sugar in the initial stages of fermentations. Indeed, one isoform of glycerol-3-phosphate dehydrogenase is regulated by osmotic stress (Hohmann 2002). However, glycerol is produced even when the sugar content reaches low concentrations, suggesting the main role of glycerol production is to act as an electron sink.

1.3.2. The Crabtree effect and the cytosol-mitochondria redox shuttles

Contrary to the common belief, fermentation is not restricted to occur only in anaerobic conditions (Henricsson et al. 2005). *Saccharomyces cerevisiae* is unusual among yeasts in the sense that it does not show the Pasteur effect (inhibition of fermentation by oxygen). On the contrary, *S. cerevisiae* carries out fermentative - rather than respiratory-metabolism under high sugar culture conditions, such as those found in winemaking. This is known as the Crabtree effect (Verduyn 1991; Walker 1998). Only in the presence of oxygen, at low sugar concentrations and low grow rates, *S. cerevisiae* shows a fully respiratory metabolism (Frick and Wittmann 2005; Jouhten et al. 2008).

Several hypotheses have been suggested to explain this phenomenon, such as catabolic repression of respiratory enzymes (Gancedo 1998), bottleneck of the carbon flux towards TCA cycle (Pronk et al. 1996), and a limitation of the yeast respiratory enzymes to reoxidize the NADH produced by glycolysis (Vemuri et al. 2007). We will explain these hypotheses below.

Glucose catabolic repression is a global transcriptional repression of genes related to metabolism of other carbon sources and possibly, respiratory and TCA cycle enzymes (Gancedo 1998). Repression of these enzymes would prevent NAD recycling and ATP production in the mitochondria. This repression is mediated by the Snf1/Hxt2 signaling pathway, which, in the presence of glucose, activates the Mig1p repressor (Zaman et al.

2008). This transcription factor is the responsible for the repression of genes such as the GAL genes, but no clear-cut evidence has been given on the union of this repressor on respiratory genes promoters.

Limitation of the activity of respiratory enzymes has also been suggested as the main cause of the Crabtree effect. Overexpression of water-forming NADH dehydrogenases causes a substantial decrease in fermentative glycerol and ethanol production in aerobic conditions, strongly suggesting that there is an increased carbon flow to respiratory pathways despite the high sugar concentration present in the medium (Vemuri et al. 2007). This strongly suggests that respiratory enzymes do not have the capacity to metabolize all the carbon and electrons arising from the sugars, when they are at high concentration levels.

How the electrons generated in the glycolytic pathways could be conveyed to the respiratory enzymes? The mitochondrial inner membrane is virtually impermeable to pyridine nucleotide coenzymes (Jagow and Klingenberg 1970). Consequently, redox balances must be established in each compartment, *i.e.* the reduced coenzymes must be reoxidized in the compartment where they are generated. However, redox-shuttle mechanisms lead a redox coupling between mitochondrial and cytoplasmatic redox equivalents through specific metabolites, which are either actively transported or diffuse freely across biological membranes.

Several redox-shuttle mechanisms have been proposed to occur in *S. cerevisiae* during anaerobic growth: 1) the glycerol-3-phosphate shuttle (Gut2p), 2) the external NADH dehydrogenase (Nde1p) shuttle and 3) the mitochondrial alcohol dehydrogenase (Adh3p) shuttle (Bakker et al. 2001; Rigoulet et al. 2004). The Adh3p reaction consumes the ethanol that diffuses from the cytoplasm and produces acetaldehyde and NADH in the mitochondrial matrix. Acetaldehyde can diffuse back to the cytoplasm, while NADH is

reoxidized by oxygen in the electron transport chain. The Nde1p reaction, on the contrary, directly couples cytosolic NADH oxidation to the respiratory chain. This is similar to the functioning of Gut2p, which shuttles electrons from glycerol 3-phosphate oxidation to the mitochondrial quinone pool. Two groups have advocated for the preeminence of the Adh3p (Bakker et al. 2001) or the Nde1p shuttles in yeast (Rigoulet et al. 2004), respectively. While only Nde1p has been assayed in nitrogen-limited conditions (Pahlman et al. 2001), most authors have accepted Adh3p as the main redox shuttle in anaerobic conditions (Bakker et al. 2001; Murray et al. 2011).

1.3.3. The TCA cycle

In anaerobic, carbon-limited conditions, it has been shown that the cycle is interrupted at the level of succinyl CoA synthetase (Camarasa et al. 2003) (Fig 1). Thus, there is an "oxidative branch" and a "reductive branch" of the cycle. This prediction was first calculated as thermodynamically feasible and it has been proposed to operate in *S. cerevisiae* (Lupiañez et al. 1974), and then this proposal was strongly supported by Metabolic Flux Analysis (MFA) (Nissen et al. 1997), where only by measuring rates of extracellular metabolites consumption and production and applying a stoichiometry-based model, the need of a reductive branch in anaerobic growth was demonstrated. These predictions were confirmed several years after by Camarasa et al (2003) using NMR isotopic filiation of ^{13}C- glucose to study the redistribution of the ^{13}C-label in anaerobic conditions. The reductive branch of the cycle has an unusual feature; *i.e.* that every reaction goes in the opposite direction that in the normal functioning in respiratory conditions. This is an important issue in the case of succinate dehydrogenase. This enzyme belongs both to the electron chain and to the TCA cycle, and its reaction is thermodynamically irreversible. The reductive branch then bypasses this enzyme and

utilizes fumarate reductase, a completely different enzyme that uses $FADH_2$ as a cofactor to transform fumarate to succinate. This is important since this pathway is responsible for the regeneration of soluble FAD in the cell. The unsolved question is, does the two-branch operation of the TCA cycle, as depicted in Fig 1C) occur under anaerobic, nitrogen-limited conditions?

1.4. Effects of oxygen in yeast physiology

1.4.1. Metabolic effects

Oxygen has a deep impact in yeast metabolism. Oxygen can shift yeast metabolism from fermentative to oxidative. However, fully oxidative operation occurs only in low sugar, low growth rates conditions. This has been reported by Jouhten et al. (Jouhten et al. 2008), where fully respiratory metabolism was achieved at a dilution rate (*i.e.* growth rate) of 0.1 h^{-1}, sparging the culture with air (20.9% oxygen). With less oxygen, the metabolism became mixed respiro-fermentative, *i.e.* ethanol was produced. However, these experiments were conducted in glucose-limited cultures, and therefore these results were not extrapolable to nitrogen-limited conditions. Indeed, it is known that a mixed respiro-fermentative metabolism occurs in nitrogen-limited conditions, regardless of the oxygen level (Larsson et al. 1993; Tai et al. 2005), because of the Crabtree effect (see above).

Few studies have carried out a detailed assessment of the oxygen effect into the global metabolism of yeast cells under nitrogen-limited conditions. Most have focused on the pathways responsible for oxygen consumption. (Fornairon-Bonnefond et al. 2002) showed that discrete additions of 218 and 1156 μM oxygen to a model batch wine fermentation affects the sterol content of the cells and, in the latter case, the excess oxygen was proposed to be consumed by respiratory pathways. This would need the induction of

respiratory metabolism; however, this was not investigated further. In a similar study, (Rosenfeld et al. 2002) determined that anaerobically grown *S. cerevisiae* can readily consume oxygen independent of protein synthesis. They also showed that 40% of the oxygen consumption depends on the functioning of the ergosterol synthesis pathway. The rest of the oxygen was unaccounted for, dismissing the function of respiration due to the inability of inhibitors such as antimycin A to have an effect on the measured oxygen consumption. However, cyanide did have an effect (33%), which raises the question about whether respiration is responsible for part of the remaining oxygen consumption. Other pathways, such as heme and unsaturated lipid synthesis showed little contribution to the overall oxygen balance in these works. Another pathway that could be responsible of oxygen consumption is proline assimilation (Ingledew et al. 1987). Proline is one of the main sources of nitrogen in grape musts (20% of total N), a medium that is remarkably low in nitrogen overall (average. 300 mg/l of available N) (Salmon and Barre 1998). Oxygen additions in winemaking improve biomass production and fermentative rate, in part by favoring proline assimilation (Sablayrolles et al. 2000). However, proline is unavailable in the absence of oxygen, since its assimilation depends on the membrane bound FAD-dependent proline oxidase enzyme (Put1p); and membrane-bound FAD cannot be regenerated in anaerobiosis since fumarate reductase (Frd1p), the enzyme that regenerates FAD in the mitochondria under these conditions, is not a membrane-bound enzyme and acts on soluble $FADH_2$. Put1p, on the other hand, is a mitochondrial membrane enzyme that directly couples ubiquinone oxidation to FAD regeneration (Wanduragala et al. 2010). Therefore, an increase in proline utilization requires ubiquinone regeneration and, consequently, respiratory oxygen consumption. Despite this knowledge, the actual contribution of respiratory pathways to oxygen consumption under wine fermentation conditions is yet unclear.

1.4.2. Regulatory effects

Besides its metabolic effect, oxygen can also be a regulatory signal. Several signaling pathways mediate oxygen regulation of gene expression. The most studied are heme-dependent pathways. Heme is a metabolite that needs oxygen for its synthesis, and whose biosynthetic pathway is constitutively expressed. Therefore, upon oxygen availability, heme begins to be synthetized. There are several transcription factors whose activity are directly proportional to the intracellular levels of heme content. The most important ones are those belonging to the *HAP* family, which exert an activating role when bounding to heme (Plakunov and Shelemekh 2009). Burke et al. (Burke et al. 1997) found that above 0.5 μM oxygen there is induction of the target genes for these transcription factors. These genes are critical for oxygen metabolism. For instance, Hap1p activates the transcription of *CYC* and *CYB* genes encoding for cytochrome c and b isoforms; and the Hap2/3/4/5p complex activates the *COX* genes encoding subunits of the cytochrome c oxidase. On the other hand, when not bound to heme (*i.e.* in anaerobic conditions), Hap1 can work as a repressor of many *ERG* genes, which encode for the oxygen-dependent biosynthetic pathway of ergosterol (Plakunov and Shelemekh 2009). Nevertheless, the Rox1p repressor, whose expression is induced by Hap1p, exerts most of the repressive activity by the heme-dependent pathway. For instance Rox1p acts on the so-called hypoxic genes such as *ERG11*, which encodes an ergosterol biosynthetic enzyme which is repressed at oxygen concentrations above 0.5 μM. A counterpart of this repressive activity is mediated by the Upc2p transcription factor, which induces hypoxic genes below the 0.5 μM dissolved oxygen threshold in response to sterol depletion, a direct consequence of oxygen limitation (Plakunov and Shelemekh 2009). Therefore, the interplay between sterol content and oxygen availability seems to control gene expression of lipid biosynthetic genes.

However, it is not yet understood how these regulatory networks contribute to the observed effects of oxygen in yeast physiology under winemaking conditions. Furthermore, no studies have dealt with the oxygen response of industrial wine yeast strains, which are known to have striking differences with laboratory yeast strains (Rossouw et al. 2009; Rossouw et al. 2011). Therefore, there is a need for transcriptomic studies that address the effect of oxygen on gene expression under winemaking conditions.

1.5. Continuous cultures as a tool for research

Scaling-down winemaking conditions to the laboratory is required to understand the molecular and metabolic effects of oxygen in wine yeast cells. For this purpose, batch cultures are not the best choice to dissect the molecular events associated with the response to oxygen. Indeed, it is known that culture conditions (*i.e.* nutrient concentrations) change continuously – and simultaneously - over time in batch systems. Steady-state continuous cultures, on the other hand, offer the unique possibility to minimize the variations of environmental conditions, as well as those related to the specific growth rate (μ), by controlling the dilution rate (D [h^{-1}]), under tightly defined nutritional conditions (Piper et al. 2002; Boer et al. 2003; Pizarro et al. 2008). The importance of the latter is highlighted by several studies that have revealed a strong overlap between genes that were reported to be regulated by temperature change and those controlled by growth rate (Regenberg et al. 2006; Castrillo et al. 2007). Thus, for example, when comparing the transcriptome of a wild type and a slow-growing *S. cerevisiae* mutant grown in batch cultures, several genes appeared to express differentially. However, when these cells were grown in continuous culture, at the same specific growth rate, only a few genes were differentially expressed (Hayes et al. 2002). Therefore, continuous cultures are more appropriate than batch cultures for well-controlled, physiological studies of the

transcriptome, proteome and metabolome, because they allow to discriminate between the direct effects of the study conditions and those indirect effects, dependent on growth rate variations (Hayes et al. 2002; Castrillo et al. 2007). In summary, this culture system allows running experiments modifying only the variable of interest, with all the other ones remaining constant. This culture system is therefore the most suitable to simulate and understand the impact of long-term, steady state increasing dissolved oxygen contents on the holistic metabolic response of yeast cells.

1.6. Metabolic models and a quantitative understanding of metabolism

Continuous cultures have the advantage of providing cells at a steady state. This steady state is an assumption of most mathematical tools dealing with metabolic processes. Achieving it, therefore, opens up the toolbox for applying mathematical models for the global understanding of the yeast metabolism.

One of the main tools for this task is the Metabolic Flux Analysis (MFA). This tool represents the metabolic network of the cell as a stoichiometric matrix *M* (equation 1), in which each reaction is represented in a *i* row and each metabolite in a *j* column. The stoichiometric coefficients (*x, y, w, z*) of the metabolites (*j, j+1,* ...) in the corresponding reactions (*i, i+1,* ...) fill the matrix, as explained in the following equation.

$$\begin{matrix} x_{i,j} & y_{i,j+1} \\ w_{i+1,j} & z_{i+1,j+1} \end{matrix} = \begin{matrix} M_{ex} \\ M_{int} \end{matrix} = M$$

Equation 1: Stoichiometric matrix

Part of the stoichiometric matrix (M_{ex}) represents reactions that can lead to extracellular products, or uptake of substrates. These are experimentally measurable rates

(*R* in equation 2), therefore, this measurements can be incorporated and equaled to the reactions in M_{ex}. For the intracellular part (M_{int}), a key assumption is the steady state of the internal metabolites (*i.e.* the rate of production and consumption of metabolites is zero). This is because these rates are much faster than the rate measurements used as an input to the model (sub-second vs. hours) and therefore they are likely to equal each other in this time framework. With this assumption, we can build and solve the following equation (Nielsen et al. 2003)

$$M * v = \begin{matrix} R \\ 0 \end{matrix}$$

Equation 2: Mass balance equation for metabolic flux analysis#

Where v is the flux vector, that is, the flux of matter through the reaction in the corresponding row in the stoichiometric matrix M. Solving the equation for "v", we can find the metabolic flux for each reaction in M_{int}, which in the end is the metabolic flux distribution through the whole metabolic network (Nielsen et al. 2003). R is the vector of extracellular specific rates of substrate consumption and product formation.

Depending on the dimension of the stoichiometric matrix, the MFA approach uses different mathematical tools to solve this equation. If it is a square matrix, this is, it has equal number of metabolites and reactions, the matrix is invertible and the solution is unique and identifiable. Non-square matrix methods appear when there is more measurements than degrees of freedom, this is, the difference between the number of metabolites and the number of reactions. An example of this is the work of Nissen et al. (Nissen et al. 1997), who used a metabolic network of the yeast central metabolism, with 37 reactions and 43 metabolites, of which 13 were measured. In this case, using 6 constraints would have been enough to obtain a unique solution. The use of 13 constraints

allowed working in an "over-determined" setting. This mean that the spare constraints could be used to check the consistency of the data, or moreover, could be all integrated into the equation as part of the *R* matrix in equation 2. In this case, solving "v" in the equation 2 is more complex, since, the matrix is not square anymore. However using the pseudo-inverse matrix operation- which is equivalent to make a least squares estimation of the model solution- we can obtain a reliable measure for the intracellular fluxes (Nielsen et al. 2003). Nissen et al. (Nissen et al. 1997) predicted several important features of yeast metabolism in anaerobic conditions, most remarkably the first indication that the TCA cycle operated in two branches, which was later confirmed experimentally (Camarasa et al. 2003).

Despite the usefulness of the over-determined setting, the most common case in metabolic flux balancing is to have more reactions than metabolites. This is the case for the genome-scale metabolic reconstructions (GSMRs) which have arisen as a promising tool to analyze cellular metabolism as a whole (Liu et al. 2010). In the case of *S. cerevisiae*, the Yeast 4.0 GSMR has 1865 reactions and 1316 metabolites (Dobson et al. 2010). In this case, the solution to equation 2 is not unique, and it is necessary to define a reaction as an "objective function" to find a solution that optimizes this function. This function is often biomass production (Feist and Palsson 2010). Using linear programming, we can search a "solution space" defined by the metabolic constraints of the organisms to find the optimal solution. This approach, dubbed Flux Balance Analysis (FBA) (Orth et al. 2010), has been of widespread use with genome-scale metabolic reconstructions such as Yeast 4.0, having the merit of covering most of the metabolic network of the cell.

However, since the solution of the FBA approaches is not unique, this approach has several drawbacks. The first has to do with the use of the objective function. While it has been assumed that growth and cell division is the main objective of microbial systems

(Feist and Palsson 2010), that is not necessarily the case, and several other objective functions have been proposed (Braunstein et al. 2008; Gianchandani et al. 2008), being still a subject of debate in the scientific community. The second is the reliability of the predictions, due to the huge scope of the solution space, the optimization can be trapped in local optima or yield flux values non-coherent with the biological knowledge, if not enough constraints are provided. Therefore, the constraints are critical to ensure the success of this approach.

Thus, for an over-determined system, the more constraints provided the better. Nevertheless, despite being smaller in scope, a properly constrained over-determined MFA model where the flux distribution is algebraically determined could yield more reliable flux estimations than a GSRM operated under the FBA approach.

Choosing between FBA-operated GSMRs and more reduced MFA approaches is a compromise between scope and accuracy of flux estimations. However, FBA approaches are more amenable for integration with other type of data. In a genome-scale model, gene-enzyme correspondence is well defined; therefore, integration with transcriptomic data has been made possible due to the availability of several computational tools, such as the TIGER or COBRA toolboxes (Becker et al. 2007; Jensen and Papin 2011). This allows use of gene expression data of the metabolic enzymes as further constraints to the solution space of the model. One of the methods to do so, called GIMME (Gene Inactivity Moderated by Metabolism and Expression) (Becker and Palsson 2008) allows for setting a zero flux toward reactions whose encoding genes have null or low expression in a particular condition. This is not feasible with small-scale MFA since, due to the reduction of the metabolic matrix, most reactions are “lumped”, (*i.e.* representations of many reactions) and so composed of multiple, unrelated genes.

The integration of metabolic and transcriptomic data in metabolic models is still in its infancy. However, it has been useful generating the so-called "context-specific" models, which are metabolic models specific for a determined condition. For example, this approach has been used to predict metabolic fluxes in bacterial or yeast strains artificially evolved to enhance growth in non-optimal substrates (Becker and Palsson 2008; Jensen and Papin 2011), for which transcriptome has been determined. Moreover, this is even more useful when the choosing of the objective function even less clear, such as in human cells (Zur et al. 2010).

1.6.1. **Final remarks**

In this thesis, we will address how *Saccharomyces cerevisiae* respond to oxygen in steady state, scaled-down, continuous cultures simulating winemaking conditions. This knowledge is organized in two chapters, which correspond to different articles, which have been or are to be submitted for publication. The first chapter deals with the impact of constant dissolved oxygen levels in the yeast physiology, quantified by a small-scale MFA model and complemented by microarray analyses. The most part of this chapter is the article published in *Applied and Environmental Microbiology vol 78 (23), pp 8340-52*, 2012. The second chapter will be a second manuscript, to be submitted to *Applied and Environmental Microbiology* or the *Journal of Biotechnology.* This deals with the oxygen consumption pathways in wine fermentation conditions, evaluated both experimentally and by the integration of transcriptome and genome-scale metabolic models. The results obtained provide strong evidence in support of respiration as a main player in wine fermentation, revealing a new dimension to the comprehension of yeast physiology under oenological conditions and providing a scientific basis to improve oxygen management during industrial winemaking.

2. HYPOTHESIS

The exposure of wine yeast cells to oxygen under oenological conditions causes global physiological responses, involving uncharacterized metabolic pathways, that can be addressed by metabolic flux analysis, metabolomic and transcriptomic studies.

3. GENERAL AIM

To characterize the wine yeast physiology in response to different levels of oxygen, in order to derive insights into global metabolism, oxygen consumption pathways and optimized oxygen management in oenological conditions.

3.1. SPECIFIC AIMS

3.1.1. To characterize the impact of different oxygen levels found in winemaking on the global metabolic and transcriptomic configuration of wine yeast

3.1.2. To evaluate the oxygen consumption of known and novel yeast metabolic pathways and its contribution to overall biological oxygen consumption in oenological conditions.

4. RESULTS

Chapter 1

Paper published in *Applied and Environmental Microbiology, Vol78, N°73, pp 8340-52*

Oxygen response of the wine yeast *Saccharomyces cerevisiae* EC1118 strain grown under carbon-sufficient, nitrogen-limited oenological conditions.

Felipe F. Aceituno[,1], Marcelo Orellana[,1], Jorge Torres[1], Sebastián Mendoza[1], Alex W. Slater[2,3], Francisco Melo[2,3]& Eduardo Agosin#[1,4].

[1]*Department of Chemical and Bioprocess Engineering, School of Engineering, Pontificia Universidad Católica de Chile, Av. Vicuña Mackenna 4860, Macul, Santiago, Chile.*

[2] *Molecular Bioinformatics Laboratory, Millenium Institute on Immunology and Immunotherapy, Av. Libertador Bernardo O'Higgins 340, Santiago, Chile.*

[3] *Department of Molecular Genetics and Microbiology, Faculty of Biological Sciences, Pontificia Universidad Católica de Chile, Av. Libertador Bernardo O'Higgins 340, Santiago, Chile.*

[4] *ASIS-UC Interdisciplinary Research Program on Tasty, Safe and Healthy Foods, Pontificia Universidad Católica de Chile, Casilla 306 Correo 22, Santiago, Chile.*

Abstract

Discrete oxygen additions play a critical role in alcoholic fermentation. However, few studies have quantified the fate of the dissolved oxygen and its impact on wine yeast cell physiology under oenological conditions. We simulated the range of dissolved oxygen concentrations that occur after a pump-over during the winemaking process, by sparging nitrogen-limited continuous cultures with oxygen-nitrogen gaseous mixtures. When the dissolved oxygen concentration increases from 1.2 to 2.7 μM, yeast cells change from a fully fermentative to a mixed respiro-fermentative metabolism. This transition is characterized by a switch in the operation of the tricarboxylic acid cycle (TCA) and an activation of NADH shuttling from the cytosol to mitochondria. Nevertheless, fermentative ethanol production remained the major cytosolic NADH sink for all oxygen conditions, suggesting the limitation of mitochondrial NADH reoxidation as the major cause of the Crabtree effect. This is reinforced by the induction of several key respiratory genes by oxygen, despite the high sugar concentration, indicating that oxygen overrides glucose repression. Genes associated with other processes such as proline uptake, cell wall remodeling and oxidative stress were also significantly affected by oxygen. The results of this study indicate that respiration is responsible for a substantial part of the oxygen response in yeast cells during alcoholic fermentation. This information will facilitate the development of temporal oxygen addition strategies to optimize yeast performance in industrial fermentations.

Introduction

Oxygen is discretely added during winemaking to avoid sluggish and stuck fermentations (Sablayrolles et al. 2000). This is generally achieved through pump-overs, where dissolved oxygen concentrations could transiently reach up to 100 μM afterwards. The oxygen is consumed completely in approx. 1 h, but depends on the wine variety and the oxygen addition method employed (Moenne and Agosin Personal communication). The wide range of resulting dissolved oxygen concentrations has a deep impact on the physiology of wine yeast cells, improving yeast fermentative rate, as well as yeast viability (Sablayrolles et al. 2000). These effects are partially explained, because oxygen is required for sterol biosynthesis, proline uptake, and unsaturated lipid biosynthesis (Ingledew et al. 1987; Valero et al. 2001; Rosenfeld et al. 2003). Prior studies have attempted to assess the fate of oxygen under winemaking culture conditions, focusing on the behavior of lipid and sterol biosynthesis (Rosenfeld et al. 2002; Rosenfeld et al. 2003). However, a global approach is required for a quantitative understanding of the impact of dissolved oxygen on yeast cells physiology, grown under oenological conditions, *i.e.* sugar-sufficient, nitrogen-limited, acidic cultures.

The presence of oxygen in the culture medium can shift the central yeast metabolism from fermentative to respiratory (Larsson et al. 1993; Tai et al. 2005; Jouhten et al. 2008; Rintala et al. 2011). However, *Saccharomyces cerevisiae* only shows a fully respiratory metabolism at low growth rates with low sugar concentrations (Frick and Wittmann 2005). Above a critical specific growth rate or sugar concentration, yeast cells synthesize ethanol, regardless of the oxygen level (Tai et al. 2005). The latter is known as the Crabtree effect (Walker 1998). Several hypotheses have been suggested to explain this phenomenon, such as catabolic repression of respiratory enzymes (Gancedo 1998), a

bottleneck of the carbon flux towards the tricarboxylic acid cycle (TCA) (Pronk et al. 1996) and limitation of yeast respiratory enzymes to reoxidize the NADH produced by glycolysis (Vemuri et al. 2007). In all cases, carbon is channeled towards ethanol biosynthesis in the cytosol, instead of the TCA cycle, causing an "overflow metabolism", the foundation of alcoholic fermentation (Nielsen et al. 2003). This overflow normally occurs under nitrogen-limited and carbon-sufficient culture conditions, *i.e.* the operation conditions of winemaking (Tai et al. 2005). However, to the best of our knowledge, it is not clear how specific oxygen uptake rate (OUR) influences overflow metabolism in nitrogen-limited conditions, and whether it is compatible or not with respiratory activity.

Understanding the overflow metabolism requires an understanding of the redox biochemistry of the alcoholic fermentation in yeast. In anaerobic conditions, the NADH spent in the glycolytic pathway must be reoxidized. Ethanol production is a way to reoxidize this NADH, although there is always an electron surplus, caused by the release of fully oxidized carbon as CO_2. Redox balance is restored by diverting carbon towards glycerol production, which also reoxidizes NADH (Vargas et al. 2010). This is the only way to achieve redox balance in anaerobic conditions. On the contrary, in aerobic conditions, oxygen can act as an electron sink and help to establish this balance. For this, two requisites are needed under oenological conditions: respiration has to be active under high-sugar, nitrogen-limited conditions; and there must be functional shuttles of NADH from the cytosol to the mitochondria.

Three redox shuttles have been proposed to be at work in yeast mitochondria: the glycerol-3-phosphate (Gut2p) shuttle; the external NADH dehydrogenase (Nde1p) shuttle; and the mitochondrial alcohol dehydrogenase (Adh3p) shuttle (Bakker et al. 2001; Rigoulet et al. 2004). The Adh3p reaction consumes the ethanol that diffuses from the cytoplasm and produces acetaldehyde and NADH in the mitochondrial matrix.

Acetaldehyde can diffuse back into the cytoplasm, while NADH is reoxidized by oxygen in the electron transport chain. The ethanol-acetaldehyde conversion is potentially reversible, and its ΔG value is low (33.5 kJ/mol at pH 5, 25°C) (Alberty 2006). The Nde1p reaction, on the contrary, directly couples cytosolic NADH oxidization to the respiratory chain. The latter is similar to Gut2p, which shuttles electrons from glycerol 3-phosphate oxidization to the mitochondrial Quinone pool. Adh3p has been regarded as the main shuttle (Celton et al. ; Varela et al. 2004; Murray et al. 2011). However, there is only one study on the function of these shuttles in nitrogen-limited conditions (Pahlman et al. 2001), emphasizing this issue deserves further investigation.

To tackle such issues, oenological conditions need to be simulated on a laboratory scale. Continuous cultures, unlike batch cultures, allow a tightly controlled environment, while keeping yeast cells at a defined specific growth rate. Thus, we can simulate culture conditions prevailing at the end of the exponential phase of wine fermentation, when assimilable nitrogen is running out (*i.e.* nitrogen limited) and the effect of oxygen addition is maximal (Sablayrolles et al. 2000). Chemostats, as they operate in steady state, are highly reproducible, making them ideal for "-omics" experiments (Hoskisson and Hobbs 2005; Tai et al. 2005).

Simulation of different oxygen conditions in a winemaking setting requires characterizing the relationship between specific oxygen uptake rates (OUR) and the dissolved oxygen concentration under these culture conditions. Specific oxygen consumption rate by yeast cells increases linearly with oxygen availability up to a critical dissolved oxygen concentration, at which the OUR is maximal, *i.e.* the "critical" OUR (Doran 1995). When an oxygen impulse is carried out during fermentation, yeast cells are subjected to oxygen contents within the oxygen-limiting regime; the whole oxygen concentration range achieved during an oxygen impulse under oenological conditions

could be simulated by increasing dissolved oxygen concentrations in nitrogen-limited continuous cultures.

Once the conditions are set, the OUR and other measured rates at the steady state are valuable inputs for Metabolic Flux Analysis (MFA). MFA allows the determination of intracellular metabolic fluxes, difficult to determine *in vivo*, from a set of extracellular uptake and production rates, which are easily measurable. MFA has been successfully used to understand yeast metabolism under anaerobic conditions, in both carbon- and nitrogen-limited settings (Nissen et al. 1997; Varela et al. 2004). Incorporation of oxygen consumption pathways to these networks is a task that could help to explain the metabolic effects and the fate of oxygen in yeast industrial fermentations.

In this research, we combined the use of carbon-sufficient, nitrogen–limited continuous cultures, MFA models and DNA microarrays to simulate and examine the *S. cerevisiae* response to increasing dissolved oxygen concentrations, under oenological conditions. MFA analysis indicated that yeast cells underwent respiro-fermentative metabolism under wine fermentation conditions above a certain dissolved oxygen threshold. Transcriptome analyses supported these findings, as they showed that respiratory genes were induced by oxygen. Other oenological-relevant processes, such as proline uptake and cell wall remodeling, were also affected by oxygen. Altogether, this research provides an understanding of the mechanisms through which oxygen can influence yeast performance in industrial fermentations.

Materials and Methods

Yeast strain and culture conditions. *Saccharomyces cerevisiae* EC1118 (Lalvin, Switzerland), an industrial strain used worldwide by the wine industry, was employed throughout this study. Initial seed cultures were grown in 50 mL YPD broth at 28ºC under aerobic conditions to a mid – logarithmic growth phase. For continuous cultivation, a 2.0 liter BIOSTAT B bioreactor (Sartorius Biotech, Germany) with a working volume of 1.5 liter, was inoculated with enough volume of the microbial broth to obtain an initial cell density of 10^6 cells ml^{-1}. The culture was allowed to grow in batch mode until reaching early-to-mid exponential growth. Constant feeding was then initiated with a defined artificial must that limited growth by nitrogen, with a constant residual carbon concentration (see below). The dilution rate (D) was set at 0.1 h^{-1}. Agitation, temperature and pH were maintained at 200 rpm, 20ºC and 3.5 respectively, to simulate white wine fermentation. All experiments were performed in triplicate.

Gases were provided by means of an Aalborg GFC Mass Flow Controller (Aalborg, USA), at a rate of 0.25-liter min^{-1} in all experiments, except for the highest dissolved oxygen concentration (21 µM, detailed below) condition, where gas flow was provided at a rate of 1 liter min^{-1}. Polyurethane tubing and butyl rubber septa were used to minimize oxygen diffusion into the anaerobic cultures. The inlet gas entered through an inline 0.2-µm pore size filter to maintain sterility. Gaseous carbon dioxide and oxygen concentrations were measured on-line with a Gascard NG (Edinburgh Instruments, UK) and a Parox 1000 (Messtechnick Engineering, Switzerland) gas analyzer, respectively. Afterwards, a condenser connected to a cryostat set at 2ºC cooled the off-gas. All the data was acquired on a SIMATIC PCS7 distributed control system with monitoring station (Siemens, Germany).

Dissolved oxygen levels. To achieve different levels of dissolved oxygen, we sparged the cultures with different oxygen/nitrogen mixtures. For anaerobic experiments, ultrapure nitrogen (certified 99.999% N_2, INDURA, Chile) was passed through an HPIOT3-2 oxygen trap (Agilent, USA) to reduce residual oxygen levels to below 15 ppb. Other oxygen levels were achieved by sparging 1%, 5% and 21% oxygen/nitrogen mixtures (INDURA, Chile) directly into the culture, reaching 1.2 μM, 2.7 μM and 5.0 μM dissolved oxygen at steady state, respectively (Table I). For the last oxygen condition, gaseous flow with the 21% mixture was increased from 0.25 to 1-liter min^{-1}. At this point, stirring was increased from 200 to 400 rpm, reaching 21 μM dissolved oxygen at a steady state. All dissolved oxygen conditions were performed in triplicate. In all cases, steady state was reached within 5 residence times (60 h) and kept for at least 1.5 more residence times. The dissolved oxygen concentration was measured online with an InPro model 6950 probe (Mettler Toledo, USA). This probe has a detection limit of 0.03 μM.

Culture Medium. A defined medium simulating standard white grape juice was used in the bioreactor fermentations. Residual glucose concentration in the chemostat outlet was targeted to 40 g $liter^{-1}$ (Table I) to sustain glucose repression at the same level in all experiments (Tai et al. 2005; Pizarro et al. 2008). Briefly, the feed glucose concentrations were 80 g $liter^{-1}$ for the cells grown anaerobically and with 1.2 μM dissolved oxygen, and 85 g $liter^{-1}$ and 95 g $liter^{-1}$ for cells grown at 2.7 μM and 5 μM of dissolved oxygen, respectively. Fructose was not included in the formulation. The composition for other nutrients was based on the MS300 medium described by Salmon and Barre(Salmon and Barre 1998), but was modified to run continuous cultures limited in nitrogen, since MS300 was designed for batch fermentations and its use in chemostats resulted in 100 mg $liter^{-1}$ of residual nitrogen (data not shown). The modified medium,

TABLE I

Nutrient concentrations and specific rates of product formation and substrate uptake in *S. cerevisiae* EC 1118 grown under different dissolved oxygen culture conditions.

Dissolved oxygen (μM)	Steady-state measurements			Physiological parameters						
	Biomass (g/l)	Glucose (g/l)	Ethanol (g/l)	Glucose[a]	Ethanol[a]	Glycerol[a]	Succinic Acid[a]	CO_2[a]	O_2[b]	RQ[c]
0 ± 0.00	3.1 ± 0.2	42.1±1.8	20.3±2.4	-43.6 ± 5.5	27.7 ± 4.0	1.5 ± 0.6	0.06 ± 0.02	13.8 ± 1.8	NA	NA
1.2± 0.06[d]	3.7 ± 0.05[d,e]	40.5±5.4	21.1±0.5	-43.9 ± 2.6	25.2 ± 0.6	1.4±0.2	0.02 ± 0.04	12.0 ± 1.2	-0.1 ± 0.0	241
2.7± 0.28[d,e]	4.2 ± 0.1[d,e]	40.7±3.0	23.5±2.8	-37.5 ± 0.0[d]	25.4 ± 1.2	1.4±0.0	0.27 ± 0.05[d]	11.5 ± 0.2[e]	-0.7 ± 0.3	17
5.0± 0.02[d,e]	5.6 ± 0.3[d,e]	37.5±3.0	24.2±2.8	-37.4 ± 1.0[e]	18.0 ± 2.3[d,e]	1.0±0.3	0.22 ± 0.00[e]	13.3 ± 0.1[d]	-2.3 ± 0.3	6
21.0± 1.1[d,e]	5.8 ± 0.2[e]	41.7±1.4	16.2± 0.8[d,e]	-21.6 ± 0.2[d,e,]	12.3 ± 0.2[d,e]	0.4±0.0[e]	0.15 ± 0.01[d,e]	11.0 ± 0.2 [d,e]	-3.9 ± 0.1[e]	2.8

[a] Cmmol gDW^{-1} h^{-1} ; [b]mmol gDW^{-1} h^{-1}; [c] Respiratory quotient; NA:Not applicable [d] Significantly different (t-test, $p<0.05$) from the dissolved oxygen level inmediatly lower; [e] Significantly different (t-test, $p<0.05$) from the anaerobic condition

called cMS300, was different from MS300 in phosphate, sulfate and biotin contents. The cMS300 medium contained (per liter): 3 g of KH_2PO_4, 5.75 g of K_2SO_4, 500 mg of $MgSO_4*7H_2O$ and 0.05 mg of biotin, following the mineral medium used by Pizarro et al. (Pizarro et al. 2008). Other vitamins and micronutrients were the same as MS300. Yeast Assimilable Nitrogen (YAN) corresponded to 380 mg N $liter^{-1}$ for all culture conditions. However, in anaerobic conditions, YAN corresponded to 300 mg N. $liter^{-1}$, since proline is not assimilable by yeast under anaerobic growth conditions (Ingledew et al. 1987). The nitrogen sources employed were (% w/w): 18.6% ammoniacal nitrogen (NH_4Cl), 20.5%; L-proline, 16.9%; L-glutamine, 1.25%; L-arginine, 6%; L-tryptophan, 4.9%; L-alanine, 4%; L-glutamic acid, 2.6%; L-serine, 2.6%; L-threonine, 1.6%; L-leucine, 1.5%; L-aspartic acid, 1.5%; L-valine,1.3%; L-phenylalanine, 1.1%; L-isoleucine, 1.1%; L-histidine, 1.1%; L-methionine, 0.6%; L-tyrosine, 0.6%; L-glycine, 0.6%; L–lysine and L-cysteine, 0.4% (Varela et al. 2004).

All culture media were supplemented with 10 mg of ergosterol and 30 mg of oleic acid, in the form of Tween 80. The final concentration of these anaerobic factors was lower than the original MS300 formulation (15 mg $liter^{-1}$ ergosterol and 90 mg $liter^{-1}$ oleic acid) for all experiments performed, to avoid masking the effect of oxygen on the synthesis of these compounds. We determined the biomass yields of both ergosterol and oleic acid of the *S. cerevisiae* EC1118 strain in chemostats, as described in (Mateles and Battat 1974). Ergosterol and oleic acid concentration in the final culture medium were set three-fold above their biomass yields to ensure excess but being still lower than the original anaerobic factor formulation. We confirmed ergosterol and oleic acid excess by detecting these anaerobic factors in the supernatant of all cultures at steady state, *i.e.* continuous cultures were limited only in nitrogen.

Metabolite sampling and analysis. For each of the three biological replicates corresponding to the dissolved oxygen levels evaluated, steady–state culture samples were taken after at least six residence times using an ice-cold sterile 50 ml plastic syringe plugged into the sampling device of the bioreactor. The samples were rapidly transferred into an ice-cold 50 ml sterile plastic tube, where either the cell dry weight of the culture was determined (see below), or it was transferred to Eppendorf™ tubes. The latter, were centrifuged at 10.000 x g by 3 min, and 1 ml supernatant aliquots were stored at -80ºC until further analysis. Biomass was determined on a dry weight basis by filtering 10 ml culture samples through a pre-weighed 0.2 µm pore size acetate ester filters (Whatman, USA). The filter was washed twice with 10 ml milliQ water, dried in an infrared drier-equipped balance (Precisa, Switzerland) to constant weight at 65ºC.

Extracellular metabolites were determined by HPLC. 20 µl of the supernatant samples were injected in a LaChrom L-7000 HPLC system (Hitachi, Japan). Organic acids, alcohols and sugars were separated using an Aminex HPX-87H anionic exchange column (Bio-Rad, USA), with H_2SO_4 5 mM as mobile phase. A LaChrom L-7450A diode array detector (Hitachi, Japan) at 210 nm detected organic acids. LaChrom L-7490 refraction index detector (Hitachi, Japan) detected sugars and alcohols. Each compound was quantified using a calibration curve made with known concentration standards. Concentrations in the culture medium and calculated rates were statistically analyzed by a t test, to determine significance of the differences observed between the different dissolved oxygen conditions.

Residual assimilable nitrogen was followed in the cultures using the σ-phthaldehyde/N-acetyl-l-cysteine spectrophotometric assay (NOPA) procedure according to (Varela et al. 2004).

Proline was determined by HPLC as described in (Liu et al. 1998). Briefly, amino acids in the supernatant samples were derivatized with 6-aminoquinoleyl-N-hydroxysuccinimidyl carbamate. Then, the amino acids were separated in a AccQ Tag column (Waters, USA). Once separated, the derivatized amino acids were detected by fluorescence, and quantified using known standards.

Sampling and RNA isolation. For RNA isolation, samples from each one of the three biological replicates for the five oxygen conditions were extracted by rapidly placing 20 ml of culture into a Falcon^{TM}tube filled with 35 to 40 ml of crushed ice(Pizarro et al. 2008). From this tube, 1 ml of sample was transferred to a 1.5 mL Eppendorf^{TM} tube; after centrifuging at 10000 x g during 3 min, the supernatant was removed and the pellet was directly frozen in liquid nitrogen and stored at -80ºC until RNA isolation.

Before RNA isolation, all water-based reagents were DEPC-treated. RNA was extracted from frozen cell pellets using the AxyPrep Multisource RNA kit (Axygen Biosciences, USA), modified for use with glass beads for cell lysis. Briefly, we re-suspended the cell pellet in the R-I kit buffer and added it to a screw-cap tube containing 250 µl of acid-washed glass beads (500 □m diameter) (Sigma, USA). We stirred the tubes in three cycles of 45 seconds in a Mini Bead Beater^{TM} (Biospec), standing an equivalent time in ice between cycles. Later, the lysate was centrifuged at 10.000 x g, and the supernatant was transferred to a tube with 250 µl of isopropanol. After this point, we followed the kit manufacturer instructions. RNA was checked for integrity in a 1.3% agarose gel, prepared in a buffer with 20 mM MOPS, 5 mM sodium acetate and 1 mM EDTA. After heating, we added 2 % v/v formaldehyde. This was also used as the electrophoresis running buffer. RNA was quantified in a NanoDrop (Thermo Scientific, USA) and samples with absorbances of 260_{nm}:280_{nm} and 260_{nm}:230_{nm}> 1.8 were used for further processing.

Microarray Analysis. We used the Yeast Genome 2.0 chip from Affymetrix. Triplicate arrays for each one of the five oxygen level conditions were performed. RNA for hybridization was prepared according to manufacturer instructions (Affymetrix. 2010). Hybridization, stain and scanning to the microarrays were performed according to manufacturer instructions (Affymetrix. 2009). Gene expression data was imported from the CEL files into R and the quality was assessed using the tools in the *simpleaffy* package from Bioconductor (Gentleman et al. 2004). After the quality check step, data was normalized in R using robust multiarray analysis (RMA) from the *affy* package from Bioconductor(Gentleman et al. 2004). Differential expression analyses between the different conditions were carried out using the Rank Products algorithm (Breitling et al. 2004), with a cut-off of false discovery rate of 0.1. We did not establish a cut-off for the magnitude of the gene expression change when comparing two conditions. We also performed hierarchical clustering on the data, using complete linkage and Euclidian distance as a distance measure. All calculations were performed using the R statistical software (Team" 2012). The resulting lists of genes from the clusters or differential expression analyses were then submitted to the AmiGO term enrichment analysis (Carbon et al. 2009) to find out which Gene Ontology annotations and functions were overrepresented among the genes regulated by oxygen levels. Full gene annotation was then extracted from Saccharomyces Genome Database (SGD) (Christie et al. 2004). Alternatively, the GO enrichment analysis was performed using the software Blast2GO (Conesa et al. 2005). This software has integrated the Gossip package for statistical assessment, which employs the Fisher's exact test and corrects for multiple testing to find enriched GO terms between two sets of sequences (Bluthgen et al. 2005). The complete set of annotated genes for *Saccharomyces cerevisiae* from SGD was used as reference control group with a false positive discovery rate value of 0.05. The raw microarray data was

submitted to Gene Expression Omnibus (GEO, http://www.ncbi.nlm.nih.gov/geo/), where it is available under the code GSE34964.

Clustering analysis. A hierarchical clustering of gene expression levels was performed using Euclidean distance to measure differences between expression vectors and group average clustering algorithm. This clustering method was selected because exhibited the highest cophenetic correlation coefficient (CCC=0.61) as compared to single linkage (CCC=0.41), Complete Linkage (CCC=0.58) and Ward's method (CCC=0.55). The CCC values were calculated as previously described (Sokal and Rohlf 1962) A distance cut-off value of 2.26 was selected to make the partition of the clustered data into 56 groups with different gene expression patterns upon the tested conditions. The specific clustering algorithm and distance cut off value were defined after a partition-based cluster structure consistency analysis using the Silhouette measure (Pearson et al. 2004). Briefly, all the possible distance cut off values to split the clustered data into *k* different groups were tested and the Silhouette associated values to each partition measured. According to this analysis, the maximum average value of 0.304 for Silhouette measure was obtained when using the group average clustering algorithm and a distance cut off value of 2.26, thus producing 56 independent gene groups. The resulting partition was then visually inspected for consistency in the dendrogram with the associated heat maps of the clustered genes in each group. The dendrogram with the heat maps for each gene was built using the iTOL webserver (http://itol.embl.de) (31). A color-coded strip illustrating the independent gene clusters was added to the dendrogram to facilitate the mapping and analysis of individual genes (Letunic and Bork 2007).

Metabolic flux analysis. We built the stoichiometric matrix based on the model developed by Varela et al (Varela et al. 2004), which includes glycolysis, TCA cycle, fermentative and anaplerotic reactions, as well as essential anabolic pathways. We added

the following oxygen-related reactions to this matrix: proline consumption, NADH- and $FADH_2$ - dependent respiration pathways (each one lumped in one reaction) and ergosterol and unsaturated fatty acid synthesis. These reactions were extracted from YeastCyc (http://pathway.yeastgenome.org). We used the approach of Nissen et al (Nissen et al. 1997) for the biomass equation, leaving every biomass component (protein, DNA, RNA, carbohydrate and lipids) as individual products. Moreover, we separated the lipids into sterols, unsaturated and saturated fatty acids, in order to have a better description of the oxygen-dependent pathways.The resulting matrix had 47 reactions and 44 metabolites, is detailed in the Supplementary Text. The condition number of the matrix was 44, indicating that the model is numerically robust (Nielsen et al. 2003).

Flux estimation. Since the model has three degrees of the system becomes over-determined if more than three extracellular rates are measured. We evaluated inputs including all of the possible combinations of rates (from 3 to 15) selected from the following set of experimentally measured extracellular rates of substrate uptake or metabolic product production: glucose, ethanol, glycerol, succinate, acetate, CO_2, oxygen, proline, biomass components (carbohydrates, DNA, RNA, proteins) and the three classes of lipids mentioned above. The procedures for measuring biomass components are stated in the Supplementary Text. Since the resulting matrix is not square, we carried out a "pseudo-inverse" operation (Stephanopoulos et al. 1998) to solve the mass balance equation and estimate the flux vector, including the unselected rates. Evaluation of the rate combinations indicated that the more rates selected for input, the more accurate the estimations of the model. This prompted us to use 13 extracellular rates as an input, leaving ethanol and CO_2 as calculated rates. This was validated by sensitivity analysis (see below). Distribution of intracellular fluxes under different oxygen conditions was assessed by determining the flux vector for the three individual replicates for each condition, using

the 13 average rates experimentally determined (see above) under each dissolved oxygen condition as the input data. We compared resulting average fluxes through each reaction to between the different dissolved oxygen condition using a *t* test, to determine statistical significance of the observed flux differences. All calculations were performed using the R computer language (Team" 2012).

Consistency and sensitivity analysis. Data consistency was checked using the method described by Wang and Stephanopoulos (Wang and Stephanopoulos 1983). After confirming the absence of gross measurement errors, we performed a custom-sensitivity analysis, based on the normalized error distribution, which was calculated as the differences between the estimated fluxes and the fluxes calculated using modified rates (specific rates plus - minus experimental error). We then calculated the square sum of these differences, and took their square root to obtain the error value. Finally, we normalized the errors by the value of the corresponding flux calculated with the unmodified rates. The specific rates were modified by the experimental error one at a time, and the sum of the errors on all the fluxes of the stoichiometric matrix was calculated. We found that ethanol and CO_2 were the rates whose errors contributed the most to the overall flux error of the model. Therefore, we used 13 rates determined in this study as input and estimated the specific rates of ethanol and CO_2 to validate the model. We also validated the model using input rates obtained from other anaerobic and/or nitrogen-limited continuous culture experiments (Nissen et al. 1997; Tai et al. 2005; Pizarro et al. 2008), and estimated the ethanol and CO_2 production for those studies.. Overall, both estimations for our data and other studies had less than 11% error (Table II), indicating this model was a reliable predictive tool. All the preceding calculations were carried out using custom scripts in R computer language.

TABLE II

Estimation error of ethanol and CO_2 production rates, measured in our experiments and other studies, by the MFA model.

	Dissolved Oxygen (µM)								
	This study					**Nissen (1997)**	**Pizarro (2008)**	**Tai (2005)**	
% of error in estimating specific rate	0	1.2	2.7	5	21	0	0	0	5*
Ethanol	-4.27	5.64	-8.99	2.68	-11.4	2.6	11.7	8.3	10.3
CO_2	1.29	8.3	-5.58	-3.88	-8.0	0.8	-5.5	-8.7	-6.2

Results

Simulation of dissolved oxygen concentrations and oxygen uptake rates in oenological conditions. To characterize the wine yeast physiology at the different dissolved oxygen concentrations found after oxygen impulses in winemaking, we built a specific OUR vs. dissolved oxygen curve (Fig. 2). The former showed a constant increase with dissolved oxygen up to 21 μM. From this critical value on, the specific OUR was constant at 3.9 mmol (g DCW h)$^{-1}$. This empirical critical value was close to the value of a previous report for the OUR under fully aerobic, nitrogen-limited continuous cultures (3.5 mmol (g DW h)$^{-1}$) (Larsson et al. 1993). Thus, five different levels of dissolved oxygen spanning were selected to cover the complete range from anaerobic to the maximum specific OUR (Table I). These concentrations covered the entire oxygen-limited range for the yeast cells under oenological conditions (Saa et al. 2012).

Carbon balances and specific rates of substrate uptake and product formation. Accounting for all the carbon inputs and outputs to and from the culture (*i.e.* the carbon balance) is a requirement for a quantitative assessment of metabolic physiology. We measured sugar and oxygen uptake, as well as accumulation of several organic compounds. Carbon balances, calculated through the yields in glucose (in Cmol Cmol^{-1}), have less than 8% error (Table III), indicating that no major product or substrate had been left out.

Biomass significantly increased with the availability of dissolved oxygen, almost doubling its concentration at 5 μM oxygen, compared to anaerobic conditions (Table I), and having a significant increase with each level of dissolved oxygen. This also correlated with an increase in proline consumption, in line with the limitation of all other nitrogen sources (Ingledew et al. 1987). Proline consumption and biomass increase matched each other, up

to 2.7 μM dissolved oxygen, according to the biomass yield in nitrogen for this strain in anaerobic conditions ((Pizarro et al. 2008) and this work) (Table IV). This correspondence did not occur for higher dissolved oxygen concentrations, likely because the biomass yield in nitrogen under aerobic conditions is different that the calculated for anaerobic conditions. Consistent with the biomass increase, the glucose consumption volumetric rate increased with increasing dissolved oxygen levels (from 141 to 197 C-mmol glucose l^{-1} h^{-1} for 0 to 5 μM dissolved oxygen, respectively). Nevertheless, increasing the dissolved oxygen further, resulted only in a modest increase in biomass and a decrease of the glucose consumption volumetric rate (to 125 C-mmol glucose l^{-1} h^{-1}). Surprisingly, the biomass yield in glucose ($Y_{x/glc}$) increased, while ethanol and CO_2 yields in glucose decreased (Table III).

The impact of oxygen on cell physiology was more evident when analyzing specific rates (Table I). A negative correlation with dissolved oxygen was observed for glucose consumption, ethanol, and glycerol specific production rates. However, in all cases, significant ethanol production was found, consistent with the presence of the Crabtree effect. Accordingly, the respiratory quotients were all larger than 1 for all oxygenated conditions (Table I). Organic acid production was also affected by oxygen availability. For instance, acetic acid was produced only under strict anaerobiosis (0.3 C-mmol $(gDCW\ h)^{-1}$). On the other hand, a striking and significant ($p < 0.01$) increase in succinic acid production occurred between 1.2 and 2.7 μM dissolved oxygen conditions (from 0.02 to 0.27 C-mmol $(gDCW\ h)^{-1}$). This increase was unexpected as there is no known mechanism of succinic acid export in yeast, though succinic acid production has been consistently reported in previous studies (Pizarro et al. 2007; Pizarro et al. 2008).

TABLE III

Dissolved oxygen and glucose yields in different oxygen feeding conditions.

Dissolved oxygen (μM)	Ygx (C-mol Biomass/C-mol glucose)	Yggly (C-mol Glycerol/C-mol glucose)	Yge (C-mol Ethanol/C-mol glucose)	Ygc (C-mol CO2/C-mol glucose)	Carbon recovery (%)
0± 0.00	0.094 ± 0.01	0.03 ± 0.01	0.60 ± 0.02	0.32 ± 0.03	107 ± 2.6
1.2± 0.06	0.094 ± 0.005	0.03 ± 0.002	0.57 ± 0.02	0.27 ± 0.02	97 ± 3.6
2.7± 0.28	0.108 ± 0.002	0.037 ± 0.001	0.61 ± 0.08	0.29 ± 0.015	107 ± 7.2
5± 0.02	0.12 ± 0.007[a]	0.027 ± 0.008	0.55 ± 0.08[a]	0.38 ± 0.02	108 ± 10.3
21± 1.1	0.18 ± 0.01[a]	0.018 ± 0.004 [a]	0.52± 0.07[a]	0.33 ± 0.04	106 ± 5.9

[a] Significantly different (t-test $p<0.05$) from the anaerobic condition

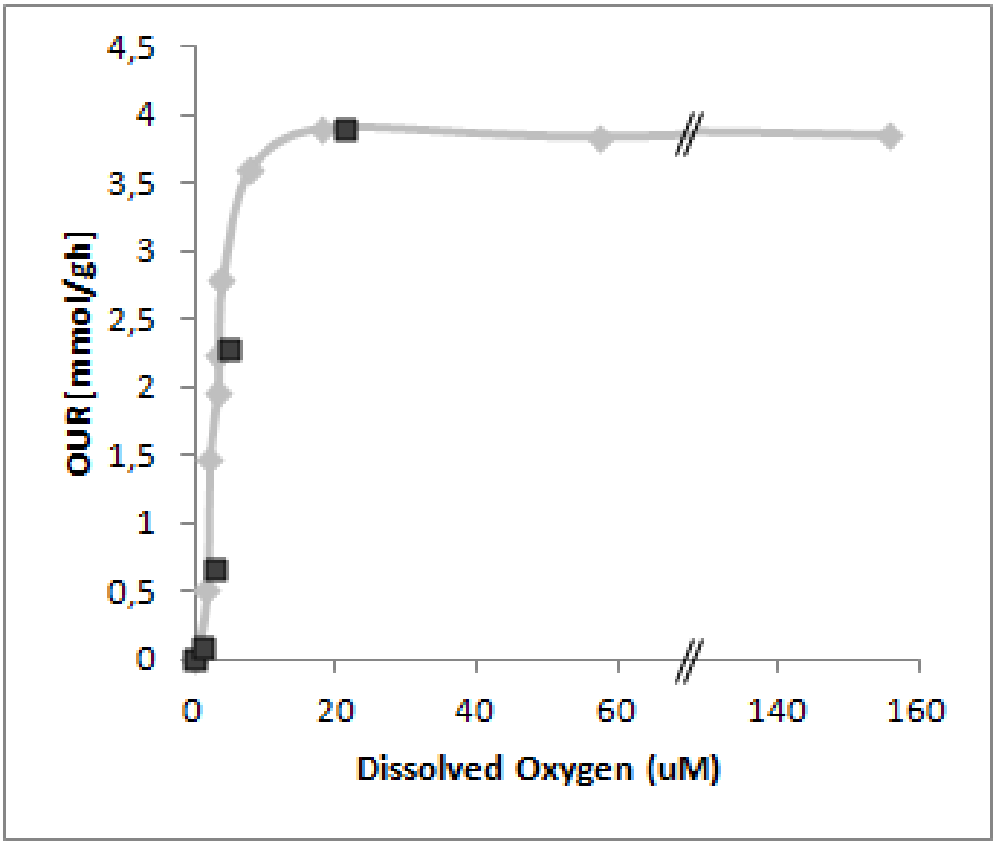

Figure 2. Relationship between specific rate of oxygen consumption (OUR) by cells of *Saccharomyces cerevisiae* strain EC1118 and dissolved oxygen concentration. Grey symbols correspond to steady-state nitrogen-limited continuous cultures with increasing dissolved oxygen concentrations. The corresponding OURs were determined in the same cultures. Black squares represent the five dissolved oxygen conditions evaluated in this research.

TABLE IV

Proline consumption and nitrogen yields.

Dissolved oxygen (μM)	Biomass (g/l)	Proline consumed (mg/l)	Nitrogen consumed in the form of proline (mg/l)	Total nitrogen consumed (mg/l)	Nitrogen necessary to get the observed biomass (mg/l) according to the anaerobic Y_{NX}[a]
0 ± 0.00	3.1 ± 0.2	0± 0.0	-	300	300
1.2± 0.06	3.7 ± 0.05	90± 1.8	21.9	321.9	308
2.7 ± 0.28	4.2 ± 0.1	239± 4.8	58.3	358.9	353
5.0 ± 0.02	5.6 ± 0.3	318± 6.3	77.4	377.4	696
21.0 ± 1.1	5.8 ± 0.2	438± 8.8	106.6	406.6	730

[a]Y_{NX} was 12.1 g biomass/ g N (experimentally calculated from anaerobic cultures)

Metabolic Flux Analyses (MFA). The redistribution of intracellular carbon fluxes in the central metabolic pathways of *Saccharomyces cerevisiae* occurring in response to increasing availability of dissolved oxygen under oenological conditions was determined using the stoichiometric model. We expressed our flux distribution as a percentage of the total carbon input to the network, which correspond to the glucose uptake rate (Fig. 3) Carbon flux towards fermentation progressively decreased, with a concomitant increase of the flux through the TCA cycle, as the dissolved oxygen content increased (Fig. 3). We confirmed that the TCA cycle under anaerobiosis was not functional and operated in two branches, as suggested previously for anaerobic, carbon-limited conditions (Nissen et al. 1997; Camarasa et al. 2003); a similar situation was observed for 1.2 μM dissolved oxygen level. However, from 2.7 μM and higher dissolved oxygen concentrations, the TCA cycle followed its canonical direction, with a large increase in carbon flux circulation through it ($p < 0.05$) (Fig 3). Another remarkable feature was the increase of the flux towards carbohydrate synthesis at 21 μM dissolved oxygen conditions, increasing more than 60% when compared with the other conditions (Fig. 3). This is supported by experimental data (Table 2).

Sources and sinks of nucleotide cofactors. MFA showed that mitochondria played an increasingly important role in NADH and ATP turnover above 2.7 μM dissolved oxygen. Fluxes through respiration and cytosol to mitochondria NADH exchange increased significantly as dissolved oxygen arises (Fig. 3). Mitochondrial NADH production and utilization significantly increased with oxygen ($p < 0.05$), rising from 25% to 60% of the total NADH production in the cell, when increasing from 2.7 to 21 μM dissolved oxygen levels, respectively. Analyses of NADH reoxidization pathways showed that ethanol production was still the dominating form for reoxidizing cytosolic NADH

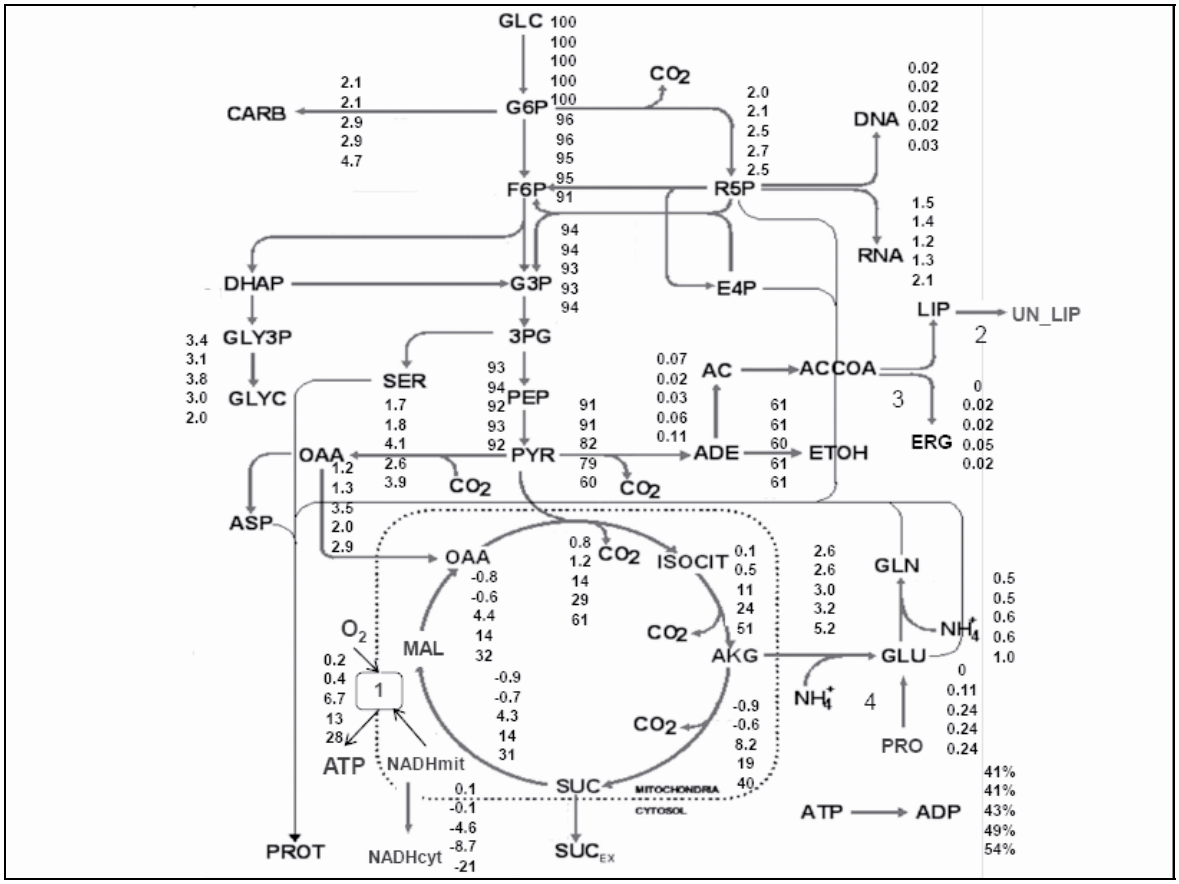

Figure 3. Flux distributions in *S. cerevisiae* EC1118 strain grown in nitrogen limited chemostats at D = 0,1 h^{-1} from anaerobic (top) to 21 µM (bottom) dissolved oxygen concentrations. Numbers indicate specific reactions related with oxygen consumption: 1) Respiration, 2) Unsaturated lipid synthesis, 3) Ergosterol synthesis, 4) Proline uptake. The fluxes are expressed as percentage of the total carbon uptake for each dissolved oxygen condition. Negative numbers indicate flux in the reverse direction. The flux for maintenance is expressed as a percentage of the total ATP produced. CARB, carbohydrates; GLC, glucose; FRUC, fructose; F6P, fructose 6-phosphate; R5P, ribose 5-phosphate; DHAP, dihydroxyacetone phosphate; G3P, glyceraldehyde 3-phosphate; E4P, erythrose 4-phosphate; GLY3P, glycerol 3-phosphate; 3PG, 3-phosphoglycerate; GLYC, glycerol; SER, serine; PEP, phosphoenolpyruvate; AC, acetate; ACCoA, acetyl coenzyme A; LIP, lipids; OAA, oxaloacetate; PYR, pyruvate; ADE, acetaldehyde; ETOH, ethanol; ASP, aspartate; ISOCIT, isocitrate; GLN, glutamine; FUM, fumarate; AKG, α-ketoglutarate; GLU, glutamic acid; PROT, protein; SUC, succinate; SUCEX, extracellular succinate; mATP, maintenance ATP; PRO, proline; $NADH_{mit}$, mitochondrial NADH; $NADH_{cyt}$, cytosolic NADH; ERG, ergosterol; UN_LIP, unsaturated lipids.

TABLE V

Biomass component production rates.

	Dissolved oxygen (μM)				
Biomass component	0	1.2	2.7	5	21
Carbohydrates	0.915 ± 0.039	0.951 ± 0.041	1.070 ± 0.048	1.020 ± 0.045	2.588 ± 0.129
DNA	0.0063 ± 0.0	0.0067 ± 0.0	0.0061 ± 0.0	0.0063 ± 0.0	0.0059 ± 0.0
Proteins	0.864 ± 0.056	0.874 ± 0.060	0.836 ± 0.054	0.877 ± 0.061	0.865 ± 0.051
RNA	0.062 ± 0.006	0.059 ± 0.005	0.044 ± 0.004	0.054 ± 0.005	0.061 ± 0.006
Ergosterol	2.13E-09 ± 0.0	0.009 ± 0.0	0.0221 ± 0.001	0.0181 ± 0.001	0.004 ± 0.0
Saturated lipids	1.15E-07 ± 0.0	1.02E-07 ± 0.0	1.56E-07 ± 0.0	1.73E-07 ± 0.0	1.73E-07 ± 0.0
Unsaturated lipid	2.20E-08 ± 0.0	2.30E-08 ± 0.0	2.60E-08 ± 0.0	2.90E-08 ± 0.0	2.90E-08 ± 0.0
Proline	0 ± 0.0	-0.108 ± 0.003	-0.244 ± 0.005	-0.242 ± 0.005	-0.322 ± 0.007

Data en C-mmol/h g dw

TABLE VI

Contribution to NADH and ATP turnover of different metabolic pathways in *S. cerevisiae* EC1118 grown under different dissolved oxygen culture conditions

Process	Dissolved Oxygen (μM)				
	0	**1.2**	**2.7**	**5**	**21**
Total NADH synthesis[a]					
Cytosolic	13.7 ± 1.7	13.8 ± 0.8	11.6 ± 0.1	11.1 ± 0.5	6.7 ± 0.5
Mitochondrial	0.12 ± 0.2	0.2 ± 0.1	3.4 ± 0.0	7.1 ± 0.2	9.5 ± 0.2
Cytosolic NADH consumed (%) for:					
Ethanol production	96.0 ± 1.7	96.0 ± 0.8	89.6 ± 0.0	85.0 ± 0.5	73.5 ± 0.5
Glycerol production	4.0 ± 0.2	4.0 ± 0.1	3.4 ± 0.0	3.0 ± 0.1	1.2 ± 0.1
Mitochondrial shuttle	0.0	0.0	7.0 ± 0.0	12.0 ± 0.0	25.3 ± 0.1
Total ATP produced[a]					
Glycolisis	27.20 ± 3.4	27.50 ± 1.6	23.10 ± 0.00	22.00 ± 0.90	13.20 ± 0.90
TCA cycle	0.0	0.0	0.61 ± 0.06	1.32 ± 0.06	1.70 ± 0.17
Oxidative phosphorylation	0.0	0.047 ± 0.05	1.45 ± 0.34	2.85 ± 0.07	3.20 ± 0.40

[a]Data in mmol gDW^{-1} h^{-1}

produced by glycolysis under all the conditions tested (Table VI). Below 2.7 μM dissolved oxygen, glycerol is the only other electron sink, albeit a minor one (~4% of NADH reoxidization). Above 2.7 μM dissolved oxygen reoxidization of cytosolic NADH through the mitochondrial redox shuttle significantly exceeds its reoxidization by glycerol synthesis (t test, $p<0.05$); moreover, glycerol synthesis showed almost no contribution at the 21 μM dissolved oxygen condition.

Oxygen also increased mitochondrial contribution to ATP production. Under anaerobic conditions, ATP was produced in glycolysis by substrate-level phosphorylation. On the other hand, ATP produced by oxidative phosphorylation had a noticeable contribution, rising from 5.7% to 21% of total ATP when dissolved oxygen increased from 2.7 μM to 21 μM, respectively. The glycolytic pathway was still the main contributor, producing more than 70% of the total ATP (Table VI). Nevertheless, the amount of ATP produced by any means is significantly reduced - decreasing by approx. 30% - at the highest dissolved oxygen level. This was also associated with an increase of the fraction of ATP used in maintenance, which increased from 43% to 54% in the 2.7 μM and 21 μM dissolved oxygen conditions, respectively.

NADPH metabolism was slightly affected by oxygen levels. The most remarkable change occurred in the aldehyde dehydrogenase reaction. NADPH production by this reaction decreased from 4% to 1% when the available oxygen increased from 0 μM to 1.2 μM dissolved oxygen. The rest of the NADPH was produced through the pentose phosphate pathway, a flux that slightly increased when comparing the anaerobic condition to the rest of the conditions. However, the flux through this pathway represents only 2% of the carbon in all conditions (See Appendix) confirming previous results reported by Varela *et al.*(Varela et al. 2004)

Gene expression analysis. To complement the metabolic flux data, global gene expression under the five dissolved oxygen conditions, was determined. As a whole, the effect of oxygen on the transcriptome was limited, since only 8.8% of the transcripts (507 genes) were affected by oxygen availability. The latter was calculated taking into account the differentially expressed genes in all possible comparisons between the different oxygen conditions. The comparison between the anaerobic and the highest dissolved oxygen conditions (21 μM) yielded 313 differentially expressed genes. This data was consistent with previous reports (Tai et al. 2005), where 371 genes were differentially expressed between anaerobic and aerobic conditions in nitrogen-limited, continuous cultures.

Analysis of oxygen level transitions. To simulate the oxygen consumption kinetics of yeast cells after an oxygen impulse during wine-making aeration operations (Moenne and Agosin Personal communication), we simulated a pseudo-dynamic setting by comparing the data of one condition with the next higher dissolved oxygen condition (Table VII). The largest effect (200 differentially expressed genes) occurred upon the onset of oxygen addition, *i.e.* between 0 and 1.2 μM dissolved oxygen. The transition between 5 and 21 μM had an equivalent impact, causing differential changes in 195 genes. Remarkably, this was the transition between oxygen-limited and oxygen-saturated conditions (Fig 2). The effect was much lower when comparing the intermediate transitions (1.2 with 2.7 μM, and 2.7 with 5 μM), affecting the expression of 25 and 19 genes, respectively.

Genes differentially expressed between 0 and 1.2 μM dissolved oxygen. These genes can be classified into two groups. The first group consisted of six genes annotated as "Siderophore transport", that participate in iron uptake. The putative increase in iron uptake could be related to the overexpression of haemoprotein-related genes, such as

TABLE VII

Characterization of the genes differentially expressed across the different oxygen levels.

Oxygen transition (gene expression effect)	Differentially expressed genes (fdr< 0.1)[a]	Enriched GO Biological Process terms (p < 0.01) [b]	Highlighted genes
0 -1.2 μM (induced)	39	Siderophore transport (10.3/0.2)[c] Amino acid transport (12.8/1.0)[c]	*FRE3* (Ferric reductase), *ENB2* (Enterobactin), *PUT4* (proline transporter),
0 -1.2 μM (repressed)	161	-	-
1.2 – 2.7 μM (induced)	11	Mitochondrial intermembrane space (27.3/0.8) [c] Inorganic anion transmembrane transporter activity (18.2/0.3)[c]	*NDE1* (External NADH dehydrogenase), *CYC1* (cytochrome c) *SUL1* (High affinity sulfate transporter), *PHO84* (Phoshapte transporter)
1.2 – 2.7 μM (repressed)	14	Cell wall (18.9/1.8)[c] sterol transport (13.5/0.9)[c]	*HPF1* (Haze-protective mannoprotein), *TIR2* (Cell wall mannoprotein), *UPC2* (Sterol regulatory element binding protein), *AUS1* (ABC-type sterol transporter)
2.7 – 5 μM (induced)	3	--	-
2.7 – 5 μM (repressed)	16	-	-

Continues in next page.

TABLE VII (cont.)

Characterization of the genes differentially expressed across the different oxygen levels.

5 – 21 µM (induced)	100	Respiratory chain (7/0.5)[c]	CYC1 (Cytochrome c, isoform 1), COX7 (Subunit VII of cytochrome c oxidase)
5 – 21 µM (repressed)	95	Iron ion homeostasis (23.2/0.9)c Transport (45.3/19.6)c	FRE3 (Ferric reductase), ENB2 (Enterobactin), PHO84 (Phosphate transporter), SUL1 (High affinity sulfate transporter,

[a]As determined by the Rank Products method

[b] As determined by the GO Term Enrichment tool at AmiGO (http://amigo.geneontolgy.org)

[c] Represents the frequency of the term among the differentially expressed genes, and in the right, the frequency among the whole transcriptome of *S. cerevisia*

cytochromes The second group comprised nine genes annotated as “aminoacid transport”, including the proline transporter *PUT4*. This highlights both the induction of respiratory genes and the impact of oxygen in regulating the nutrient uptake of yeast.

Genes differentially expressed between 1.2 and 2.7 µM dissolved oxygen. Between these conditions, key mitochondrial genes such as *CYC1* (cytochrome c) and *NDE1* (external NADH dehydrogenase,) were induced. NDE1p is responsible for the shuttling of cytosolic redox equivalents directly into the respiratory chain. *GUT2,* another gene responsible for a shuttle mechanism (Rigoulet et al. 2004) was also induced between 0 and 2.7 µM dissolved oxygen. Among repressed genes, two members of the *TIR* genes and the *HPF1* gene – all encoding cell wall mannoproteins - were found. It is worthy to note that the repression of mannoproteins could have several consequences on wine quality, modulating astringency and other organoleptic properties (Gonzalez-Ramos et al. 2008). The *AUS1* gene involved in fatty acids and sterol uptake was also repressed.

Genes differentially expressed between 5 and 21 µM dissolved oxygen. This transition consolidated the trend in induction of respiratory genes. Induced genes included more respiratory genes, such as *CYC1* and *COX7* (subunit of Complex IV), supporting the idea of active respiration, even under these high-glucose conditions. Other induced genes were stress response genes, such as *CTT1* (catalase), *HSP12* (membrane heat-shock protein) and *GRX4* (glutaredoxin) hinting to a potential oxidative stress occurring at this condition. The repressed genes at this transition included genes involved in iron metabolism, as well as those involved in sulfate and phosphate ion transport (Table VII).

Other gene expression changes. The genes annotated to the “TCA cycle” GO term showed no differential expression in the analyzed transitions. However, when comparing anaerobic and 21 µM dissolved oxygen conditions, the TCA cycle term was statistically enriched among induced genes ($p < 0.01$), including *ACO1* (aconitase)

and*CIT1* (citrate synthase). On the other hand, *FRD1* was significantly repressed when comparing anaerobic with 5 μM dissolved oxygen conditions. *FRD1* encodes a soluble fumarate reductase that is responsible for the operation of the reductive branch of the TCA cycle. This observation was in line with the redistribution of metabolic carbon fluxes observed by MFA with increasing dissolved oxygen concentrations: increase of TCA fluxes and disappearance of the anaerobic, two-branch operation of the TCA cycle.

Clustering analysis. Genes that respond to oxygen in at least one condition were classified into 56 clusters (Fig. 4), by means of hierarchical clustering. We classified the clusters according to their major tendencies with regard to the dissolved oxygen concentration. We analyzed the 12 clusters that showed at least one enriched GO term according to the GO-term enrichment analysis (Table VIII). We classified the clusters according to their general trends in relation to the dissolved oxygen concentration. We found four broad categories: Clusters with genes down-regulated at 21 μM dissolved oxygen, clusters with genes down-regulated with 1.2 μM dissolved oxygen, genes negatively and positively correlated with dissolved oxygen. We describe the genes in these clusters below.

Genes down-regulated at 21 μM dissolved oxygen. Several gene clusters show this behavior. Four clusters (2, 8, 26 and 52) related to iron metabolism are repressed under 21 μM dissolved oxygen. From these, clusters 2, 26 and 52 are induced with 1.2 μM dissolved oxygen, confirming the induction of iron uptake at low oxygen levels a trend that is reversed at high oxygen concentrations. Besides the iron metabolism genes, several genes involved in ergosterol metabolism were downregulated at high oxygen levels. This

Figure 4. Hierarchical clustering of the *S. cerevisiae*transcriptome data obtained for the five dissolved oxygen conditions. From center to outside, the dendrogram depicts: 1) Hierachical clustering tree; 2) Color ribbons indicate each of the 56 clusters; 3) Heatmaps of gene expression values, where black and green represent low and high gene expression levels, respectively. Increasing dissolved oxygen concentrations, from 0 (most internal) to 21 μM (most external), are shown. The scale of the calculated distances in the dendrogram is also illustrated.

TABLE VIII

Functional terms enrichment for the genes in each cluster

Cluster number[d]	Number of genes	Representative enriched GO terms (fdr< 0.05) [a,b]	Highlight genes[c]
2	5	Iron ion transport	*FRE2, FRE3* (Ferric and cupric reductase), *ENB2* (Enterobactin)
8	23	Iron ion homeostasis	*FRE1, FRE6* (Ferric and cupric reductase)
13	18	-	*UPC2* (sterol regulatory element binding protein)
16	13	Response to zinc ion	*EEB1* (acylCoA-ethanol O-acyltransferase)
25	60	Transcription, DNA-dependent	*DAL 81, GZF3* (nitrogen metabolism regulators)
26	3	Iron ion transport	*FET3* (ferrous ion transport)
29	16	Oxoacid metabolic process	-
32	10	Mitochondrial respiratory chain complex IV	*COX4, COX5A, COX13* (cytochrome c oxidase subunits)
37	5	DNA integration	-
43	23	1-acylglycerol-3-phosphate O-acyltransferase activity	*FRD1* (fumaratereductase), *SLC1* (1-acylglycerol-3-phosphate O-acyltransferase)
51	5	Cellular alcohol biosynthetic process	*ERG1,ERG2,ERG3* (ergosterol biosynthetic process), *OLE1* (fatty acid desaturase)
52	4	Iron ion transmembrane transport	*SIT1* (siderophoreirontransport)
53	2	Structural constituent of cell wall	*TIR1, TIR2* (cell wall mannoproteins)

[a]As determined by the Rank Products method; [b] As determined by the GO Term Enrichment tool at AmiGO (http://amigo.geneontolgy.org); [c] Annotations extracted from SGD (www.yeastgenome.org), [d] Clusters not described in the table did not show any enriched GO terms.

suggests a possible product repression, when enough oxygen is present to synthesize these compounds (Hazelwood et al. 2008).

Genes down-regulated with 1.2 µM dissolved oxygen. Several clusters show a common negative response to low levels of oxygen. Gene expression in clusters 25 and 29 drop significantly at 1.2 µM dissolved oxygen, although it increases concomitantly with oxygen concentration for the higher oxygen levels (Fig. 3). Several transcription factors belong to these clusters, most notably two positive regulators of nitrogen catabolism, such as *DAL81* and *GZF3* (Georis et al. 2009). Other genes, such as those from cluster 37, show a very low expression. This is characteristic of silenced transposable elements, which are further lowered with oxygen increase. Cluster 43 also shows this pattern. The latter includes *FRD1,* the fumarate reductase gene, confirming the two–branch TCA transition analysis, as well as *SLC1,* a key enzyme in phospholipid metabolism (Athenstaedt and Daum 1997).

Genes negatively correlated with dissolved oxygen. The family of *TIR* genes appears in both cluster 53 and the 1.2 - 2.7 µM oxygen transition, showing a dose-dependent response to oxygen (Fig 3). These results suggest that cell wall remodeling is taking place as oxygen increases, which could be also linked to the increasing ergosterol production (Table 2). Consistently, the *UPC2* transcription factor, which regulates ergosterol biosynthesis and *TIR* genes (Davies and Rine 2006), was also repressed as the oxygen level increases (Cluster 13).

Genes positively correlated with dissolved oxygen. Supporting the idea of a respiratory metabolism under these conditions, several genes related to the complex IV of the respiratory chain are induced together with dissolved oxygen, and they are grouped in cluster 32 (Fig 4).

Despite these findings, some metabolic pathways showed phenotypic changes that were not reflected on gene expression, such as acetate production. For instance, we observed that *ALD* genes, coding for aldehyde dehydrogenases responsible for acetate production (Boubekeur et al. 2001), were not affected by oxygen levels, despite acetate is only detected in anaerobic cultures.

Discussion

This research addresses the impact of different levels of dissolved oxygen on the physiology of an industrial strain of *S. cerevisiae* under oenological (*i.e.* carbon-sufficient, nitrogen-limited) conditions. We experimentally captured a subset of dissolved oxygen concentrations, aiming to represent the oxygen-limiting range of dissolved oxygen concentrations found in the discrete oenological aeration operations (Saa et al. 2012). We found that oxygen had major metabolic effects, reflected by changes in the production of several extracellular compounds and metabolic flux redistribution within the cell. For instance, ethanol and glycerol specific production rates decreased with oxygen, along with the respiratory quotient. This is an indication of a transition from fermentative to mixed respiro-fermentative metabolism. Nevertheless, the respiratory quotient values indicate that respiratory metabolism was never achieved completely. Although this has been already reported for laboratory strains under nitrogen-limited conditions (Tai et al. 2005), evidence of an active respiratory metabolism under oenological conditions is striking, since there is a general belief that respiration is under catabolic repression under these conditions (Gancedo 1998; Walker 1998; Rosenfeld and Beauvoit 2003).

Respiratory quotient showed a large decrease between 1.2 and 2.7 μM dissolved oxygen. Consistently, Metabolic Flux Analysis predicts two very different metabolic configurations depending on the concentration of dissolved oxygen: a fully fermentative

(including 0 and 1.2 μM dissolved oxygen conditions) and a mixed respiro-fermentative metabolism (from 2.7 μM and higher dissolved oxygen content). Fully fermentative conditions featured low carbon fluxes and two-branch operation of the TCA cycle; ethanol and glycerol as the only redox sinks; and glycolysis as the major source for ATP and NADH. The two-branch TCA cycle operation for anaerobic conditions was initially suggested by MFA (Nissen et al. 1997) and later proven by ^{13}C based metabolomic analysis (Camarasa et al. 2003), under carbon-limited conditions. To the best of our knowledge, this is the first report of a two-branch TCA cycle operation under carbon sufficient, nitrogen-limited conditions.

Cultures with more than 2.7 μM dissolved oxygen showed a mixed respiro-fermentative metabolism, despite the high external sugar concentration (40 g/l). It is worthy to note that the model assumes that respiration is working under these conditions. Under this assumption, the estimations of ethanol and CO_2 production were reliable (Table II), providing further support for a functional and active respiratory pathway under these culture conditions. The main features of putative mixed respiro-fermentative metabolic configuration were: significant respiratory activity; TCA cycle operation in its canonical direction; increased succinic acid production; and mitochondrial redox shuttle working as a significant cytosolic NADH sink. This effect of oxygen on yeast metabolism is mirrored by gene expression, *i.e.* induction of *COX* and *CYC1* genes (respiration), the repression of fumarate reductase gene (reductive branch of the TCA cycle) and the induction of the *NDE1* and *GUT2* genes (mitochondrial electron shuttles). Moreover, TCA genes such as *ACO1* (aconitase) and *CIT1* (citrate synthase) are induced at the highest level of oxygen tested. Altogether, the data confirm the occurrence of a respiratory metabolism. Nevertheless, ATP and NADH were still mainly produced by glycolysis, confirming that this is the major pathway regarding carbon flow operating in these conditions.

One of the hallmarks of mixed respiro-fermentative metabolism was the large increase (approx. 10 fold) of succinic acid production between 1.2 and 2.7 μM dissolved oxygen. Most likely, this resulted from the much larger flux towards the TCA cycle, as compared to the two-branch TCA cycle operation, since this was not observed above 1.2 μM dissolved oxygen. Nevertheless, how succinic acid is exported remains unclear. Several succinic acid transporters of the mitochondrial membrane are known that could account for export out of this organelle (Palmieri et al. 2000). However, no transporter for succinic acid has been identified at the plasma membrane yet. Therefore, succinic acid could be exported either by diffusion and/or active transport, though the diffusion mechanism implicates an actual production rate six fold higher than the one observed (See Supplementary Text). Preliminary experiments argued in favor of an active transport mechanism, since batch cultures of *S. cerevisiae* EC1118 with approx. 2.7 μM dissolved oxygen were able to export succinic acid, despite being supplemented with exogenous succinic acid.

The export of acetic acid also shows an interesting trend, being only present in strict anaerobic conditions. With a low dissolved oxygen level (1.2 μM), acetic acid production disappears. This correlates with decrease of the flux through the aldehyde dehydrogenase reaction, and a slight increase of flux through the pentose phosphate pathway. Therefore, it is likely that acetate production in anaerobiosis is necessary to provide NADPH to the cell, a function that is taken over by the pentose phosphate pathway when oxygen is available. In fact, both pathways are complementary and, together, they are the only source of NADPH in glucose-containing media (Grabowska and Chelstowska 2003). While the mechanism for the coordination of these two pathways is unclear, the lack of change in the expression of *ALD6* gene (encoding aldehyde dehydrogenase) in response to oxygen, suggests a non-transcriptional mechanism. Ald6p involvement in a calcium/calmodulin-dependent signaling pathway supports this hypothesis, (Butcher and Schreiber 2004).

Another feature of the mixed respiro-fermentative metabolism under the culture conditions of this study was the increase of shuttling redox equivalents from the cytoplasm to the mitochondria. MFA analysis suggested that the functioning of Adh3p shuttle is necessary to explain ethanol reduction under the 21 μM dissolved oxygen condition. However, the function of neither Nde1p nor Gut2p can be ruled out in respiro-fermentative metabolism, since replacing Adh3p with Nde1p does not change model estimations. Moreover, inclusion of the Gut2p shuttle in the MFA model yielded good estimations for all aerobic conditions (data not shown). Experimental evidence for Nde1p and Gut2p suggests that both mechanisms are active, as enzymatic activity of both was detected under aerobic, nitrogen-limited conditions (Pahlman et al. 2001). Moreover, at the oxygen metabolic threshold (between 1.2 and 2.7 μM dissolved oxygen), we found an induction of the Nde1p gene at the transcriptional level. Gut2p gene was also gradually induced by oxygen, contradicting previous studies where this gene was reported to be catabolically repressed (Rigoulet et al. 2004). Therefore, the increased mitochondrial capacity for cytosolic NADH reoxidization could be attributed to the presence of these shuttles, as well as of the Adh3p shuttle, which showed a constant, significant gene expression regardless of the oxygen level.

Despite the increase in mitochondrial shuttle activity, mitochondria showed a limited reoxidization capacity, as reflected by the large contribution of the ethanol production pathway to NADH reoxidization, even when the yeast is at its fastest OUR (Table VI). This limited capacity, and not catabolic repression, was the most likely cause of the Crabtree effect (Vemuri et al. 2007) and, overall, of the inability of *Saccharomyces cerevisiae* to develop a fully respiratory metabolism under nitrogen limitation. Whether this limitation occurs at the shuttle level or at the activity of the respiratory enzymes level, is unclear from our experiments. Nevertheless, the shuttle hypothesis is in line with recent

reports that have proposed that mitochondrial membrane surface availability is crucial in regulating the respiro-fermentative transition (Zhuang et al. 2011). Therefore, focusing on the shuttles can be a valuable and novel approach to shift yeast metabolism to a more oxidative state. This could be useful, for example, to lower ethanol production in oenological fermentation, an active area of research in metabolic engineering (see, for example, (Ehsani et al. 2009)

The hypothesis of a limited mitochondrial reoxidization as the major cause of the Crabtree effect was reinforced by gene expression analyses. We found little evidence of glucose catabolic repression of respiratory enzymes, as the *COX,* cytochromes b and c (*CYB2 and CYC1*) genes are responsive to oxygen despite high external sugar concentrations. This was also observed by Tai et al (Tai et al. 2005). Even under anaerobic conditions, expression of these genes was higher than the average (Fig 4), discarding any repressive effect from the high external glucose concentration. The data also suggest that oxygen was able to override glucose catabolic repression, as the expression of many responsive genes (such as *COX*) was positively correlated with dissolved oxygen concentrations (Fig. 4). Therefore, heme-dependent oxygen induction, through the *HAP* transcription factors (Plakunov and Shelemekh 2009), could be able to by-pass catabolic repression. However, it was not possible to detect significant changes in transcription factor activities using Network Component Analysis (Liao et al. 2003), suggesting that the mechanisms involved in this phenomenon are too elaborated to be inferred only from gene expression profiles. This regulatory landscape appears to encompass all conditions in the presence of oxygen. However, at the highest dissolved oxygen level (21 μM) a puzzling gene expression scheme occurred. Respiratory genes were induced, but those encoding for ion transporters, such as iron and copper, were repressed. This is the opposite of what occurs upon oxygen exposure, where both iron transport and respiratory genes are induced

coordinately, since iron is a requirement for building the essential hemoproteins of the respiratory chain. The situation at 21 μM could be a major physiological reconfiguration when maximal OUR capacity of yeast cells is reached (Fig 2). One component of this reconfiguration could be oxidative stress, which will also explain the iron uptake restriction, as an excess of iron generates more free radicals into the cell (Eide 1998). Furthermore, some oxidative stress marker genes are induced, such as *GRX4.* Grx4p negatively regulates the activity of Aft1p (Pujol-Carrion et al. 2006), the master transcriptional factor regulating iron metabolism. The latter provides a mechanism to explain iron transporter repression. Aft1p could also influence nitrogen metabolism (52); which is indeed the case under high oxygen conditions. For instance, *DAL81,* (regulator of allantoin utilization), a transcription factor that positively regulates the utilization of alternative nitrogen sources, shows the highest expression at anaerobic and 21 μM dissolved oxygen as well, both conditions where nitrogen is effectively unavailable. Aft1p could influence other nutrients metabolism (Shakoury-Elizeh et al. 2004), for which we also found transporter repression (Table VII).

Repression of the nutrient transporters could explain the modest biomass increase when comparing 21 μM with 5 μM dissolved oxygen condition. Also, a limited nutrient availability could play a role in establishing OUR saturation at 21 μM dissolved oxygen (Fig. 2) since nutrient limitation can impair the cell capacity to build more respiratory complexes and/or mitochondria. This is supported by the fact that the critical OUR is much higher in carbon-limited cultures (Larsson et al. 1993), indicating that the catalytic capacity of the respiratory chain can sustain a higher OUR. Therefore, the low critical OUR under nitrogen-limited culture conditions is more likely related to the total respiratory complexes available.

The evidence presented suggests some degree of both oxidative and nutritional stress, in the oxygen-saturated conditions (21 μM). Consistently, we have observed that with dissolved oxygen higher than 21 μM (Fig. 2), biomass can drop as low as 4 g l^{-1} (data not shown), suggesting that at 21 μM dissolved oxygen yeast are at the edge of its biomass producing capacities. Additionally, at this condition there is a strong increase in carbohydrate synthesis (Table 2), which is a landmark of physiological stress responses in microorganisms (Li et al. 2009). Altogether this data suggests that yeasts are possibly under multi-factorial stress under nitrogen-limited conditions at the OUR saturation regime. Increased carbohydrate synthesis also explain the simultaneous increase of biomass/glucose yield and decrease of ethanol and CO_2/glucose yields, another puzzling feature of the 21 μM dissolved oxygen condition (Table III).

The changes in dissolved oxygen concentrations also affect the cell wall. For instance, *SLC1,* encoding a key enzyme in phospholipid metabolism, is repressed at 1.2 μM dissolved oxygen. At the highest oxygen concentration, these changes can be another source of stress. For example, ergosterol and unsaturated lipid biosynthetic gene expression significantly decreased at 21 μM dissolved oxygen. In fact, the ergosterol content and synthesis rate decreased by 77% when comparing 5 and 21 μM dissolved oxygen conditions (Table 2). This ergosterol reduction could also contribute to establish a stress phenotype, as ergosterol has been regarded as a protective compound against oxidative stress (Landolfo et al. 2010). On the other hand, oxygen represses several mannoprotein-encoding genes (*TIR*) in a dose-dependent fashion This could be caused by Upc2p, an inducer of the ergosterol biosynthesis and of *TIR* genes (Davies and Rine 2006). Upc2p decreases at high dissolved oxygen level (Table VIII) by a yet unknown mechanism. Moreover, oxygen represses another cell wall-related gene, *MUC1, (*also called *FLO11*), which is critical to yeast flocculation (Govender et al. 2011).

From a winemaking perspective, metabolic flux analysis and gene expression data suggest that elevated dissolved oxygen concentrations could affect yeast performance during and after fermentation. During fermentation, reaching oxygen levels above 2.7 μM would reduce the ethanol yield (Table III); and reaching 21 μM or higher would induce a severe stress on the yeast cell, further decreasing its fermentative capacity. These oxygen levels are easily achieved in industrial winemaking practice (Moenne and Agosin Personal communication). Therefore, these results indicate that it is advisable not to keep wine yeast cells at these oxygen levels for an extended period. Furthermore, mannoprotein genes repression by oxygen could also be damaging, since their presence in wine has been linked to many beneficial effects, such as increased mouthfeel, aroma retention and astringency reduction (Gonzalez-Ramos et al. 2008). Furthermore, one of these mannoproteins (Hpf1p) is a key contributor to white wine clarification by protein haze removal (Dupin et al. 2000). Another repressed gene product, Flo1p, is crucial for flocculation, a process needed for removing yeast out of wine. Repression of these proteins could be a novel mechanism of how oxygen can affect wine quality, besides its known oxidative effect on phenolic compounds (Waterhouse and Laurie 2006).

On the contrary, low oxygen levels could be beneficial for winemaking. For instance, with 1.2 μM dissolved oxygen, ethanol production is similar to anaerobiosis, with no acetic acid production, what is beneficial since acetic acid is a common "off-flavor" in wine. Viability and stress resistance of the wine yeast might also increase, as specific ergosterol content, a protective compound against stresses in wine fermentation (Landolfo et al. 2010), increases to its maximum (see Chapter 2). Moreover, nitrogen-deficient musts can be more efficiently utilized in winemaking since the proline carrier (*PUT4*) is induced and proline assimilation effectively increased at 1.2 μM oxygen (Table

2), in turn increasing biomass synthesis. Further research will be aimed to find a tradeoff between oxygen addition and limitation under winemaking conditions.

In conclusion, we found that, under a nitrogen-limited setting, oxygen exerted a large metabolic effect on yeast mitochondria, and there is a threshold setting apart fermentative and respiro-fermentative metabolism. This is related to the expression of some key genes, such as *COX*, *NDE1* and *GUT2* and *FRD1*. Changes in these genes could explain most of the flux changes estimated in relation to respiration, cytosolic NADH shuttling to the mitochondria and two-branch cycle operation. Furthermore, gene induction casts doubts on the operation of glucose catabolic repression under nitrogen-limited conditions, since it can be overridden by oxygen. Other genes affected by oxygen were mannoprotein–encoding genes, which were repressed as part of global remodeling of the cell wall. This repression could have negative consequences in winemaking, highlighting the dual role of oxygen in "making or breaking wines."

Acknowledgments

This research was supported by FONDECYT grant #1090520 from CONICYT, Chile, to E.A., the "Doctoral thesis support" grant AT-24100170 from CONICYT, Chile, to F.F.A., and ICM (Iniciativa Científica Milenio, Chile; No. P09-016-F) to F.M. We are grateful to Lallemand, Inc. (Canada) for financial support and INDURA S.A. (Chile) for providing gas mixtures. We thank Paulina Torres, Pablo Cañón and Camila Orellana for technical support, Mr. Leonardo I. Almonacid (*Molecular Bioinformatics Laboratory, Millenium Institute on Immunology and Immunotherapy*) for bioinformatics support and GO enrichment analysis, Dra. Elena Vidal and Dr. Rodrigo A. Gutierrez (*Department of Molecular Genetics and Microbiology, Faculty of Biological Sciences, Pontificia Universidad Católica de Chile*) for use of microarray facilities and technical support.

F.F.A., M.O. and A.W.S. were supported by CONICYT and VRI-UC doctoral fellowships.

Supplemental Data

1. Supplementary Methods

Biomass component determination. Samples were treated as the samples for RNA. DNA extraction was performed using the Wizard SV Genomic DNA extraction kit (Promega, USA). Total lipids were determined gravimetrically, and saturated and unsaturated fatty acids measured by gas chromatography by an external service (ANALAB Ltda., Chile). Total carbohydrates were determined using the phenol method (Varela et al. 2004). Proteins were determined using the BCA assay (Santa Cruz Biotech, USA). RNA amount was determined from the extractions described in the main manuscript. All the determinations were normalized to the biomass dry weight of the corresponding samples. From this, we calculated the rates shown in Table 2, which were used for Metabolic Flux Analysis calculations.

Ergosterol extraction and determination. We collected 50 ml samples from the reactors. We centrifuged the cells at 5000 rpm for 5 min, discarded the supernatant, and froze the cells in liquid nitrogen. The pellet was kept at-80ºC until used. Ergosterol was extracted with ethyl ether, using a method based in those of Nylund (Nylund and Wallander 1992). Briefly, we mixed the cells with 8M KOH for saponification. A 10% of ethanol was added to improve cell disaggregation. We boiled the mixture in reflux by 3 h and then we extracted 4 times with 100 ml ethyl ether. Then, we washed the organic phase 2 times with 100 ml Milli-Q water and removed the remaining humidity by filtering in anhydrous sodium sulfate. The organic phase was then evaporated in a rotary evaporator at 60 ºC, obtaining yellow oil that was dissolved in methanol up to 5 ml. 1 ml of this extract was then used for HPLC analysis (Salmanowicz et al. 1990). A C-18 column was used with

pure methanol as mobile phase. Ergosterol appeared at 4 min in these conditions, detected at 280 nm with a diode array detector. Ergosterol concentration was determined by interpolation of a standard curve ranging between 2 and 50 mg/l. From this, we calculated the rates shown in Table 2, which were used for Metabolic Flux Analysis calculations.

2. Reactions included in the MFA model.

In the following biochemical reactions the subscripts CYT, MIT, and EX indicate cytosolic, mitochondrial, and extracellular metabolites, respectively; AICAR refers to 5_-phosphoriboxyl-5-aminoimidazole-4-carboxamide; THF refers to tetrahydrofolate.

Glycolysis

1. Glucose + 1/6 ATP →Glucose 6-phosphate + 1/6 ADP + 1/6 H^+

2. Glucose 6-phosphate ⇒Fructose 6-phosphate

3. Fructose 6-phosphate + 1/6 ATP ⇒3/6 Glyceraldehyde 3-phosphate+ 3/6 Dihydroxyacetone phosphate + 1/6 ADP + 1/6 H^+

4. Dihydroxyacetone phosphate ⇒Glyceraldehyde 3-phosphate

5 Glyceraldehyde 3-phosphate + 1/3 NAD^+_{CYT} + 1/3 ADP + 1/3P + 1/3 H_2O ⇒3-Phosphoglycerate + 1/3 ATP + 1/3 $NADH_{CYT}$ + 2/3H^+

6. 3-Phosphoglycerate ⇒Phosphoenolpyruvate + 1/3 H_2O

7. Phosphoenolpyruvate + 1/3 ADP + 1/3 H^+⇒Pyruvate + 1/3 ATP

Ethanol, glycerol, and acetate synthesis

8. Pyruvate + 1/3 H^+⇒2/3 Acetaldehyde + 1/3 CO_2

9. Acetaldehyde + 1/2 $NADH_{CYT}$ + 1/2 H^+⇒Ethanol + 1/2 NAD^+_{CYT}

10. Acetaldehyde + 1/2 $NADP^+_{CYT}$ + 1/2 H_2O ⇒Acetate + 1/2 $NADPH_{CYT}$+ H^+

11. Dihydroxyacetone phosphate + 1/3 $NADH_{CYT}$ + 1/3 H^+⇒Glycerol3-phosphate + 1/3 NAD^+_{CYT}

12. Glycerol 3-phosphate + 1/3 H^+ → Glycerol + 1/3 P

Pentose phosphate pathway

13. Glucose 6-phosphate + 2/6 $NADP^+_{CYT}$ + 1/6 H_2O → 5/6 Ribose5-phosphate + 2/6 $NADPH_{CYT}$ + 2/6 H^+ + 1/6 CO_2

14. Ribose 5-phosphate → 2/5 Erythrose 4-phosphate + 3/5 Fructose6-phosphate

15. 5/9 Ribose 5-phosphate + 4/9 Erythrose 4-phosphate → 6/9Fructose 6-phosphate + 3/9 Glyceraldehyde 3-phosphate

Tricarboxylic acid cycle

16. 3/7 Pyruvate + 4/7 $Oxaloacetate_{MIT}$ + 1/7 NAD^+_{MIT} + 1/7 H_2O → 6/7 Isocitrate + 1/7 CO_2 + 1/7 $NADH_{MIT}$ + 1/7 H^+

17. Isocitrate + 1/6 NAD^+_{MIT} → 5/6 α-Ketoglutarate + 1/6 CO_2 +1/6 $NADH_{MIT}$

18. α-Ketoglutarate + 1/5 NAD^+_{MIT} + 1/5 ADP + 1/5 P + 1/5 H_2O → 4/5 Succinate + 1/5 ATP + 1/5 CO_2 + 1/5 $NADH_{MIT}$ + 1/5 H^+

19. Succinate + 1/4 FAD → Malate +1/4 FADH2 + 1/4 H^+

20. Malate + 1/4 H_2O + 1/4 NAD^+_{MIT} → $Oxaloacetate_{MIT}$ + 1/4$NADH_{MIT}$ + 1/4 H^+

21. Acetate + 1/2 Coenzyme A + ATP + H^+ → Acetylcoenzyme A +ADP + P + 1/2 H_2O

22. Isocitrate + 1/6 $NADP^+_{MIT}$ → 5/6 α-Ketoglutarate + 1/6 CO_2+ 1/6 $NADPH_{MIT}$

Anaplerotic reaction: pyruvate carboxylase

23. 3/4 Pyruvate + 1/4 CO_2 + 1/4 ATP → $Oxaloacetate_{CYT}$ + 1/4ADP + 1/4 P + 1/4 H^+

Carbohydrate synthesis

24. Glucose 6-phosphate + 1/6 ATP → Carbohydrates + 1/6 ADP +2/6 P

Nitrogen metabolism and amino acid biosynthesis

25. α-Ketoglutarate + 1/5 NH_4^+ + 1/5 $NADPH_{CYT}$ + 1/5 H^+ → Glutamate+ 1/5 H_2O + 1/5 $NADP^+_{CYT}$

26. Glutamate + 1/5 NH_4^+ + 1/5 ATP → Glutamine + 1/5 ADP + 1/5P + 1/5 H_2O

27. 4/9 $Oxaloacetate_{CYT}$ + 5/9 Glutamate→ 4/9 Aspartate + 5/9α-Ketoglutarate

28. 3/8 3-Phosphoglycerate + 5/8 Glutamate + 1/8 NAD^{+}_{CYT}→ 3/8Serine + 5/8 α-Ketoglutarate + 3/8 P + 1/8 $NADH_{CYT}$

29. NH_4ex + ATP → NH_4 + ADP +Pi

Synthesis of DNA, RNA, proteins, and lipids

30. 5/23 Ribose 5-phosphate + 10/23 Glutamine + 3/23 Serine+ 4/23 Aspartate + 1/23 CO_2 + 6/23 ATP + 1/23 $NADP^{+}_{CYT}$→9/23AICAR + 10/23 Glutamate + 4/23 Fumarate + 1/23 $NADPH_{CYT}$ + 6/23ADP + 6/23 Pi + 5/23 H^+ + 2/23 H_2O

31. 0.4579 AICAR + 0.4371 Glutamine + 0.0842 THF + 0.3313 Aspartate+ 0.2544 Ribose 5-phosphate + 0.4625 ATP + 0.0509 $NADPH_{CYT}$ +0.1540 NAD^{+}_{CYT} + 0.3301 H_2O →DNA + 0.4371 Glutamate + 0.1278Fumarate + 0.0509 $NADP^{+}_{CYT}$ + 0.1540 $NADH_{CYT}$ + 0.5166 H^+ + 0.4625ADP + 0.4625 Pi

32. 0.5112 AICAR + 0.5271 Glutamine + 0.0568 THF + 0.2993 Aspartate+ 0.2400 Ribose 5-phosphate + 0.4890 ATP + 0.0568 $NADP^{+}_{CYT}$ +0.1348 NAD^{+}_{CYT} + 0.3427 H_2O →RNA + 0.5271 Glutamate + 0.1073Fumarate + 0.1348 $NADH_{CYT}$ + 0.0568 $NADPH_{CYT}$ + 0.7080 H^+ + 0.4890ADP + 0.4890 Pi

33. 0.0263 Ribose 5-phosphate + 0.7189 Glutamate + 0.1311 Glutamine+ 0.2319 Aspartate + 0.3944 Pyruvate + 0.0869 Serine + 0.0597Erythrose 4-phosphate + 0.0895 Phosphoenolpyruvate + 1.0084ATP + 0.0522 $NADPH_{MIT}$ + 0.0742 NAD^{+}_{MIT} + 0.0201 $NADH_{CYT}$ + 0.0883$NADPH_{CYT}$ + 0.0083 SO_4^{-2} + 0.7685 H_2O →Proteins + 0.5596α-Ketoglutarate + 0.0518 Fumarate + 0.0044 Glyceraldehyde 3-phosphate+ 0.1155 CO_2 + 0.0110 NH_4^+ + 0.0124 THF + 0.0742 $NADH_{MIT}$ + 1.0617H^+ + 0.0522 $NADP^{+}_{MIT}$ + 0.0201 NAD^{+}_{CYT} + 0.0883 $NADP^{+}_{CYT}$ + 1.0084ADP + 1.0084 Pi

34. 0.8326 Acetyl coenzyme A + 0.0662 Glyceraldehyde 3-phosphate+ 0.1012 Serine + 0.4000 ATP + 0.7111 $NADPH_{CYT}$ + 0.0259 H^+→ Lipids + 0.0258 H_2O + 0.4000 ADP + 0.4000 Pi + 0.4163 CoenzymeA + 0.7111 $NADP^+_{CYT}$

Manteinance ATP

35. ATP-> ”manteinance”

Oxaloacetate shuttle

36.$Oxaloacetate_{CYT}$ + 1/4 ATP →$Oxaloacetate_{MIT}$ + 1/4 ADP + 1/4Pi

Mitochondrial synthesis of ethanol

37. Acetaldehyde + 1/2 $NADH_{MIT}$ + 1/2 H → Ethanol + 1/2 NAD^+_{MIT}

FAD oxidation

38. $FADH_{2\ MIT}$ + 1/2O_2 +ADP +Pi → ATP + FAD^+_{MIT} 2H2O

Proline consumption

39. Proline + FAD^+ + NAD^+_{MIT}+ 2H_2O → $NADH_{MIT}$ + $FADH_2$ + Glutamate + H^+

Unsaturated lipid synthesis

40. 0.061 O_2 + Lipids + 0.12H^+→ Unsaturated lipids+ 0.12 H_2O

Squalene synthesis

41. AcetylCoA + 0.5 ATP + 0.361 NADPH +0.361H^+→ 0.833 Squalene + 0.5ADP + 0.361 $NADP^+$ + 0.167 CO_2 + CoA

Ergosterol synthesis

42.Squalene + 0.367 O_2 +0.367 NADPH + 0.1 NADH + 0.533 H^+→ 0.934 Ergosterol + 0.033 CO_2 + 0.033 formate + 0.567 H_2O

Formate incorporation

43. Formate + ATP → THF

Electron transport chain

44. $NADH_{MIT}$ + 1/2O_2 + ADP + 1/2Pi +H^+→ ATP +NAD^+_{MIT}+ H2O

3. Succinic acid transport.

The observed production rate of succinic acid (Table I) is the actual production rate only if there is no intracellular accumulation of the product, i.e, it is exported against concentration gradient. Since active succinic acid transporters in yeast are unknown, we evaluated a diffusion mechanism. In the first case, the diffusion is governed by the intracellular and extracellular pH. Since the pK_a1 of succinic acid is 4.21, assuming an intracellular pH of 5 (Walker 1998) and extracellular pH of 3.5, most of the succinic acid should be in an anionic, monocarboxylic form that is unable to cross the membrane. This arises from the following calculations, using the equation for diffusion of weak acids in (Nielsen et al. 2003).

$$\frac{C_{intracelular}}{C_{extracellular}} = \frac{1 + 10^{pH - pKa}}{1 + 10^{pH - pKa}}$$

Replacing the values for compartment pH and pKa, we obtain that the ratio intracellular/extracellular concentration is 6 at this pH conditions. Therefore, to achieve a production rate of succinic acid of 0.24 C-mmol/ gDW h, (the rate in the 4 µM condition), which corresponds to an extracellular concentration of 2.54 mM, the cell should to accumulate 15.24 mM of intracellular succinic acid. This would correspond to an actual production rate of 1.44 C-mmol/ gDW h of succinic acid, six-fold higher than the observed production rate.

To differentiate between active transport and passive diffusion, we carried out batch cultures of in presence of (0.2 g/l) exogenous succinic acid, with should inhibit diffusion but not active transport. These cultures were performed in 250 ml flasks filled with cMS300 medium up to 225 ml. They were inoculated and incubated in an orbital shaker at 150 RPM at 20ºC. These cultures had aprox. 2.7 uM dissolved oxygen.. We found that

succinic acid is produced at roughly the same rate (0.11 C-mol /h) despite the exogenous succinic acid, giving evidence of active transport. Although there is no known transporter for succinic acid, we tested the Pdr12p transporter. This is an ATP-dependent transporter of the ABC family that is known to transport monocarboxylic acids and it is induced by succinic acid (Hatzixanthis et al. 2003). We evaluated batch cultures of a *PDR12* null mutant in a BY4743 strain background; however, it produced succinic acid in the same amount as the control with 2.7 μM dissolved oxygen. Despite this setback, we can conclude that a so far unknown transporter should actively export succinic acid.

Chapter 2

Draft paper (to be submitted to *Applied and Environmental Microbiology* or *Journal of Biotechnology*)

The respiratory chain is the main contributor to oxygen consumption by *Saccharomyces cerevisiae* EC1118 in wine fermentation conditions.

Felipe F. Aceituno, Marcelo Orellana, Pablo Cañón & Eduardo Agosín*.

Department of Chemical and Bioprocess Engineering, School of Engineering, Av. Vicuña Mackenna 4860, Macul, Santiago, Chile[1]

*Corresponding author

Abstract

The fate of the oxygen added by pump-overs and other processes during oenological fermentation at an industrial scale has not been clearly established. While there have been attempts to quantify oxygen consumption pathways in yeast in oenological conditions, results have been contradictory on the contribution of respiration to this consumption. To shed light on the issue, we integrated transcriptome and metabolome data in a genome-scale metabolic model of *Saccharomyces cerevisiae* framework, to answer the question of oxygen fate during winemaking. We carried out Flux Balance Analysis (FBA) to estimate the metabolic flux through each oxygen-utilizing pathway in yeast. The model predicts that respiration has the largest contribution to oxygen consumption at any dissolved oxygen condition (1.2, 2.7 or 5 μM) in the oxygen-limiting range in oenological conditions. To confirm this findings, we experimentally measured proline uptake and ergosterol and unsaturated fatty acids synthesis. From this data we calculated that the contribution of the synthesis of these lipids to oxygen consumption is always less than the contribution of proline assimilation, which in turn depends on a functional electron transport chain to occur. Therefore, theoretical and experimental data points to respiration as the main biological oxygen sink during winemaking.

Introduction

Alcoholic fermentation is a complex and dynamic process where sugars are transformed into ethanol by yeast fermentative activity. In industrial oenological fermentations, oxygen pulses are periodically added to improve yeast fermentative rate, viability and biomass (Sablayrolles et al. 2000). The fate of the oxygen added has been debated and investigated in several studies. For instance, Fornairon-Bonnefond et al. (Fornairon-Bonnefond et al. 2002) showed an increase of the sterol biosynthesis with oxygen, but not enough to explain total oxygen consumption. Rosenfeld et al. (Rosenfeld et al. 2003) determined that anaerobically grown *S. cerevisiae* could readily consume oxygen and that 25% of the oxygen consumption was dependent on the ergosterol synthesis pathway. Although the 75% of the consumed oxygen was unaccounted for, cyanide inhibition of oxygen consumption raised the possibility of respiratory oxygen consumption. Supporting this hypothesis, David and Poyton (David and Poyton 2005) reported that yeast cells have a functional respiratory chain under anoxic conditions. Other potential oxygen-utilizing pathways, such as heme and unsaturated lipid synthesis, showed a limited contribution to the overall oxygen balance (Fornairon-Bonnefond et al. 2002; Rosenfeld et al. 2003). Nevertheless, the amount of oxygen unaccounted for raises the possibility that a unexpected or so far unknown pathway is actually consuming oxygen.

Another pathway that could be involved in oxygen consumption is proline assimilation (Ingledew et al. 1987). Proline is one of the main nitrogen sources of grape musts (20% of total N) (Salmon and Barre 1998). However, this amino acid is not assimilable under anoxic conditions, since its assimilation depends on the FAD-dependent proline oxidase enzyme, Put1p. Put1p is a mitochondrial membrane enzyme that directly couples proline turnover with ubiquinone oxidation and FAD reduction, likewise succinate dehydrogenase (Wanduragala et al. 2010). Membrane-bound mitochondrial FAD, which is

the only form of FAD that can be used by Put1p, is only generated by $FADH_2$ reoxidation with oxygen through the respiratory chain(Ingledew et al. 1987).

Despite the previous knowledge on oxygen consumption pathways, it has proven difficult to achieve a sound, quantitative estimation that could account for all the oxygen consumed by yeast. Genome-scale metabolic modeling is suitable for this purpose as it includes most metabolically important pathways in terms of mass quantity for which there is some evidence in yeast (Dobson et al. 2010). By using the Flux Balance Analysis approach (FBA), it is possible to simulate through linear optimization the fluxes through the whole yeast metabolic network. The latter results, for example, in a prediction of the mass flux through all oxygen consumption pathways present in the model. Besides the unbiased coverage of the metabolic network, metabolic models have also the advantage to be amenable to integrate with transcriptomic data. Several methods, such as GIMME (Becker and Palsson 2008) and others, allow to exclude from the model those genes – hence, reactions- that are scarcely expressed, incorporating the regulatory dimension and yielding more optimal estimations.

To be able to integrate genome scale metabolic modeling and transcriptomic tools, a suitable experimental setting is needed to obtain reliable and reproducible information. We took advantage of an already operating system that simulates winemaking conditions at different oxygen levels (Aceituno et al. 2012). Unlike previous studies, this system is based in continuous cultures, which allow a greater degree of reproducibility while simulating the growth phase and medium of a late exponential phase, the phase of wine fermentation where oxygen additions have maximal effects (Sablayrolles et al. 2000). The reliability of chemostat systems allowed us to generate transcriptomic and exo-metabolomic data of good quality to feed the metabolic model and achieve optimal estimations.

In this study, we perform the first genome-wide assessment of oxygen consumption in oenological conditions, and provide theoretical and experimental evidence on the role of respiration, either classical or coupled to proline consumption, as the main contributor to oxygen consumption by yeast during winemaking.

Materials & Methods

Yeast strain and culture conditions. *Saccharomyces cerevisiae* EC1118 (Lalvin, Switzerland), an industrial strain used worldwide by the wine industry, was employed throughout this study. Initial seed cultures were grown in 50 mL YPD broth at 28ºC under aerobic conditions to a mid – logarithmic growth phase. For continuous cultivation, a custom-modified MS300 medium was employed as described elsewhere (Aceituno et al. 2012). We used this medium in a 2.0 liter BIOSTAT B bioreactor (Sartorius Biotech, Germany) with a working volume of 1.5 liter, was inoculated with enough volume of the microbial broth to obtain an initial cell density of 10^6 cells ml^{-1}. The culture was allowed to grow in batch mode until reaching early-to-mid exponential growth. Constant feeding was then initiated with a defined artificial must that limited growth by nitrogen, with a constant residual carbon concentration (see below). The dilution rate (D) was set at $D = 0.1\ h^{-1}$. Agitation, temperature and pH were maintained at 200 rpm, 20ºC and 3.5 respectively, to simulate white wine fermentation. All experiments were performed in triplicate.

Gases were provided by means of an Aalborg GFC Mass Flow Controller (Aalborg, USA), at a rate of 0.25 liter min^{-1} in all experiments. Polyurethane tubing and butyl rubber septa were used to minimize oxygen diffusion into the anaerobic cultures. The inlet gas entered through an inline 0.2 μm pore size filter to maintain sterility. Gaseous carbon dioxide and oxygen concentrations were measured on-line with a

GascardNG (Edinburgh Instruments, UK) and a Parox 1000 (Messtechnick Engineering, Switzerland) gas analyzer, respectively. Afterwards, a condenser connected to a cryostat set at 2ºC cooled the off-gas. All the data was acquired on a SIMATIC PCS7 distributed control system with monitoring station (Siemens, Germany).

Dissolved oxygen levels. To achieve different levels of dissolved oxygen, we sparged the cultures with different oxygen/nitrogen mixtures. For anaerobic experiments, ultrapure nitrogen (certified 99.999% N_2, INDURA, Chile) was passed through an HPIOT3-2 oxygen trap (Agilent, USA) to reduce residual oxygen levels to below 15 ppb. Other oxygen levels were achieved by sparging 1%, 5% and 21% oxygen/nitrogen mixtures (INDURA, Chile) directly into the culture, reaching 1.2 μM, 2.7 μM and 5.0 μM dissolved oxygen at steady state, respectively (Table I). In all cases, steady state was reached within 5 residence times (60 h) and kept for at least 1.5 more residence times. The dissolved oxygen concentration was measured online with an InPro model 6950 probe (Mettler Toledo, USA). This probe has a detection limit of 0.03 μM.

Sampling. The continuous cultures were sampled using a sterile 50 ml plastic syringe plugged into the sampling device of the bioreactor. This sample was rapidly transferred into a 50-ml sterile plastic tube, from which the culture was taken from dry weight determination, or was transferred to eppendorf tubes of 2 or 1,5 ml. Then, they were centrifuged at 10.000 x g by 3 min, and 1 ml supernatant aliquots were transferred to clean tubes and stored at -80ºC until analysis Alternatively, the sample was centrifuged at 4000 x g during 5 min, supernatant was removed, and the pellet directly frozen in liquid nitrogen and stored at -80ºC for further processing.

Dry weight determination. We determined dry weight by filtering 10 ml culture samples through 0,2 uM acetate ester filters (Whatman. The filters were dried and weighted before use. After filtering the sample, the filter was washed twice with 10 ml

miliQ water, and then removed and dried in a Precisa 220M balance equipped with a Precisa HA 300 infrared drying module balance up to constant weight. The yeast dry weight was then calculated by subtracting this value to the weight of the filter prior to the filtering, and multiplied by 100 to obtain the culture biomass content in g/l.

Proline determination. Proline in the culture supernatant was determined by HPLC performed after derivatization of aminoacids with 6-aminoquinoleyl-N-hydroxysuccinimidyl carbamate to detect it by fluorescence. This analysis was subcontracted (IADET Ltda., Chile)

Biomass component determination. Samples were treated as the samples for RNA. DNA extraction was performed using the Wizard SV Genomic DNA extraction kit (Promega, USA). Total lipids were determined gravimetrically following acid hydrolysis, and saturated and unsaturated fatty acids measured by gas chromatography by an external service (ANALAB Ltda., Chile). Total carbohydrates were determined using the phenol method (Schulze et al. 1996). Proteins were determined using the BCA assay (Santa Cruz Biotech, USA). RNA amount was determined from the extractions described above. All the determinations were normalized to the biomass dry weight of the corresponding samples.

Ergosterol extraction and determination. We collected 50 ml samples from the reactors. We centrifuged the cells at 5000 rpm for 5 min, discarded the supernatant, and froze the cells in liquid nitrogen. The pellet was kept at-80ºC until used. Ergosterol was extracted with ethyl ether, using a method based in those of Nylund (Nylund and Wallander 1992). Briefly, we mixed the cells with 8M KOH for saponification. A 10% of ethanol was added to improve cell disaggregation. We boiled the mixture in reflux by 3 h and then we extracted 4 times with 100 ml ethyl ether. Then, we washed the organic phase 2 times with 100 ml Milli-Q water and removed the remaining humidity by filtering in

anhydrous sodium sulfate. The organic phase was then evaporated in a rotary evaporator at 60 ºC, obtaining yellow oil that was dissolved in methanol up to 5 ml. 1 ml of this extract was then used for HPLC analysis (Salmanowicz et al. 1990).A C-18 column was used with pure methanol as mobile phase. Ergosterol appeared at 4 min in these conditions, detected at 280 nm with a diode array detector. Ergosterol concentration was determined by interpolation of a standard curve ranging between 2 and 50 mg/l.

Oxygen balance calculations. In order to determinate the contribution of proline assimilation and ergosterol and unsaturated fatty acids synthesis to the oxygen consumption, we calculated the uptake and synthesis rates of each compounds as follows: For proline, we determined the proline concentration difference between the unused media and the culture media,. For ergosterol, we determined the content of ergosterol of a cell sample, and then we scaled it to the whole culture. Finally, for unsaturated fatty acids, we measured the relative content of the different fatty acids in the biomass, and the total fat content of the culture samples to obtain absolute values. We normalized all these data by biomass dry weight of the corresponding culture and its dilution rate. The calculated specific rate was multiplied by the stoichiometric coefficient of oxygen in each relevant reaction, and normalized by the total oxygen uptake rate determined en each condition, in order to determine the contribution of the pathway to the oxygen consumption. For proline, as it uses one equivalent of FAD, and one of NAD, therefore, the equivalents of oxygen used for proline assimilation equals 1, using the stoichiometry of NADH- and $FADH_2$ respiration reactions. For ergosterol, it was calculated to be 12. This coefficient was obtained for the conversion from squalene to ergosterol, since it has been reported that anaerobically-grown yeast cells, in oenological conditions accumulate squalene (Valero et al. 2001). For unsaturated fatty acids, we determined the coefficient ranged between 1.4 and 1.8. This was calculated by averaging the oxygen needed to synthesize different

unsaturated fatty acids experimentally found for the different dissolved oxygen conditions in yeast. The equations were formulated from the metabolic information obtained from MetaCyc (Caspi et al. 2008) for an Metabolic Flux Analysis model for the different dissolved oxygen conditions as reported elsewhere (Aceituno et al. 2012)

Flux Balance Analysis at genomic scale. In order to quantify the overall metabolic pathways contribution to oxygen and to enable integration with transcriptomic data, we aimed to use a metabolic model that covers the entire metabolic network of yeast. The latest version of such a model is the so called "YEAST 4.0" (Dobson et al. 2010) that has 1865 reactions and 1319 metabolites including 75 oxygen-consuming reactions in the different cell compartments. In this case, since there are much more reactions than metabolites, is not possible to obtain a unique solution to the mass-balanced equations (Stephanopoulos et al. 1998). So, we use the strategy of constraint-based model, that seek to optimize a function, subject to certain restrictions, in order to define a solution space that is explored by linear programming to find an optimum flux distribution that is compliant with the restrictions. In our case, we restricted using 8 extracellular rates (glucose, oxygen, ethanol, CO_2, glycerol and acetic acid, succinic acid and proline) and defined biomass production as the optimization objective. We used these constraints as they were all the measurements available that were able to constrain this model. All this was done using the COBRA toolbox (Becker et al. 2007) in MATLAB^{TM} (Mathworks, USA).

Integration of gene expression and flux balance analysis. In order to add constraints to our genome-scale flux balance analysis approach, we sought to integrate the previously obtained gene expression data for these conditions (Aceituno et al. 2012). To this aim, we used the GIMME approach (Becker and Palsson 2008) as implemented in the COBRA toolbox (Schellenberger et al. 2011). This approach consists in eliminating from

the model those reactions that correspond to genes expressed under a certain threshold. If there is no solution for the trimmed model with the eight restrictions (see previous section), the algorithm seeks to re-incorporate the minimum number of reactions, resulting in a functional model that can attain a 90% of the objective function, *i.e.* a 90% of the biomass production. This was performed for each of the four oxygen conditions, setting the threshold at the first quartile of the gene expression distribution. This yielded four flux distributions that were a closer representation of the intracellular fluxes that accounted for the reactions that were actually expressed.

RNA extraction. For RNA extraction, frozen cell pellets were used. RNA was extracted using the AxyPrep Multisource RNA kit (Axygen Biosciences, USA), modified for the use with glass beads for cell lysis. Briefly, we used the lysis buffer to resuspend the cell pellet, added to 250 ul of 500 uM acid-washed glass beads and stirred in three cycles of 45 seg in a Mini-BeadBeater standing an equivalent time in ice between cycles. Later, the lysate was centrifuged at 10.000 x g and supernatant was transferred to a tube with 250ul of isopropanol. After this point, we followed the kit manufacturer instructions.

RNA visualization and quantification. RNA was visualized by electrophoresis in a MOPS/formaldehyde gel. The gel was prepared with 1.3 % w/v agarose, in a buffer with MOPS solution 1X (MOPs buffer winkler) and 10% v/v formaldehyde. This was also the composition of the running buffer for this electrophoresis. RNA was quantified in a NanoDrop (Thermo Scientfic, USA) and those with Absorbance 260_{nm}:280_{nm} and 260_{nm}:230_{nm}> 1.8 were used for further processing

RT-PCR. 1 μg of extracted RNA was treated with DNAse I (Invitrogen, USA). This was used for reverse transcription with the SuperScript III kit (Invitrogen, USA), all according to manufacturer instructions. Gene expression was assessed semi-quantitatively by amplifying both the *COX4* and the *ACT1* (actin) gene as a normalizing control, from the

same sample. Primer sequences were, for *COX4;* Left: 5'-ATTTTTCAAGCCAGCCACAA-3', Right: 5'-TGATGGTGGTCATCATTTGG-3'. For *ACT1;* Left: 5'-TGTCACCAACTGGGACGATA-3', Right: 5'-CGGTGATTTCCTTTTGCATT-3'. The products have a size of 438 bp and 731 bp, respectively. The products were then analyzed by electrophoresis in 1% agarose gel, stained with SybrGreen (Invitrogen, CA) and photographed using the PhotoDocIt system (UVP, USA). The quantification of expression was determined by quantifying the pixels in the bands with the ImageJ software. The expression of *COX4* was determined as the ratio of intensity between the *COX4* band and the *ACT1* band.

Results

Experimental setting. This study aims to determine the relative contribution of different metabolic pathways for oxygen consumption under oenological conditions. To this aim, we worked in culture conditions prevailing at the end of exponential phase of oenological fermentation, where the impact of oxygen additions is the most significant (Sablayrolles et al. 2000). In these conditions, we achieved four different dissolved oxygen levels, representative of what is commonly found during winemaking. Importantly, we concentrated in the limiting oxygen uptake rate range (0, 1.2. 2.7 and 5 μM) (Larsson et al. 1993; Aceituno et al. 2012) where all oxygen

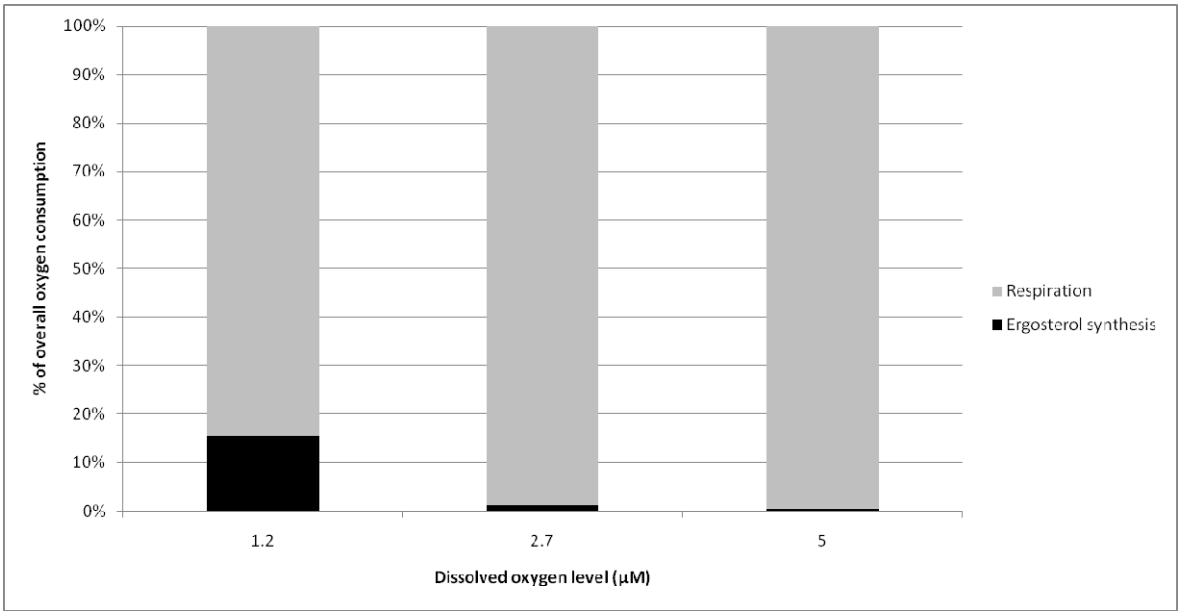

Figure 5. Contribution of different metabolic pathways to oxygen consumption as predicted by the Yeast 4.0 model after constraining with gene expression data. Only ergosterol synthesis and respiration contributed significantly to oxygen consumption; the other pathways that had reactions that consume oxygen either were unexpressed or had very low flux values

provided is consumed, to minimize the occurrence of radical oxygen species that are generated in the oxygen-saturating range (Aceituno et al. 2012), that can confound oxygen consumption results.

Flux balance analysis at the genome scale. The flux distributions obtained after integrating flux balance analyses and gene expression data by the GIMME algorithm clearly indicated that respiratory oxygen consumption was predominant at all oxygen levels. This was an 84% of the oxygen consumed with 1.2 μM dissolved oxygen, and 99% of the oxygen consumed at higher dissolved oxygen conditions. On the other hand, non-respiratory consumption pathways are important only at the lowest dissolved oxygen level (1.2 μM). At this condition, the reactions involved in the ergosterol biosynthetic pathway consumed approx 15% of the total oxygen, as previously reported(Fornairon-Bonnefond et al. 2002).For higher oxygen levels (2.7 and 5 μM dissolved oxygen), the model predicted that the contribution of this pathway to the overall oxygen consumption was lower than 1% (Fig 5). It is worthy to note that unrecognized or novel pathways were not found to have significant contribution to oxygen consumption.

Experimental assesment of oxygen consumption pathways. Experimental confirmation of *in silico* results was carried out by determining proline consumption, as well as ergosterol and unsaturated fatty acid synthesis in the continuous cultures described above. These rates are all null when no oxygen is available, as determined experimentally (data not shown), although the cells in anaerobic conditions contain ergosterol and unsaturated fatty acids since they were exogenously provided in the medium. Proline uptake rate increases from 2.2 to 4.9 μm gDW^{-1} h^{-1} when comparing 1.2 to 2.7 μM dissolved oxygen conditions. Then, it reached a plateau at 5 μM dissolved oxygen. However, this is not the upper limit of proline uptake capacity of yeast adding more

oxygen would result in a higher proline uptake rate (Aceituno et al. 2012). Ergosterol synthesis rate have a somewhat similar pattern, rising from 1.2 μM oxygen but even decreasing at 5 μM oxygen. However, the specific ergosterol content of yeast cells is roughly the same regardless the level of oxygen (~3.23 mg/gDW). This content only increases (to 0.61 mg/gDW) when oxygen goes up to 21 μM, to the saturated oxygen uptake zone (Aceituno et al. 2012). Unsaturated fatty acid synthesis was lower at 2.7 μM dissolved oxygen, and higher at 5 μM oxygen. The total fraction of unsaturated and poly-unsaturated fatty acids was 36.4, 34.6 and 47.6% of the total lipids in the 1.2, 2.7 and 5 μM dissolved oxygen conditions, which resulted in the synthesis rates showed in Table IX.

From this experimental data, we calculated that proline assimilation explained approx. the 43% of oxygen consumption at 1.2 μM dissolved oxygen, decreasing to 7.2% and 0.2% of the oxygen consumed with 2.7 and 5 μM dissolved oxygen, respectively. Regarding the ergosterol pathway, it explained a lesser fraction of the oxygen consumption (8% oxygen consumption at 1.2 μM dissolved oxygen), and even much lesser for the more aerobic conditions (1.4% and 0.3% of the overall oxygen consumption for 2.7 and 5 μM dissolved oxygen, respectively). It is worthy to note that the experimental values of

TABLE IX

Inlet gas (% oxygen)	Dissolved oxygen (µM)	Total rO_2[a]	Proline uptake rate[a]	$rO_{2\text{-}pro.}$(%)[b]	Ergosterol synthesis rate[a]	$rO_{2\text{-}erg.}$(%)	Unsaturated lipid synthesis rate[a]	$rO_{2\text{-}uns}$ (%)	Total rO_2 explained (%)
1	1.2 ± 0,06	50	2.17	21.7 (43.4)	0.33	4.0 (8.0)	9.8	14.9 (30)	81
5	2.7 ± 0,28	670	4.88	48.8 (7.3)	0.79	9.4 (1.4)	7.9	14.6 (2.2)	10.9
20	5.0 ± 0,02	2280	4.85	48.5 (0.2)	0.65	7.6 (0.3)	11.9	20 (0.5)	1

Oxygen balance obtained from experimental measurement of oxygen consumption pathways.

[a] µmol *g dry weight^{-1} h^{-1}. Data are the average of duplicate measurements. Standard deviation is less than 10% in all cases.
[b]Oxygen consumption rate corresponding to the pathway. In parenthesis is the percentage of the total consumption explained by the pathway

fluxes through the ergosterol pathway roughly agreed with FBA predictions (Fig 5 and Table IX). Synthesis of unsaturated lipids contributed significantly, explaining 30% of the overall oxygen consumption at 1.2 μM dissolved oxygen. Under aerobic conditions, the contribution of unsaturated lipids to the overall oxygen consumption was much lower and comparable to the oxygen consumed for ergosterol synthesis (2.2% and 0.5% overall consumption of oxygen). In both cases, the results did not agree with the model, which predicted no flux in the reactions of unsaturated fatty acid synthesis. As these compounds were detected in the biomass, this discrepancy suggests there are still improvements needed in the model. Indeed, lipid metabolism has been the subject of several revisions in yeast metabolic reconstruction (Nookaew et al. 2008).

Respiration contribution to oxygen consumption and glucose catabolic repression. The prediction of oxygen consumption by respiration, supported by the proline consumption data, is a striking one since respiratory enzymes are thought to be under glucose repression at high-sugar concentrations (>40 g/l in our study) (Gancedo 1998). However, microarray analysis (Aceituno et al. 2012) showed that respiratory genes were indeed induced in response to oxygen in our conditions, having a more than average expression level even in anaerobiosis (Tai et al. 2005; Aceituno et al. 2012) (Table X). This was confirmed by RT-PCR analysis for the gene *COX4*, a key subunit of cytochrome c oxidase (Fig 6). *COX4* was induced by oxygen both in steady-state oxygen conditions and in response to a discrete oxygen addition (Orellana et al. 2013). Concordantly, it has been reported that yeast mitochondria can respire in wine fermentation medium (Rosenfeld et al. 2002) when exposed to constant levels of oxygen. Therefore, it seems clear that glucose repression did affect neither respiratory genes nor metabolic fluxes.

TABLE X.
Gene expression of key respiratory genes according to Affymetrix microarray data (Aceituno et al. 2012).

			Dissolved oxygen concentration			
Gene code	Gene name	Function	0	1.2	2.7	5
YGL187C	COX4	Complex IV subunit	8.69	9.43	9.85	10.12
YNL052W	COX5A	Complex IV subunit	8.60	9.19	9.95	10.30
YJR048W	CYC1	Cytochrome c	6.55	5.49	7.09	8.67
YOR065W	CYT1	Complex III catalytic subunit	7.51	7.13	7.33	8.27
		Average gene expression of the whole transcriptome	6.69	6.40	6.50	6.66

Data is deposited at Gene Expression Ominbus under the number GSE34964.

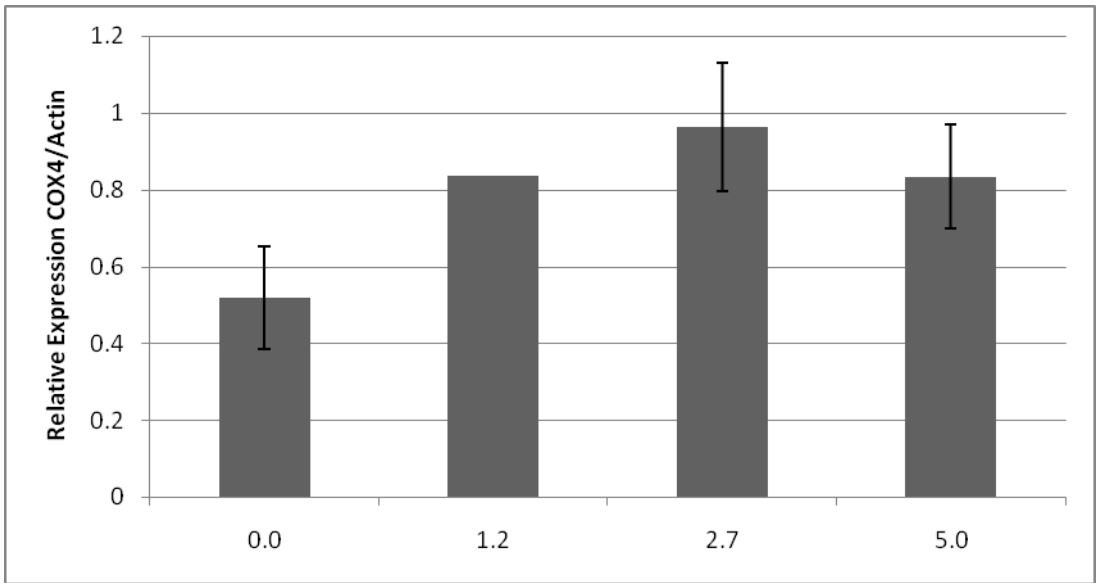

Figure 6. Relative expression of the *COX4* gene under different dissolved oxygen conditions as determined by conventional RT-PCR. Bars represent relative band intensity with respect to the actin (*ACT1)* gene. Standard deviation is shown.

Discussion

This work intended to assess the relative contribution of yeast metabolic pathways to oxygen consumption occurring under oenological conditions. We set up a continuous culture system able to seize the physiological state of aerated yeast cells during winemaking, such as occurring in pump-overs. We were able to control and monitor oxygen in both the liquid and gaseous phases. This experimental set up allowed to precisely determining the oxygen uptake rates, by balancing oxygen inputs and outputs. With this parameter confidently estimated, we could quantify the amount of oxygen consumed through each known pathway involved in oxygen consumption, both by metabolic modeling and by experimental mass balancing.

Fluxes distribution through the genome-scale metabolic network did not predict the necessity of any novel pathway to account for all the oxygen consumed during the fermentation. Therefore, the most relevant known oxygen-consuming pathways were experimentally measured to confirm model predictions. The most relevant prediction, confirmed by experimental data, is that non-respiratory pathways have a relatively small contribution to the overall oxygen consumption, while respiratory pathways have the largest contribution. For example, at 1.2 µM dissolved oxygen, where the experimental oxygen balance is closest to 100%, the major contributor is proline consumption, accounting for 43% of the oxygen consumed. Proline assimilation can be considered as a respiratory pathway, since the key enzyme of this pathway, proline oxidase (Put1p), has an absolute need of a functional respiratory chain to function (Wanduragala et al. 2010). Therefore, this 43% of oxygen is actually consumed by the respiratory chain. While the model predicts larger respiratory oxygen consumption in these conditions, the caveats of the model regarding unsaturated lipid metabolism could account for this difference. In

fact, non respiratory pathways such as unsaturated lipids and ergosterol biosynthesis accounted for the ~38% of the oxygen consumed according to experimental data

Under more aerobic conditions, experimental data indicated that proline consumption, ergosterol and unsaturated lipids biosyntheses were able to account for less than 10% of the oxygen actually consumed. This is coherent with the model prediction, which is that 99% of oxygen under these conditions is consumed by respiratory chain, coupled to NADH and succinate oxidation rather than proline. In turn, non-respiratory pathways dramatically decreased its contribution as oxygen increased, even though the actual flux through the pathways increased according to the experimental data. This is coherent with a situation where most oxygen is consumed by respiration.

This suggestion contradicts previous hypothesis by other authors (Rosenfeld et al. 2002), who have neglected the respiratory oxygen consumption in oenological fermentations since glucose repression of respiratory enzymes was thought to be in force due to the high-sugar conditions. However, we experimentally showed that respiratory enzymes are indeed expressed at the transcript level even in anaerobiosis. This was also evident at the metabolic flux level, which was constrained by gene expression patterns, *i.e.*, respiration should not have appeared in the FBA analysis if any of the respiratory enzymes were repressed. Moreover, Metabolic Flux Analysis of this experimental system that included respiration as a working reaction showed good rate estimations (Aceituno et al. 2012). Furthermore, Rosenfeld et al (Rosenfeld et al. 2002) showed that cyanide-sensitive respiratory activity increases with qualitative oxygen levels in winemaking conditions, despite neglecting respiratory contribution. Finally, Rosenfeld et al. did not assess proline consumption in their experiments, what raises the possibility that the oxygen unaccounted for in their experiments (~50%) is ultimately consumed by Put1p. With this evidence, we cannot neglect respiration and their associated pathways as contributors to

oxygen consumption in oenological conditions. Rather, our data provided evidence that respiration is the main pathway that consumes the oxygen added in oenological fermentations.

In parallel, our data allowed us to give a picture of ergosterol metabolism and regulation in oenological conditions. The ergosterol content found in the oxygenated conditions is much higher than the content observed for this yeast strain in anaerobic conditions (1.1 mg gDW^{-1}), which is higher than most wine yeast strains in anaerobiosis (Valero et al. 2001; Fornairon-Bonnefond et al. 2002). Interestingly, the ergosterol content is constant regardless of the oxygen level, suggesting that while necessary, oxygen is not limiting to ergosterol production. The limiting factor is not NADPH either, as MFA analysis indicates that there is a relatively low flux to the ergosterol pathway (Aceituno et al. 2012). Despite not being the limiting factor, oxygen increase relieves the dependency exogenous ergosterol uptake, what is negligible with 5 μM dissolved oxygen. This is puzzling since it has been proposed that ergosterol represses its own synthesis (Plakunov and Shelemekh 2009). The complex interplay of the regulation of the *ERG* genes in this conditions have been described elsewhere (Aceituno et al. 2012), and deserves further investigation.

In conclusion, respiratory chain, either directly or associated with proline consumption, consumes more oxygen than biosynthesis of unsaturated lipids and sterols in winemaking conditions. Furthermore, at low oxygen levels, nitrogen metabolism is a priority over other oxygen-dependent metabolic pathways, since nitrogen assimilation (in the form of proline) consumes more oxygen than other pathways. We can even order this requirement, as the use of oxygen is higher for proline assimilation, then for unsaturated lipid synthesis and least for ergosterol synthesis. This can be regarded as an adaptive response of the yeast to the nitrogen-limited conditions prevailing during wine

fermentation. In this sense, oxygen additions are beneficial to winemaking because: 1) they fuel a more efficient energy metabolism in the form of respiration; and 2) they allow an efficient utilization of the available nitrogen sources, being less important for unsaturated lipid synthesis, and even lesser for ergosterol synthesis.

Acknowledgments

This research was supported by FONDECYT grant #1090520 from CONICYT, Chile, to E.A., the "Doctoral thesis support" grant AT-24100170 from CONICYT, Chile, to F.F.A. We are grateful to Lallemand, Inc. (Canada) for financial support and INDURA S.A. (Chile) for providing gas mixtures. F.F.A. and M.O. were supported by CONICYT and VRI-UC doctoral fellowships.

5. GENERAL DISCUSSION

In this thesis, we performed a global assessment of wine yeast physiology in oenological conditions. To that aim, we set up an experimental system to simulate alcoholic fermentation conditions at the late exponential growth phase. This set up allowed us to control and monitor both dissolved oxygen and oxygen uptake rate, which is an improvement compared to previous studies related with oxygen response in yeast (Valero et al. 2001; Rosenfeld et al. 2002; Jouhten et al. 2008). With this information, we were able to:

1) Physiologically characterize wine yeast cells in oenological conditions at different dissolved oxygen conditions, gaining a better understanding of wine yeast metabolism in a nitrogen-limited setting, determining that respiration may account for most of the oxygen consumed in these conditions.

2) Define several guidelines that could be of importance for winemaking and industrial yeast biotechnology operation in general, provided they are proven at industrial scale.

5.1. Global characterization of wine yeast physiology in oenological conditions.

After examining the transitions between every dissolved oxygen condition achieved, several insights were found. The transition from anaerobic to microaerobic conditions (0 to 1.2 μM) seems to be the most important effect of oxygen in terms of the yeast transcriptome (200 genes with differential expression). Most of the genes highlighted in this work (respiratory genes, mannoproteins, iron metabolism genes, etc.) are induced or repressed in this transition. This is in line with the hypothesis of (Kwast et al. 1998) who postulate that at 1 μM dissolved oxygen there is a threshold for the induction of oxygen dependent-genes, in carbon-limited conditions. This also appears to be true for our

nitrogen-limited culture conditions, suggesting that oxygen exerts its regulatory effect by a generic component, independent on the nutritional status of the yeast. This is likely mediated, at least partially, by the *HAP* transcription factor system, a known inducer of respiratory among other genes (Plakunov and Shelemekh 2009).

Nevertheless, the magnitude of change of gene expression is very limited in response to oxygen. Only 19 genes are induced/or repressed over four-fold when taking into account all the transitions. These include genes already described such as members the *TIR* and *PAU* family, and others related to sterol binding and uptake (*HES1, IZH4)* and iron transport (*FIT2)* among other transport-related genes. Therefore, we can suggest that oxygen has a quantitatively important effect on plasma membrane components of yeast, and yeast exchange with the medium. On the other hand, regulatory effect of oxygen on metabolic genes is subtle when compared with other studies (Tai et al. 2005; Rintala et al. 2009). Moreover, we cannot discard a post-transcriptional effect of oxygen, which have been reported for some metabolic genes such as for TCA cycle enzymes and aldehyde dehydrogenases (*ALD* genes) when measuring proteome and transcriptome altogether (Rintala et al. 2009). This might explain, for example, the disappearance of acetic acid at 1.2 μM dissolved oxygen, in spite of there was not effect of oxygen on the expression of the *ALD* genes. Notwithstanding, the coordination of many of these regulatory changes with the metabolic flux changes we report in this thesis, supports the significance of the oxygen impact at the metabolic level, as we describe below.

5.1.1. Respiration induction by oxygen

The most remarkable feature of the oxygen response of yeast to the lowest oxygen concentration is the induction of respiratory genes. While this is not surprising for carbon-limited conditions, where yeast can achieve a fully respiratory metabolism (Frick and

Wittmann 2005; Jouhten et al. 2008), there is a widespread belief that respiration cannot work in nitrogen-limited, high sugar conditions due to glucose catabolite repression (Gancedo 1998; Walker 1998; Rosenfeld et al. 2002). The first evidence contradicting this idea came from our analysis of a microarray compendium (Knijnenburg et al. 2009), that complied several chemostat-based experiments for laboratory yeast strains in different nutrient conditions. The authors showed that respiratory chain gene expression (*COX* genes) actually increased upon exposure to oxygen in nitrogen-limited conditions and the genes were by no means repressed in anaerobic conditions. The same result was obtained for a wine yeast strain in our winemaking-simulating continuous cultures, when we performed RT-PCR analysis of a key gene, *COX4*, a subunit of the complex IV of the respiratory chain, known to be induced by oxygen in carbon-limited conditions (Burke et al. 1997). Therefore, *COX* gene induction by oxygen, regardless of the external sugar content, appeared to be a universal trait, medium, strain or specific sugar concentration – independent. A more global proof came from our microarray analyses, that showed that many *COX* genes, along with *CYC* (cytochrome c), and *NDE* (NADH dehydrogenase) genes have a significant basal expression in anaerobiosis and are induced by oxygen, overriding the supposed catabolic repression effect.

Further evidence about respiration occurring in the presence of oxygen under oenological conditions comes from Metabolic Flux Analysis. We built a metabolic model including respiration and the estimations of ethanol and CO_2 production with this model were consistent with experimental data (~10% error at most), supporting the existence of an active respiration system and argues against the existence of novel oxygen consumption pathways. Nevertheless, this metabolic model had 44 reactions, and, while useful to determine fluxes through the central metabolism, it could be missing other pathways that could be taking the role of respiration. To avoid bias due to model size, we carried out

another Flux Balance Analysis with the stoichiometric network Yeast 4.0, a genome-scale metabolic model, comprises most of documented reactions in yeast. This analysis, that also integrated transcriptome data to constrain the number of reactions, suggested that respiration, and specifically complex IV of the respiratory chain, carried most of the flux of oxygen consumption among all the yeast metabolic pathways, leaving non-respiratory pathways to a quantitatively secondary role. No unknown or unexpected pathway was necessary to invoke to fulfill the oxygen balance when predicted from the GSMR-based model. While it remains to be demonstrated if respiration can be experimentally determined from yeast cells grown in our experimental set up, there has been evidence, that mitochondria extracted from yeast cells grown in synthetic must media can actually respire when they are exposed to oxygen (Rosenfeld and Beauvoit 2003). Therefore, we can postulate that respiration takes place in yeast during aeration operations in winemaking.

5.1.2. The transition to respiro-fermentative metabolism

In addition to the occurrence of respiration itself, we found that oxygen causes a wider metabolic transition: the shift from a fully fermentative to a respiro-fermentative metabolism. This transition happens at a slightly higher oxygen concentration (1.2 and 2.7 μM dissolved oxygen) than the respiratory gene induction and occurs despite fully respiratory metabolism in oenological conditions is never reached. This is reflected by the change of operation mode of the TCA cycle, from the two-branch operation typical of anaerobic physiology in yeast to the canonical, cyclic operation, associated to an increased succinic acid production. The transition to canonical operation goes together with a significant flux increase through it, which can equal the flux through fermentation when oxygen reaches saturating concentrations. It is worthy to note that this thesis is the first to

show that two-branch operation of the TCA cycle is still compatible with oxygen uptake, and that it takes place under nitrogen-limited conditions. This transition, unlike other metabolic transitions such as the diauxic shift (DeRisi et al. 1997) or the respiratory-fermentative transition that occur with dilution rate change (Frick and Wittmann 2005), involves the differential expression of only 25 genes. However, the expression changes are very relevant, since at 2.7 μM dissolved oxygen, mitochondria-cytosol redox shuttle genes (*NDE1, GUT2)* are induced and *FRD1* (fumarate reductase that is responsible for TCA cycle two-branch operation) is repressed, all coordinated with respiratory metabolism onset. Hence, we hypothesize the existence of a fine-tuning adaptation system, according to the actual oxygen concentrations in the culture medium. The latter is a common feature during winemaking, since wine yeast cells are normally exposed to significant oxygen gradients according to their spatial position in the tank after aeration operations or when the must is incidentally exposed to air (Moenne and Agosin Personal communication).

5.1.3. Respiration vs. fermentation: the Crabtree effect and the role of NADH shuttles.

Despite the above evidence, there is one point that has not been answered: why, if respiration takes place, is the Crabtree effect still present, this is, there is ethanol production in wine yeast in oenological condition regardless the oxygen level? Furthermore, ethanol production (*i.e.* fermentation) is the main ATP producer and NADH recycler even in oxygen-saturated conditions according to Metabolic Flux Analysis. Most authors have assumed that this is due to glucose repression of respiratory enzymes (Walker 1998), and fermentation is a "default" pathway in the absence of an efficient respiration. While we provided evidence that this is not caused by a transcriptional effect, the idea of a somehow impaired respiration has support in the fact that the upper limit of the oxygen uptake rate is much lower than in carbon-limited conditions, where fully respiratory

metabolism is achieved (3.9 vs 5.4 mmol gDW^{-1} h^{-1}, respectively) (Larsson et al. 1993; Aceituno et al. 2012). This argues in favor of an effect of the nitrogen limitation on the production of respiratory complexes, which might not be enough to sustain the demand of reducing equivalent reoxidization given the high concentration of sugar. However, this is not the whole story. Together with the availability of respiratory chain proteins, the compartmentalization of reducing equivalents in the cell needs to be accounted for. Most of NADH in the cell is produced by glycolysis when there is high external sugar, and this NADH has to be incorporated into the mitochondria in order to transfer its electrons to oxygen through the respiratory chain. What if the OUR cannot increase more because the import of respiration substrate (NADH) into the mitochondria cannot be done faster? Supporting this hypothesis is the key work of (Vemuri et al. 2007), who heterologously expressed a water-forming NADH oxidase, located facing the cytoplasm, in yeast mitochondria. Expression of this enzyme resulted in a complete outage of the Crabtree effect, due to its ability to reoxidize the cytosolic NADH. Moreover, recent work proposes that the transition between fermentative and respiratory metabolism is governed by the economics of mitochondrial membrane occupancy (Zhuang et al. 2011). This means, for this case, that the redox shuttles that are responsible for exchanging reducing equivalents between cytosol and mitochondria have an upper limit on its effective concentration, which is lower for nitrogen-limited than for carbon-limited culture conditions. The involvement of these shuttles, such as Nde1p (external NADH dehydrogenase), Gut2p (glycerol-3-phosphate dehydrogenase) or Adh3p (ethanol-acetaldehyde shuttle) is supported by their coordinated induction with the metabolic fermentative to respiro-fermentative transition as well as by Metabolic Flux Analysis. As the shuttles are located in the membrane (*NDE1, GUT2*), or require a lipid bilayer for metabolite diffusion (Adh3p), their functioning is constrained by membrane occupancy, and they can be,

individually or collectively, the limiting step in transferring reducing equivalents for respiration. However, it cannot be ruled out that the shuttles *and* the respiratory chain are also limited by membrane constraints. It remains to be seen if there is evidence to support this hypothesis; for instance, if mitochondrial morphology in nitrogen-limited condition was different from that in carbon-limited conditions.

5.1.4. Physiology of yeast under oxygen-saturated conditions

Another important "phase change" in terms of metabolism and transcriptome is the transition between limiting and saturating oxygen conditions (5-21 μM dissolved oxygen, 195 genes induced or repressed). Actually, most measured rates were different between these conditions. Furthermore, all measured parameters are significantly different between the anaerobic and the 21 μM dissolved oxygen condition. However, this condition shows a non-significant biomass increase despite the proportionally large oxygen increase. Besides, it is difficult to experimentally maintain a continuous culture in this condition, because biomass often drops significantly, not reaching a steady-state (data not shown). The transcriptome of the saturated condition showed a down regulation of nutrient uptake functions, which can be linked to the saturation of biomass and perhaps of respiratory capacity. This is very different to the oxygen-limiting condition, where biomass and specific OUR increases with dissolved oxygen increase. Oxidative stress is the most likely causative of these responses in the oxygen-saturating zone, being thus a "third state" on the oxygen response of wine yeast.

5.2. Insights from the oxygen response of wine yeast- relevance to applied research

5.2.1. Deleterious effects of the oxygen saturation zone in oenological conditions

Under our experimental conditions, the transition between oxygen-limited and oxygen-saturated conditions occur around 18 μM dissolved oxygen. This information could be critical for winemakers, as we recommend that steady-state oxygen concentrations should not surpass this limit in winemaking (however, this is a rare condition (Moenne and Agosin Personal communication). We found that oxidative stress markers, such as glutaredoxin gene induction and carbohydrate accumulation appear in wine yeast cultured in these conditions. For winemaking, this result in a 40% decrease in volumetric sugar consumption and a 30% decrease in volumetric ethanol production; this is likely to cause a sluggish fermentation. Moreover, we found a novel deleterious effect of high dissolved oxygen contents, *i.e.* the repression of cell wall mannoproteins, which have been reported to have beneficial effects, such as protein haze removal and improved wine bodyness and mouthfeel (Dupin et al. 2000; Gonzalez-Ramos et al. 2008). Therefore, if oxygen remains high for a long period, these organoleptic wine features may be compromised. This is in line with empirical oenological knowledge, which dictates that oxygen additions must be performed carefully in order to keep wine quality.

5.2.2. The optimal oxygen level for winemaking.

If oxygen-saturated conditions are deleterious, which is the oxygen range that best suits wine fermentation? From our evidence, sparging the culture with gas with 1% oxygen (resulting in 1.2 μM dissolved oxygen) would be the best steady-state condition for oxygen addition in winemaking among those evaluated. In this condition, there is a significant biomass increase by adding this low oxygen level, which in turn results in a significant volumetric increase of ethanol production (24%) and sugar consumption (20%), coherent with a fermentative metabolism. The beneficial effect of oxygen in this condition

also arises from the proline uptake increase, which relieves the nitrogen limitation of the culture (the cause of most sluggish and stuck fermentations (Varela et al. 2004), which in turn fully explains the biomass increase. Moreover, unsaturated fatty acids and ergosterol cell content increase when compared to anaerobic conditions. Furthermore, another beneficial effect would be the abolishment of acetic acid production, which is perhaps the most typical off-flavor in wines (Boulton et al. 1998). Therefore, winemaking would benefit of low, constant oxygen addition.

6. GENERAL CONCLUSIONS AND PROJECTIONS

6.1 The three stages of the yeast oxygen response in oenological conditions.

The goal of this thesis was to characterize the oxygen response of wine yeast in oenological conditions, aiming to identify global effects. In the process, we successfully set up a chemostat-based system for the simulation of wine fermentation conditions at the laboratory scale. We also set up a Metabolic Flux Analysis model suited for fermenting wine yeast in presence of oxygen, and obtained metabolic and transcriptomic data that allowed us to achieve our aim. We found three general oxygen-dependent physiological states in yeast in oenological conditions. First is the fermentative state, which can be strict (in anoxic condition) or only metabolic (below 2.7 μM dissolved oxygen). Second, the respiro-fermentative, oxygen-limiting state, and a third, stress-related, oxygen saturated state. In the latter states, respiration dominates as the main oxygen consumption pathway and contributes significantly to redox and energetic metabolism, despite the Crabtree effect is still in force, probably due to the limitations in the electron transport between cytosol and mitochondria.

The effects of oxygen on yeast metabolism and transcriptome do not seem to encompass a major part of the regulatory or metabolic network of the cell, as neither transition associates to a gene expression change of more than 3.5% of the transcriptome. Therefore, the drivers of the transitions may lie elsewhere. For instance, they can be driven directly by substrate (*i.e.* oxygen) availability, and/or post-transcriptional mechanisms at the enzyme level. In fact this is a regulatory level affected by oxygen in carbon-limited conditions (Rintala et al. 2011). The fact that we did not detect such issues could be due to the inherent limitation of any experimental setting. First, we simulated only one point in the growth curve of a wine fermentation, and put it in a steady-state condition that is

amenable for systemic analysis but also lacks the information from other growth stages or dynamic oxygen additions. In addition, we predicted metabolic fluxes from exo-metabolomic measurements, lacking internal metabolite and enzyme/protein level measurements. Connecting transcriptome data with flux measurements is not always straightforward (Nielsen 2003). Therefore, completing this analysis with the rest of the regulatory landscape (protein level and enzyme activity, for example) would surely make an impact on our current understanding on the yeast response to oxygen. Despite these limitations, our multilevel integration of data from transcriptomics, modeling and metabolomics allowed us to find several specific and coordinated transcriptional and metabolic changes that mark the yeast oxygen-response stages, such as TCA cycle reversal, cytosol-mitochondria redox shuttle induction, and especially the onset of respiration regardless high sugar conditions. It is interesting to note that the acknowledgment of the functioning of a classical pathway, rather than the discovery of new ones, is the main result from our research towards explaining the fate of the oxygen consumed by wine yeast. It is also worthy to note that the integration of transcriptomics with metabolic models (which in turn integrate exo-metabolomic measurements) of different scopes and different algorithms produced similar results on the respiration issue, which supports our findings. In the end, the steps we have taken towards a systemic view of wine yeast physiology have provided significant insights on its oxygen response.

6.2 Projections on applied winemaking

In the applied realm, our insights on the benefit avoiding oxygen-saturating conditions and of a 1% continuous oxygen sparging, could be applied. The former is well-known by oenologists, and we provide a mechanistic explanation on one of the deleterious effects of excess oxygen in wine (decrease of mannoprotein-associated organoleptic

features). The latter insight could be valuable but with some degree of caution. First, our system only simulate white wine fermentation; we cannot directly extrapolate oxygen concentration effect to red wine fermentation, since we did not include phenolic compounds present in red wines, which does consume oxygen chemically (Waterhouse and Laurie 2006). Moreover, we worked at 20°C, a temperature closer to white wine fermentation run (Boulton et al. 1998). Another caution to observe relates to scaling up, since in industrial winemaking a steady-state addition of a 1% oxygen gas mixture could be expensive and complex. In fact, work from our laboratory has shown that most oxygen additions in industrial operations are discrete events of pump-over or rack and return operations where the fermenting must is re-circulated and exposed to air, with little control of the oxygen actually incorporated in the must (Moenne and Agosin Personal communication). Therefore, industrial application of the knowledge generated in this work needs to overcome two major challenges: a technological challenge, for better controlling of the oxygen added in industrial operations; and a scientific one, to study a more close-to-real situation using our experimental system, feeding it with an oxygen pulse instead of a continuous supply. For the latter, an experimental system have been already set up and future work is aimed to characterize the transcriptome of wine yeast after an oxygen pulse (Orellana et al. 2013). We expect that comparison of the data of these experiments with those reported in this thesis would allow us to draw more straightforward conclusions to be applied at the winery level.

6.3 Projections on cancer research: The Warburg and Crabtree effects.

Moving beyond the microbiology field, our study on global physiology of a microbial cell can have ramifications to a radically different biological system: cancer cells. The Crabtree effect and the metabolic transitions due to oxygen are not exclusive of

wine yeast, but they are present in this system. Cancer cells present the so-called Warburg effect, producing lactate -instead of ethanol- even in aerobiosis (Diaz-Ruiz et al. 2011). It seems that this allows cancer cells to proliferate faster than when they show respiratory metabolism. Our experimental setting could be useful to study this phenomenon, since cancer cells appear to be limited in nitrogen and/or phosphorous, since they are particularly avid on glutamine and phosphate (Elser et al. 2007; Wise and Thompson 2010). Moreover, cancer cells are also exposed to different levels of oxygen (hypoxia) during tumor growth. Some studies showed that killing efficiency of radiotherapy and other drugs presents an inflection point around 1 μM dissolved oxygen (Wilson and Hay 2011). Whether this is linked to the shift between fermentative and mixed metabolism remains to be seen. Nevertheless, insight obtained from yeast in nitrogen-limited conditions might be useful to shed light into the causes of the Warburg effect, for example, by studying the redox exchange mechanisms between mitochondria and cytosol that could be involved in establishing this phenotype, with the aim of finding potential therapeutic targets.

6.4 Final Remarks

The study of the global interplay of oxygen and yeast transcriptome and metabolism can affect several fundamental and applied fields of knowledge. The idea that respiratory metabolism can occur in high-sugar, nitrogen limiting conditions, together with the fact that respiration itself is the main oxygen consumption pathway in oenological conditions, is the main finding of this thesis. This new knowledge, obtained by global approaches, supported the general formulation of our hypothesis but contradicts our statement on the involvement of novel, uncharacterized metabolic pathways in the wine yeast oxygen response.

7. APPENDIX

Average fluxes for each reaction (numbered as in Supplemental Data 2, Chapter 1, for the five dissolved oxygen conditions. Data is in C-mmol/gDw h

Dissolved Oxygen (micromolar)	0	1.2	2.7	5	21
01	43.56791	43.93017	37.45833	35.40776	21.62141
02	41.74124	42.05062	35.42772	33.4213	19.63494
03	42.27222	42.61684	35.99882	33.99629	20.20993
04	19.65378	19.9032	16.58607	15.9513	9.682103
05	40.91255	41.34309	34.71817	33.08311	19.92073
06	40.80399	41.23453	34.61269	32.97763	19.81525
07	40.72317	41.15371	34.53187	32.89681	19.73443
08	39.70785	40.01887	30.83968	27.55615	12.92306
09	26.37516	26.71167	22.28275	21.43511	13.07627
10	0.031122	0.01129	0.011266	0.022955	0.022955
11	1.482331	1.40522	1.413343	1.046845	0.422862
12	1.482331	1.40522	1.413343	1.046845	0.422862
13	0.911807	0.964684	0.96061	0.966462	0.966462
14	0.509793	0.539161	0.543223	0.546467	0.546467
15	0.337649	0.364081	0.367738	0.370658	0.370658
16	0.367146	0.557225	5.241644	10.17779	13.17587
17	0.057972	0.220897	4.236103	8.467075	11.03685
18	-0.40121	-0.26544	3.080556	6.606354	8.747821
19	-0.38068	-0.32281	1.617522	5.060879	6.848967
20	-0.32882	-0.27094	1.663335	5.106699	6.894788
21	-0.00027	0.01129	0.011266	0.022955	0.022955
22	0.256723	0.256723	0.25672	0.256719	0.256719
23	0.754398	0.805152	1.538157	0.915469	0.84057
24	0.914864	0.914864	1.07	1.02	2.588
25	1.156713	1.15673	1.139657	1.139674	1.139674
26	0.237184	0.237206	0.217369	0.217391	0.217391
27	0.485519	0.485544	0.464089	0.464115	0.464115
28	0.289491	0.289499	0.281267	0.281275	0.281275
29	0.270135	0.270143	0.262761	0.262769	0.262769
30	0.048963	0.04899	0.025329	0.025357	0.025357
31	0.006806	0.006819	0.006862	0.006875	0.006875
32	0.063172	0.063181	0.045031	0.04504	0.04504
33	0.864406	0.864403	0.864393	0.86439	0.86439
34	1.39E-07	1.39E-07	1.39E-07	1.39E-07	1.39E-07
35	11.20334	11.40328	10.86781	12.85686	10.18332
36	0.538614	0.589357	1.331898	0.709197	0.634299
37	0.065756	-0.04358	-1.73413	-3.08721	-4.4838
38	-0.09517	-0.1023	0.35558	1.21682	1.712242

39	6.7E-15	-0.108	-0.244	-0.242	-1.26E-14
40	-0.00596	-0.0058	-0.00635	-0.00618	-0.00618
41	2.2E-08	2.2E-08	2.2E-08	2.2E-08	2.20E-08
42	-0.00027	0.01129	0.011266	0.022955	0.022955
43	-0.00023	0.009405	0.009384	0.019121	0.019121
44	0.095335	0.1954	2.537532	4.469145	6.053723

8. REFERENCES

Aceituno, F. F., M. Orellana, et al. (2012). "Oxygen response of the wine yeast Saccharomyces cerevisiae EC1118 strain grown under carbon-sufficient, nitrogen-limited oenological conditions." Appl Environ Microbiol **78**(23).

Affymetrix. (2009). Gene Chip Expression Analysis Technical Manual.

Affymetrix. (2010). GeneChip® 3' IVT Express Kit Manual.

Alberty, R. A. (2006). "Biochemical thermodynamics: applications of Mathematica." Methods Biochem Anal **48**: 1-458.

Athenstaedt, K. and G. Daum (1997). "Biosynthesis of phosphatidic acid in lipid particles and endoplasmic reticulum of Saccharomyces cerevisiae." J Bacteriol **179**(24): 7611-6.

Bakker, B. M., K. M. Overkamp, et al. (2001). "Stoichiometry and compartmentation of NADH metabolism in Saccharomyces cerevisiae." FEMS Microbiol Rev **25**(1): 15-37.

Becker, S. A., A. M. Feist, et al. (2007). "Quantitative prediction of cellular metabolism with constraint-based models: the COBRA Toolbox." Nature Protocols **2**(3): 727-738.

Becker, S. A. and B. O. Palsson (2008). "Context-specific metabolic networks are consistent with experiments." Plos Computational Biology **4**(5).

Bluthgen, N., K. Brand, et al. (2005). "Biological profiling of gene groups utilizing Gene Ontology." Genome Inform **16**(1): 106-15.

Boer, V. M., J. H. de Winde, et al. (2003). "The genome-wide transcriptional responses of Saccharomyces cerevisiae grown on glucose in aerobic chemostat cultures limited for carbon, nitrogen, phosphorus, or sulfur." J Biol Chem **278**(5): 3265-74.

Boubekeur, S., N. Camougrand, et al. (2001). "Participation of acetaldehyde dehydrogenases in ethanol and pyruvate metabolism of the yeast Saccharomyces cerevisiae." European Journal of Biochemistry **268**(19): 5057-5065.

Boulton, R. B., V. L. Sinlgleton, et al. (1998). Principles and Practices of Winemaking. Gaithersburg, , Aspen Publishers, Inc.

Braunstein, A., R. Mulet, et al. (2008). "Estimating the size of the solution space of metabolic networks." Bmc Bioinformatics **9**.

Breitling, R., P. Armengaud, et al. (2004). "Rank products: a simple, yet powerful, new method to detect differentially regulated genes in replicated microarray experiments." Febs Letters **573**(1-3): 83-92.

Burke, P. V., D. C. Raitt, et al. (1997). "Effects of oxygen concentration on the expression of cytochrome c and cytochrome c oxidase genes in yeast." J Biol Chem **272**(23): 14705-12.

Butcher, R. A. and S. L. Schreiber (2004). "Identification of Ald6p as the target of a class of small-molecule suppressors of FK506 and their use in network dissection." Proc Natl Acad Sci U S A **101**(21): 7868-73.

Camarasa, C., J. P. Grivet, et al. (2003). "Investigation by 13C-NMR and tricarboxylic acid (TCA) deletion mutant analysis of pathways for succinate formation in Saccharomyces cerevisiae during anaerobic fermentation." Microbiology **149**(Pt 9): 2669-78.

Carbon, S., A. Ireland, et al. (2009). "AmiGO: online access to ontology and annotation data." Bioinformatics **25**(2): 288-289.

Caspi, R., H. Foerster, et al. (2008). "The MetaCyc Database of metabolic pathways and enzymes and the BioCyc collection of Pathway/Genome Databases." Nucleic Acids Res **36**(Database issue): D623-31.

Castrillo, J. I., L. A. Zeef, et al. (2007). "Growth control of the eukaryote cell: a systems biology study in yeast." J Biol **6**(2): 4.

Cejudo-Bastante, M. J., I. Hermosin-Gutierrez, et al. (2011). "Hyperoxygenation and bottle storage of Chardonnay white wines: effects on color-related phenolics, volatile composition, and sensory characteristics." J Agric Food Chem **59**(8): 4171-82.

Celton, M., A. Goelzer, et al. "A constraint-based model analysis of the metabolic consequences of increased NADPH oxidation in Saccharomyces cerevisiae." Metab Eng **14**(4): 366-79.
Christie, K. R., S. Weng, et al. (2004). "Saccharomyces Genome Database (SGD) provides tools to identify and analyze sequences from Saccharomyces cerevisiae and related sequences from other organisms." Nucleic Acids Research **32**: D311-D314.
Conesa, A., S. Gotz, et al. (2005). "Blast2GO: a universal tool for annotation, visualization and analysis in functional genomics research." Bioinformatics **21**(18): 3674-6.
David, P. S. and R. O. Poyton (2005). "Effects of a transition from non-noxia to anoxia on yeast cytochrome c oxidase and the mitochondrial respiratory chain - Implications for hypoxic gene induction." Biochimica Et Biophysica Acta-Bioenergetics **1709**(2): 169-180.
Davies, B. S. J. and J. Rine (2006). "A role for sterol levels in oxygen sensing in Saccharomyces cerevisiae." Genetics **174**(1): 191-201.
DeRisi, J. L., V. R. Iyer, et al. (1997). "Exploring the metabolic and genetic control of gene expression on a genomic scale." Science **278**(5338): 680-6.
Diaz-Ruiz, R., M. Rigoulet, et al. (2011). "The Warburg and Crabtree effects: On the origin of cancer cell energy metabolism and of yeast glucose repression." Biochim Biophys Acta **1807**(6): 568-76.
Dobson, P. D., K. Smallbone, et al. (2010). "Further developments towards a genome-scale metabolic model of yeast." BMC Syst Biol **4**: 145.
Doran, P. M. (1995). Bioprocess Engineering Principles. London, UK, Academic Press.
Dupin, I. V. S., V. J. Stockdale, et al. (2000). "Saccharomyces cerevisiae mannoproteins that protect wine from protein haze: Evaluation of extraction methods and immunolocalization." Journal of Agricultural and Food Chemistry **48**(4): 1086-1095.
Ehsani, M., M. R. Fernandez, et al. (2009). "Engineering of 2,3-butanediol dehydrogenase to reduce acetoin formation by glycerol-overproducing, low-alcohol Saccharomyces cerevisiae." Appl Environ Microbiol **75**(10): 3196-205.
Eide, D. J. (1998). "The molecular biology of metal ion transport in Saccharomyces cerevisiae." Annu Rev Nutr **18**: 441-69.
Elser, J. J., M. M. Kyle, et al. (2007). "Biological Stoichiometry in Human Cancer." Plos One **2**(10).
Feist, A. M. and B. O. Palsson (2010). "The biomass objective function." Current Opinion in Microbiology **13**(3): 344-349.
Fornairon-Bonnefond, C., V. Demaretz, et al. (2002). "Oxygen addition and sterol synthesis in Saccharomyces cerevisiae during enological fermentation." J Biosci Bioeng **93**(2): 176-82.
Frick, O. and C. Wittmann (2005). "Characterization of the metabolic shift between oxidative and fermentative growth in Saccharomyces cerevisiae by comparative C-13 flux analysis." Microbial Cell Factories **4**.
Gancedo, J. M. (1998). "Yeast carbon catabolite repression." Microbiol Mol Biol Rev **62**(2): 334-61.
Gentleman, R. C., V. J. Carey, et al. (2004). "Bioconductor: open software development for computational biology and bioinformatics." Genome Biology **5**(10).
Georis, I., A. Feller, et al. (2009). "The yeast GATA factor Gat1 occupies a central position in nitrogen catabolite repression-sensitive gene activation." Mol Cell Biol **29**(13): 3803-15.
Gianchandani, E. P., M. A. Oberhardt, et al. (2008). "Predicting biological system objectives de novo from internal state measurements." Bmc Bioinformatics **9**.
Gonzalez-Ramos, D., E. Cebollero, et al. (2008). "A recombinant Saccharomyces cerevisiae strain overproducing mannoproteins stabilizes wine against protein haze." Applied and Environmental Microbiology **74**(17): 5533-5540.
Govender, P., S. Kroppenstedt, et al. (2011). "Novel wine-mediated FLO11 flocculation phenotype of commercial Saccharomyces cerevisiae wine yeast strains with modified FLO gene expression." Fems Microbiology Letters **317**(2): 117-126.

Grabowska, D. and A. Chelstowska (2003). "The ALD6 gene product is indispensable for providing NADPH in yeast cells lacking glucose-6-phosphate dehydrogenase activity." J Biol Chem **278**(16): 13984-8.
Hatzixanthis, K., M. Mollapour, et al. (2003). "Moderately lipophilic carboxylate compounds are the selective inducers of the Saccharomyces cerevisiae Pdr12p ATP-binding cassette transporter." Yeast **20**(7): 575-85.
Hayes, A., N. Zhang, et al. (2002). "Hybridization array technology coupled with chemostat culture: Tools to interrogate gene expression in Saccharomyces cerevisiae." Methods **26**(3): 281-90.
Hazelwood, L. A., J. M. Daran, et al. (2008). "The Ehrlich pathway for fusel alcohol production: a century of research on Saccharomyces cerevisiae metabolism." Appl Environ Microbiol **74**(8): 2259-66.
Henricsson, C., M. C. de Jesus Ferreira, et al. (2005). "Engineering of a Novel Saccharomyces cerevisiae Wine Strain with a Respiratory Phenotype at High External Glucose Concentrations." Applied and Environmental Microbiology **71**(10): 6185-6192.
Hohmann, S. (2002). "Osmotic stress signaling and osmoadaptation in yeasts." Microbiol Mol Biol Rev **66**(2): 300-72.
Hoskisson, P. A. and G. Hobbs (2005). "Continuous culture--making a comeback?" Microbiology **151**(Pt 10): 3153-9.
Ingledew, W. M., C. A. Magnus, et al. (1987). "Influence of oxygen on proline utilization during the wine fermentation." Am J. Enol. Vitic. **38**: 246-248.
Jagow, G. and M. Klingenberg (1970). "Pathways of hydrogen in mitochondria of Saccharomyces carlsbergensis." European Journal of Biochemistry **12**(3): 583-592.
Jensen, P. A. and J. A. Papin (2011). "Functional integration of a metabolic network model and expression data without arbitrary thresholding." Bioinformatics **27**(4): 541-547.
Jouhten, P., E. Rintala, et al. (2008). "Oxygen dependence of metabolic fluxes and energy generation of Saccharomyces cerevisiae CEN.PK113-1A." BMC Syst Biol **2**: 60.
Knijnenburg, T. A., J. M. Daran, et al. (2009). "Combinatorial effects of environmental parameters on transcriptional regulation in Saccharomyces cerevisiae: a quantitative analysis of a compendium of chemostat-based transcriptome data." BMC Genomics **10**: 53.
Kwast, K. E., P. V. Burke, et al. (1998). "Oxygen sensing and the transcriptional regulation of oxygen-responsive genes in yeast." J Exp Biol **201**(Pt 8): 1177-95.
Landolfo, S., G. Zara, et al. (2010). "Oleic acid and ergosterol supplementation mitigates oxidative stress in wine strains of Saccharomyces cerevisiae." Int J Food Microbiol **141**(3): 229-35.
Larsson, C., U. Vonstockar, et al. (1993). "Growth and Metabolism of Saccharomyces-Cerevisiae in Chemostat Cultures under Carbon-Limiting, Nitrogen-Limiting, or Carbon-Limiting and Nitrogen-Limiting Conditions." Journal of Bacteriology **175**(15): 4809-4816.
Letunic, I. and P. Bork (2007). "Interactive Tree Of Life (iTOL): an online tool for phylogenetic tree display and annotation." Bioinformatics **23**(1): 127-8.
Li, L., Y. Ye, et al. (2009). "The induction of trehalose and glycerol in Saccharomyces cerevisiae in response to various stresses." Biochem Biophys Res Commun **387**(4): 778-83.
Liao, J. C., R. Boscolo, et al. (2003). "Network component analysis: Reconstruction of regulatory signals in biological systems." Proceedings of the National Academy of Sciences of the United States of America **100**(26): 15522-15527.
Liu, H., M. C. Sanuda-Pena, et al. (1998). "Determination of submicromolar concentrations of neurotransmitter amino acids by fluorescence detection using a modification of the 6-aminoquinolyl-N-hydroxysuccinimidyl carbamate method for amino acid analysis." J Chromatogr A **828**(1-2): 383-95.
Liu, L., R. Agren, et al. (2010). "Use of genome-scale metabolic models for understanding microbial physiology." Febs Letters **584**(12): 2556-64.

Lupiañez, J. A., A. Machado, et al. (1974). "Succinic acid production by yeasts grown under different hypoxic conditions." Molecular and cellular biochemistry **3**(2): 113-116.
Mateles, R. I. and E. Battat (1974). "Continuous culture used for media optimization." Appl Microbiol **28**(6): 901-5.
Moenne, M. I. and E. Agosin (Personal communication). Kinetics of oxygen consumption during fermentation of red wines.
Murray, D. B., K. Haynes, et al. (2011). "Redox regulation in respiring Saccharomyces cerevisiae." Biochim Biophys Acta **1810**(10): 945-58.
Nielsen, J. (2003). "It is all about metabolic fluxes." J Bacteriol **185**(24): 7031-5.
Nielsen, J., J. Villadsen, et al. (2003). Bioreaction Engineering Principles. New York, Kluwer Academic/Plenum Publisher.
Nissen, T. L., U. Schulze, et al. (1997). "Flux distributions in anaerobic, glucose-limited continuous cultures of Saccharomyces cerevisiae." Microbiology **143 (Pt 1)**: 203-18.
Nookaew, I., M. C. Jewett, et al. (2008). "The genome-scale metabolic model iIN800 of Saccharomyces cerevisiae and its validation: a scaffold to query lipid metabolism." BMC Syst Biol **2**: 71.
Nylund, J. E. and H. Wallander (1992). "Ergosterol Analysis as a Means of Quantifying Mycorrhizal Biomass." Methods in Microbiology **24**: 77-88.
Orellana, M., F. F. Aceituno, et al. (2013). "Transcriptomic analysis of wine yeast after an oxygen pulse in oenological conditions." in preparation.
Orth, J. D., I. Thiele, et al. (2010). "What is flux balance analysis?" Nature Biotechnology **28**(3): 245-248.
Pahlman, I. L., L. Gustafsson, et al. (2001). "Cytosolic redox metabolism in aerobic chemostat cultures of Saccharomyces cerevisiae." Yeast **18**(7): 611-20.
Palmieri, L., M. J. Runswick, et al. (2000). "Yeast mitochondrial carriers: bacterial expression, biochemical identification and metabolic significance." J Bioenerg Biomembr **32**(1): 67-77.
Parpinello, G. P., F. Plumejeau, et al. (2011). "Effect of micro-oxygenation on sensory characteristics and consumer preference of Cabernet Sauvignon wine." J Sci Food Agric **92**(6): 1238-44.
Pearson, R. K., T. Zylkin, et al. (2004). Quantitative Evaluation of Clustering Results Using Computational Negative Controls. Proceedings of the Fourth SIAM International Conference on Data Mining. M. W. Berry, D. Umeshwar, C. Kamath and D. Skilliconr, Society for Industrial and Applied Mathematics.
Piper, M. D., P. Daran-Lapujade, et al. (2002). "Reproducibility of oligonucleotide microarray transcriptome analyses. An interlaboratory comparison using chemostat cultures of Saccharomyces cerevisiae." J Biol Chem **277**(40): 37001-8.
Pizarro, F., C. Varela, et al. (2007). "Coupling kinetic expressions and metabolic networks for predicting wine fermentations." Biotechnol Bioeng **98**(5): 986-98.
Pizarro, F. J., M. C. Jewett, et al. (2008). "Growth temperature exerts differential physiological and transcriptional responses in laboratory and wine strains of Saccharomyces cerevisiae." Appl Environ Microbiol **74**(20): 6358-68.
Plakunov, V. K. and O. V. Shelemekh (2009). "Mechanisms of Oxygen Regulation in Microorganisms." Microbiology **78**(5): 535-546.
Pronk, J. T., H. Yde Steensma, et al. (1996). "Pyruvate metabolism in Saccharomyces cerevisiae." Yeast **12**(16): 1607-33.
Pujol-Carrion, N., G. Belli, et al. (2006). "Glutaredoxins Grx3 and Grx4 regulate nuclear localisation of Aft1 and the oxidative stress response in Saccharomyces cerevisiae." J Cell Sci **119**(Pt 21): 4554-64.
Regenberg, B., T. Grotkjaer, et al. (2006). "Growth-rate regulated genes have profound impact on interpretation of transcriptome profiling in Saccharomyces cerevisiae." Genome Biol **7**(11): R107.

Rigoulet, M., H. Aguilaniu, et al. (2004). "Organization and regulation of the cytosolic NADH metabolism in the yeast Saccharomyces cerevisiae." Mol Cell Biochem **256-257**(1-2): 73-81.
Rintala, E., P. Jouhten, et al. (2011). "Transcriptional Responses of Saccharomyces cerevisiae to Shift from Respiratory and Respirofermentative to Fully Fermentative Metabolism." Omics-a Journal of Integrative Biology **15**(7-8): 461-476.
Rintala, E., M. Toivari, et al. (2009). "Low oxygen levels as a trigger for enhancement of respiratory metabolism in Saccharomyces cerevisiae." BMC Genomics **10**: 461.
Rosenfeld, E. and B. Beauvoit (2003). "Role of the non-respiratory pathways in the utilization of molecular oxygen by Saccharomyces cerevisiae." Yeast **20**(13): 1115-44.
Rosenfeld, E., B. Beauvoit, et al. (2003). "Oxygen consumption by anaerobic Saccharomyces cerevisiae under enological conditions: effect on fermentation kinetics." Appl Environ Microbiol **69**(1): 113-21.
Rosenfeld, E., B. Beauvoit, et al. (2002). "Non-respiratory oxygen consumption pathways in anaerobically-grown Saccharomyces cerevisiae: evidence and partial characterization." Yeast **19**(15): 1299-321.
Rossouw, D., D. Jacobson, et al. (2011). "Transcriptional Regulation and the Diversification of Metabolism in Wine Yeast Strains." Genetics.
Rossouw, D., R. Olivares-Hernandes, et al. (2009). "Comparative Transcriptomic Approach To Investigate Differences in Wine Yeast Physiology and Metabolism during Fermentation." Applied and Environmental Microbiology **75**(20): 6600-6612.
Saa, P. A., M. I. Moenne, et al. (2012). "Modeling oxygen dissolution and biological uptake during pulse oxygen additions in oenological fermentations." Bioprocess Biosyst Eng.
Sablayrolles, J. M., A. Julien, et al. (2000). "Comparison of nitrogen and oxygen demands of enological yeasts: Technological consequences." American Journal of Enology and Viticulture **51**(3): 215-222.
Salmanowicz, B., J. E. Nylund, et al. (1990). "High-Performance Liquid-Chromatography - Assay of Ergosterol - a Technique to Estimate Fungal Biomass in Roots with Ectomycorrhiza." Agriculture Ecosystems & Environment **28**(1-4): 437-440.
Salmon, J. M. and P. Barre (1998). "Improvement of nitrogen assimilation and fermentation kinetics under enological conditions by derepression of alternative nitrogen-assimilatory pathways in an industrial Saccharomyces cerevisiae strain." Appl Environ Microbiol **64**(10): 3831-7.
Schellenberger, J., R. Que, et al. (2011). "Quantitative prediction of cellular metabolism with constraint-based models: the COBRA Toolbox v2.0." Nat Protoc **6**(9): 1290-307.
Schulze, U., G. Liden, et al. (1996). "Physiological effects of nitrogen starvation in an anaerobic batch culture of Saccharomyces cerevisiae." Microbiology **142 (Pt 8)**: 2299-310.
Shakoury-Elizeh, M., J. Tiedeman, et al. (2004). "Transcriptional remodeling in response to iron deprivation in Saccharomyces cerevisiae." Mol Biol Cell **15**(3): 1233-43.
Sokal, R. R. and F. J. Rohlf (1962). "The comparison of dendrograms by objective methods." Taxon **11**: 33-40.
Stephanopoulos, G., A. Aristidou, et al. (1998). Metabolic engineering: principles and methodologies. San Diego, Academic Press.
Tai, S. L., V. M. Boer, et al. (2005). "Two-dimensional transcriptome analysis in chemostat cultures. Combinatorial effects of oxygen availability and macronutrient limitation in Saccharomyces cerevisiae." J Biol Chem **280**(1): 437-47.
Team", R. D. C. (2012). "R: A language and environment for statistical computing.".
Valero, E., C. Millan, et al. (2001). "Influence of oxygen addition during growth phase on the biosynthesis of lipids in Saccharomyces cerevisiae (M(3)30-9) in enological fermentations." J Biosci Bioeng **92**(1): 33-8.
Varela, C., F. Pizarro, et al. (2004). "Biomass content governs fermentation rate in nitrogen-deficient wine musts." Appl Environ Microbiol **70**(6): 3392-400.

Vargas, F. A., F. F. Aceituno, et al. (2010). Biochemistry and Molecular Biology of Yeast Alcoholic Fermentation. Comprehensive Food Fermentation and Biotechnology. A. Pandey, C. R. Soccol, E. Gnansounouet al. New Delhi, India, Asiatech Publishers. **2**.
Vemuri, G. N., M. A. Eiteman, et al. (2007). "Increasing NADH oxidation reduces overflow metabolism in Saccharomyces cerevisiae." Proc Natl Acad Sci U S A **104**(7): 2402-7.
Verduyn, C. (1991). "Physiology of yeasts in relation to biomass yields." Antonie Van Leeuwenhoek **60**(3): 325-353.
Walker, G. M. (1998). Yeast physiology and biotechnology. West Sussex, UK, John Wiley & Sons.
Wanduragala, S., N. Sanyal, et al. (2010). "Purification and characterization of Put1p from Saccharomyces cerevisiae." Arch Biochem Biophys **498**(2): 136-42.
Wang, N. S. and G. Stephanopoulos (1983). "Application of macroscopic balances to the identification of gross measurement errors." Biotechnol Bioeng **25**(9): 2177-208.
Waterhouse, A. L. and V. F. Laurie (2006). "Oxidation of wine phenolics: A critical evaluation and hypotheses." American Journal of Enology and Viticulture **57**(3): 306-313.
Wilson, W. R. and M. P. Hay (2011). "Targeting hypoxia in cancer therapy." Nature Reviews Cancer **11**(6): 393-410.
Wise, D. R. and C. B. Thompson (2010). "Glutamine addiction: a new therapeutic target in cancer." Trends in Biochemical Sciences **35**(8): 427-433.
www.vinosdechile.cl (2012). "Informacion y Estadisticas." **2012**.
Zaman, S., S. I. Lippman, et al. (2008). "How Saccharomyces responds to nutrients." Annu Rev Genet **42**: 27-81.
Zhuang, K., G. N. Vemuri, et al. (2011). "Economics of membrane occupancy and respiro-fermentation." Mol Syst Biol **7**: 500.
Zur, H., E. Ruppin, et al. (2010). "iMAT: an integrative metabolic analysis tool." Bioinformatics **26**(24): 3140-2.